

INTERVAL HYPERGRAPHIC POLYTOPES (OR DEFORMED ASSOCIAHEDRA), TAMARI INTERVAL POSETS, AND WEEPING WILLOWS

JOSE BASTIDAS, FÉLIX GÉLINAS, VINCENT PILAUD, GERMAIN POULOT, ANDREW SACK,
AND ELENI TZANAKI

ABSTRACT. For a hypergraph \mathbb{H} on $[n]$, the hypergraphic polytope $\Delta_{\mathbb{H}}$ is the Minkowski sum of the standard simplices Δ_H for all $H \in \mathbb{H}$. We focus here on interval hypergraphs, where all hyperedges are intervals of $[n]$. They are precisely the deformations of Loday’s associahedron. Their vertex posets are Tamari interval posets, and we describe which Tamari interval poset appears as a vertex poset in which interval hypergraphic polytope. We also characterize the interval hypergraphs \mathbb{I} for which the hypergraphic polytope $\Delta_{\mathbb{I}}$ is simple, and we study their vertex posets, which we call weeping willows.

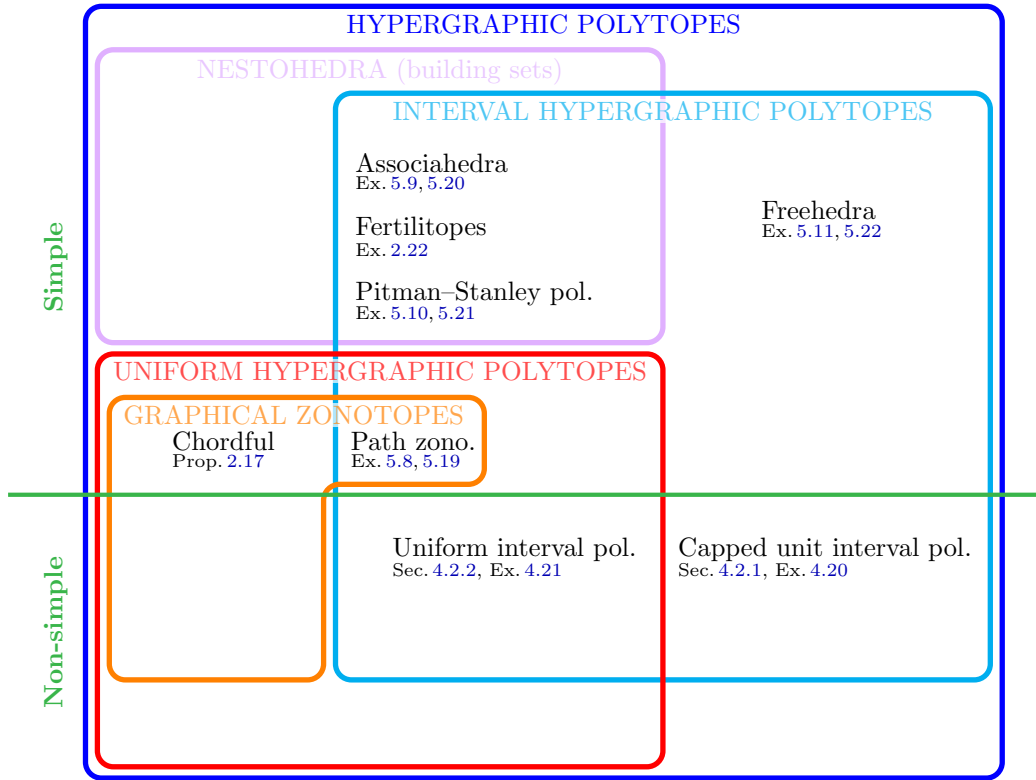


FIGURE 1. The main families of hypergraphic polytopes discussed in this paper.

VP was supported by the Spanish project PID2022-137283NB-C21 of MCIN/AEI/10.13039/501100011033 / FEDER, UE, by the Spanish–German project COMPOTE (AEI PCI2024-155081-2 & DFG 541393733), and by the Severo Ochoa and María de Maeztu Program for Centers and Units of Excellence in R&D (CEX2020-001084-M).

CONTENTS

1. Introduction	3
2. Preliminaries	5
2.1. Deformed permutahedra	5
2.2. Hypergraphic polytopes	6
2.3. Acyclic orientations and vertices of hypergraphic polytopes	7
2.4. Acyclic preorientations and faces of hypergraphic polytopes	7
2.5. Three families of hypergraphic polytopes	8
2.6. Two Genocchi families of interval hypergraphic polytopes	10
3. Simple interval hypergraphic polytopes	12
3.1. Necessity	12
3.2. Sufficiency	14
3.3. Counting simple interval hypergraphic polytopes	15
3.4. Characterizing simple hypergraphic polytopes?	16
4. Tamari interval posets and vertices of interval hypergraphic polytopes	18
4.1. Tamari interval posets	18
4.2. Two families of Tamari interval posets	19
4.3. Counting Tamari interval posets	21
4.4. Tamari interval posets and interval hypergraphic polytopes	22
4.5. A finer description	23
5. Weeping willows and vertices of simple interval hypergraphic polytopes	26
5.1. Weeping willows	26
5.2. Four families of weeping willows	28
5.3. Counting weeping willows	28
5.4. Weeping willows and simple interval hypergraphic polytopes	30
5.5. A finer description	31
6. Tamari interval preposets and faces of interval hypergraphic polytopes	34
6.1. Tamari interval preposets	34
6.2. Inclusion versus refinement	35
6.3. Two families of Tamari interval preposets	35
6.4. Counting Tamari interval preposets	37
6.5. Tamari interval preposets and interval hypergraphic polytopes	37
6.6. A finer description	37
7. Schröder weeping willows and faces of simple interval hypergraphic polytopes	39
7.1. Schröder weeping willows	39
7.2. Inclusion versus refinement	39
7.3. Four families of Schröder weeping willows	40
7.4. Counting Schröder weeping willows	41
7.5. Schröder weeping willows and simple interval hypergraphic polytopes	43
7.6. A finer description	43
Acknowledgements	43
References	44

1. INTRODUCTION

Hypergraphic polytopes. We fix an integer $n \geq 1$, and denote by $(\mathbf{e}_i)_{i \in [n]}$ the standard basis of \mathbb{R}^n . The *hypergraphic polytope* of a hypergraph $\mathbb{H} \subseteq 2^{[n]}$ on $[n]$ is the Minkowski sum $\Delta_{\mathbb{H}} := \sum_{H \in \mathbb{H}} \Delta_H$, where Δ_H is the simplex given by the convex hull of the points $\mathbf{e}_h \in \mathbb{R}^n$ for $h \in H$ (Section 2.2). The face lattice of $\Delta_{\mathbb{H}}$ was described combinatorially in terms of acyclic orientations of \mathbb{H} in [BBM19] (Sections 2.3 and 2.4).

Hypergraphic polytopes (or some special cases) have been studied in [FS05, PRW08, Pos09, AM09, Agn17, BBM19, PPP22, Reh22, AA23, CHM⁺23, CS25, ABG⁺25, BP26] among others. Important examples of hypergraphic polytopes include the permutahedron (when $\mathbb{H} = \binom{[n]}{2}$ is the complete graph), the associahedron of [SS93, Lod04] (when $\mathbb{H} = \{[i, j] \mid 1 \leq i \leq j \leq n\}$ is the complete interval hypergraph), graphical zonotopes (when $\mathbb{H} \subseteq \binom{[n]}{2}$ is a graph), graph associahedra [CD06], nestohedra [FS05, Pos09], multiplihedra [Sta70, SU04, For08, AD13, CP24, PP25], constrainahedra [BP22, CP24, PP25], and other more specific examples given below (Section 2.5).

Hypergraphic polytopes belong to the more general class of *deformed permutahedra* (aka. *generalized permutahedra* [Pos09], or *polymatroids* [Edm70]). The later are all deformations of the permutahedron, *i.e.* polytopes whose normal fans coarsen the braid arrangement (Section 2.1). They are all obtained as Minkowski sums and differences of faces of the standard simplex $\Delta_{[n]}$. Within the class of deformed permutahedra, the hypergraphic polytopes are precisely those which can be constructed using only Minkowski *sums* of faces of the standard simplex.

The edge directions of deformed permutahedra are all of the form $\mathbf{e}_i - \mathbf{e}_j$. Hence, each vertex \mathbf{v} of a deformed permutahedron \mathbb{P} defines a directed graph, called its *vertex digraph*, with nodes $[n]$ and where there is an arc $i \rightarrow j$ if \mathbb{P} has a neighboring vertex \mathbf{w} of \mathbf{v} such that $\mathbf{w} - \mathbf{v}$ is a positive multiple of $\mathbf{e}_j - \mathbf{e}_i$. The corresponding *vertex poset* is the transitive closure of the vertex digraph. Similarly, each face of a deformed permutahedron defines a preposet (*i.e.* a reflexive and transitive relation), called its *face preposet*. In this paper, we will study the combinatorics of these vertex posets and face preposets for certain hypergraphic polytopes.

Interval hypergraphic polytopes. Following [BP26], we study in this paper the case of *interval hypergraphs* \mathbb{I} , *i.e.* when all hyperedges of \mathbb{I} are intervals of $[n]$, namely $\mathbb{I} \subseteq \{[i, j] \mid 1 \leq i \leq j \leq n\}$. Note that the family of interval hypergraphic polytopes includes

- the classical associahedron of [SS93, Lod04] when \mathbb{I} contains all intervals of $[n]$,
- the Pitman–Stanley polytope [SP02] when \mathbb{I} is the set of all initial intervals $[i]$ for $i \in [n]$,
- the freehedron of [San09] when \mathbb{I} is the set of all initial intervals $[i]$ for $i \in [n]$ and all final intervals $[n] \setminus [i]$ for $i \in [n - 1]$,
- the fertilitopes of [Def23] when any two intervals of \mathbb{I} are either nested or disjoint.

See Section 5.2. The permutahedron, graphical zonotopes, graph associahedra, nestohedra, multiplihedra and constrainahedra are not interval hypergraphic polytopes (except for trivial examples).

Two combinatorially interesting families of interval hypergraphs are those closed under intersection, and those closed under union (of intersecting hyperedges). The former corresponds to interval hypergraphic lattices [BP26, Thm. A] while the latter corresponds to interval nestohedra (in the sense of [FS05, Pos09]). An elementary size preserving bijection between these two families of interval hypergraphs was described in [Pil25], passing through certain permutations known to be counted by median Genocchi numbers. We reproduce this argument (Section 2.6) in order to place it in a more formal context, noting that interval nestohedra form an important class of simple interval hypergraphic polytopes.

By definition, the interval hypergraphic polytopes are deformations of the classical associahedron, *i.e.* all polytopes whose normal fan coarsens the sylvester fan. It actually follows from [BMCLD⁺23, PPP23, PPP23] that the converse also holds when we allow for positive scaling of the Minkowski summands (which preserves the normal fan). Namely, any deformation of the associahedron is an interval hypergraphic polytope $\sum_{1 \leq i \leq j \leq n} \lambda_{ij} \Delta_{[i, j]}$ with $\lambda_{ij} \geq 0$ for all $1 \leq i < j \leq n$ and $\lambda_{ii} \in \mathbb{R}$ for $i \in [n]$.

Tamari interval (pre)posets. Interval hypergraphic polytopes are also closely related to the Tamari interval posets of [CP15]. These are the posets \triangleleft on $[n]$ such that $a \triangleleft c$ implies $a \triangleleft b$ while $a \triangleright c$

implies $b \triangleright c$ for all $1 \leq a < b < c \leq n$ (Sections 4.1 and 4.2). They are in correspondence with intervals of the Tamari lattice, are counted by remarkable product formulas [Cha07, Cha18], and are also in bijection with relevant families of planar maps [BB09, FFN25] (Section 4.3). The following connects Tamari interval posets and interval hypergraphic polytopes (Section 4.4).

Proposition A (Propositions 4.15 and 4.16). *The interval hypergraphic polytopes are precisely the deformed permutahedra whose vertex posets are Tamari interval posets. Moreover, any Tamari interval poset is a vertex poset of some interval hypergraphic polytope.*

In more detail (Section 4.5), we characterize which Tamari interval posets appear as vertex posets of which interval hypergraphic polytopes (Theorem 4.18). We then consider, for a given Tamari interval poset \triangleleft , the inclusion poset $\mathcal{I}_{\triangleleft}$ of interval hypergraphs \mathbb{I} such that \triangleleft is a vertex poset of $\Delta_{\mathbb{I}}$. This poset $\mathcal{I}_{\triangleleft}$ is an order convex subposet of the boolean lattice, always admits a maximum, and we characterize when it admits a minimum (Proposition 4.22).

In this paper, we also consider the face preposets of interval hypergraphic polytopes. We prove (Section 6.5) that they are precisely the preposets \blacktriangleleft on $[n]$ such that $a \blacktriangleleft c$ implies $a \blacktriangleleft b$ while $a \blacktriangleright c$ implies $b \blacktriangleright c$ for all $1 \leq a < b < c \leq n$, which we call *Tamari interval preposets* (Section 6.1). We again describe which Tamari interval preposets appear as face preposets of which interval hypergraphic polytopes (Theorem 6.15) and study the inclusion poset $\mathcal{I}_{\blacktriangleleft}$ of interval hypergraphs \mathbb{I} such that \blacktriangleleft is a face preposet of $\Delta_{\mathbb{I}}$ (Proposition 6.18).

Simple interval hypergraphic polytopes. A polytope is *simple* if each vertex is incident to dimension-many edges (or, equivalently, facets). For a generalized permutahedron, this means that its vertex digraphs are forests (actually trees if the polytope is of maximal dimension $n - 1$). Among the above-mentioned examples of hypergraphic polytopes, the permutahedron, associahedron, graph associahedra, and nestohedra are all simple, while the multiplihedra and constrainahedra are not (except in low dimension). As observed in [Kim08, Rem. 6.2] (see also [PRW08, Prop. 5.2] and [Pil24, Prop. 53]), the graphical zonotope of a graph G is simple if and only if G is *chordful* (meaning that any cycle induces a clique). In contrast, it is unclear whether simple hypergraphic polytopes admit an elementary characterization (Section 3.4). Going back to interval hypergraphs, we prove the following characterization of simple interval hypergraphic polytopes.

Theorem B (Theorem 3.1). *The hypergraphic polytope $\Delta_{\mathbb{I}}$ of an interval hypergraph \mathbb{I} is simple if and only if the following two conditions hold for all $I, J \in \mathbb{I}$:*

- (i) *if $I \cap J \neq \emptyset$ and there exists $K \in \mathbb{I}$ with $I \cup J \subseteq K$, then $I \cup J \in \mathbb{I}$, and*
- (ii) *if $|I \cap J| \geq 2$, then $I \cup J \in \mathbb{I}$ or there exists $K \in \mathbb{I}$ with $I \cap J \subseteq K$ and $I \not\subseteq K$ and $J \not\subseteq K$.*

(Schröder) weeping willows. We then consider the vertex trees of these simple interval hypergraphic polytopes. We call *weeping willow* any directed tree WW on $[n]$ such that for all $1 \leq a < b < c \leq n$, if WW contains the arc (a, c) (resp. (c, a)), then it contains a directed path from a to b (resp. from c to b) (Section 5.1). In other words, these are precisely the Hasse diagrams of the Tamari interval posets which are trees. We first observe that these trees have interesting counting formulas (Section 5.3). We then specialize Proposition A to the following statement.

Proposition C (Propositions 5.15 and 5.16). *The simple interval hypergraphic polytopes are precisely the deformed permutahedra whose vertex digraphs are weeping willows. Moreover, any weeping willow is a vertex tree of some simple interval hypergraphic polytope.*

This result can even be extended to characterize interval nestohedra (*i.e.* when the underlying interval hypergraph is closed under union of intersecting hyperedges).

Proposition D (Propositions 5.17 and 5.18). *The interval nestohedra are precisely the deformed permutahedra whose vertex digraphs are rooted weeping willows. Moreover, any rooted weeping willow is a vertex tree of some interval nestohedron.*

Again, using our characterization of which Tamari interval posets appear as vertex posets of which interval hypergraphic polytopes, we describe the posets of simple hypergraphic polytopes and of interval nestohedra containing a given weeping willow (Propositions 5.23 and 5.27). We finally extend these results to face preposets of simple interval hypergraphic polytopes, which we call *Schröder weeping willows* (Section 7).

2. PRELIMINARIES

2.1. Deformed permutahedra. The *Minkowski sum* of two polytopes $\mathbb{P}, \mathbb{Q} \subseteq \mathbb{R}^n$ is the polytope $\mathbb{P} + \mathbb{Q} := \{\mathbf{p} + \mathbf{q} \mid \mathbf{p} \in \mathbb{P}, \mathbf{q} \in \mathbb{Q}\}$. A *deformation* of a polytope \mathbb{P} is a polytope \mathbb{Q} which satisfies the following equivalent conditions:

- \mathbb{Q} is a weak Minkowski summand of \mathbb{P} , meaning that there exists $\lambda > 0$ and a polytope \mathbb{R} such that $\lambda\mathbb{P} = \mathbb{Q} + \mathbb{R}$,
- the normal fan of \mathbb{Q} coarsens the normal fan of \mathbb{P} ,
- \mathbb{Q} can be obtained from \mathbb{P} by parallelly translating its facets without moving past vertices,
- \mathbb{Q} can be obtained from \mathbb{P} by moving its vertices in such a way that all edge directions and orientations are preserved.

The *permutahedron* $\text{Perm}(n)$ is the polytope in \mathbb{R}^n obtained equivalently as:

- the convex hull of the points $\sum_{i \in [n]} i \mathbf{e}_{\sigma(i)}$ for all permutations σ of $[n]$, see [Sch11],
- the intersection of the hyperplane $\mathbb{H} = \{\mathbf{x} \in \mathbb{R}^n \mid \sum_{i \in [n]} x_i = \binom{n+1}{2}\}$ with the half-spaces $\{\mathbf{x} \in \mathbb{R}^n \mid \sum_{i \in I} x_i \geq \binom{|I|+1}{2}\}$ for all $\emptyset \neq I \subsetneq [n]$, see [Rad52],
- (a translation of) the Minkowski sum of the segments $[e_i, e_j]$ for $1 \leq i < j \leq n$.

See Figure 2. The (outer) normal fan of the permutahedron $\text{Perm}(n)$ is the *braid fan*, defined by the (type A) Coxeter arrangement formed by the hyperplanes $\{\mathbf{x} \in \mathbb{R}^n \mid x_i = x_j\}$ for all $1 \leq i < j \leq n$. Each permutation σ of $[n]$ corresponds to a maximal cone $\mathbf{C}_\sigma := \{\mathbf{x} \in \mathbb{R}^n \mid x_{\sigma(1)} \leq \dots \leq x_{\sigma(n)}\}$ of the braid fan, consisting of all points whose coordinates are ordered by the permutation σ .

A *deformed permutahedron* (aka. *generalized permutahedron* [Pos09], or *polymatroid* [Edm70]) is a deformation of the permutahedron $\text{Perm}(n)$. A classical example of a deformed permutahedron is the *associahedron* $\text{Asso}(n)$, defined equivalently as

- the convex hull of the points $\sum_{i \in [n]} \ell(T, i) r(T, i) \mathbf{e}_i$ for all binary trees T on n nodes, where $\ell(T, i)$ and $r(T, i)$ respectively denote the numbers of leaves in the left and right subtrees of the i -th node of T in infix labeling, see [Lod04],
- the intersection of the hyperplane \mathbb{H} with the halfspaces $\{\mathbf{x} \in \mathbb{R}^n \mid \sum_{i \leq \ell \leq j} x_\ell \geq \binom{j-i+2}{2}\}$ for all $1 \leq i < j \leq n$, see [SS93],
- the Minkowski sum of the faces $\Delta_{[i,j]}$ of the standard simplex $\Delta_{[n]}$ for $1 \leq i < j \leq n$, see [Pos09].

See Figure 2. The (outer) normal fan of the associahedron is the *sylvester fan*. Each binary tree T with n nodes corresponds to a maximal cone $\mathbf{C}_T := \{\mathbf{x} \in \mathbb{R}^n \mid x_i \leq x_j \text{ for } i \text{ child of } j \text{ in } T\}$ of the sylvester fan. Other examples of deformed permutahedra include matroid polytopes, graphical zonotopes, graph associahedra [CD06], nestohedra [FS05], quotientopes [PS19, PPR23], brick polytopes [PS12], multiplihedra [Sta70, SU04, For08, AD13, CP24], constrainahedra [BP22, CP24], and many others.

Following [PRW08], we now recall the dictionary between vertices (resp. faces) of deformed permutahedra and integer posets (resp. preposets). Note that our convention for vertex poset and face preposets is reversed from that of [PRW08] in order to fit with that of [BBM19, BP26]. In

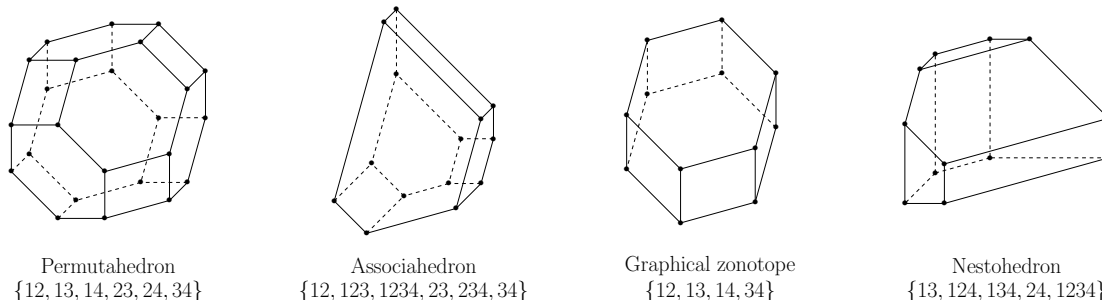


FIGURE 2. Examples of 3-dimensional hypergraphic polytopes.

particular, several of our arguments are formulated in terms of minimizing directions rather than maximizing ones.

For a vertex \mathbf{v} of a deformed permutahedron \mathbb{Q} , we call *vertex digraph* of \mathbf{v} in \mathbb{Q} the directed graph on $[n]$ with an arc $i \rightarrow j$ for each neighbor \mathbf{w} of \mathbf{v} in \mathbb{Q} such that $\mathbf{w} - \mathbf{v}$ is a positive multiple of $\mathbf{e}_j - \mathbf{e}_i$, and *vertex poset* \triangleleft of \mathbf{v} in \mathbb{Q} its transitive closure (note that vertex digraphs are acyclic, otherwise it would contradict \mathbf{v} being a vertex). In other words, the (outer) normal cone of \mathbf{v} in \mathbb{Q} is given by $\{\mathbf{x} \in \mathbb{R}^n \mid x_i \geq x_j \text{ for all } i \triangleleft j\}$. In particular, the linear extensions of the opposite of the vertex poset of \mathbf{v} in \mathbb{Q} are precisely the permutations σ such that the cone \mathbb{C}_σ of the braid arrangement is contained in the normal cone of \mathbf{v} in \mathbb{Q} . Moreover, note that \mathbf{v} is a simple vertex of \mathbb{Q} if and only if its vertex digraph is a forest.

More generally, for a face \mathbb{F} of \mathbb{Q} , we call *face preposet* \triangleleft of \mathbb{F} in \mathbb{Q} the preposet on $[n]$ such that the (outer) normal cone of \mathbb{F} in \mathbb{P} is given by $\{\mathbf{x} \in \mathbb{R}^n \mid x_i \geq x_j \text{ for all } i \triangleleft j\}$. Recall that a *preposet* \triangleleft is a reflexive and transitive relation, and defines an equivalence relation $\{(a, b) \mid a \triangleleft b \text{ and } b \triangleleft a\}$ and a poset $\{(A, B) \mid a \triangleleft b \text{ for some (or all) } a \in A \text{ and } b \in B\}$ on the equivalence classes of this equivalence relation. We will always denote by \triangleleft the poset associated to the preposet \triangleleft . We call *face digraph* of \mathbb{F} in \mathbb{Q} the Hasse diagram of the poset \triangleleft (its vertex set being a partition of $[n]$). If \mathbf{v} is a simple vertex, then the face digraphs of the faces containing \mathbf{v} are precisely the forests obtained by iterative edge contractions in the vertex digraph of \mathbf{v} .

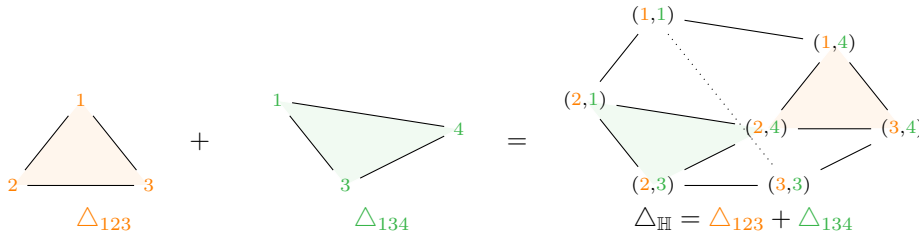
For instance, the vertex (resp. face) digraphs of the associahedron $\text{Asso}(n)$ are precisely the binary (resp. Schröder) trees with $n + 1$ leaves, labeled in inorder, and oriented towards their leaves, see Example 5.9 (resp. Example 7.8). Recall that a *Schröder tree* is a rooted plane tree where each node has at least two children (or equivalently a tree obtained from a binary tree by iterative edge contractions).

2.2. Hypergraphic polytopes. A *hypergraph* \mathbb{H} on $[n]$ is a collection of subsets of $[n]$. The *hypergraphic polytope* $\Delta_{\mathbb{H}}$ is the Minkowski sum

$$\Delta_{\mathbb{H}} := \sum_{H \in \mathbb{H}} \Delta_H,$$

where $\Delta_H := \text{conv}\{\mathbf{e}_h \mid h \in H\}$ is the simplex given by the convex hull of the points $\mathbf{e}_h \in \mathbb{R}^n$ for $h \in H$. Note that $\Delta_{\mathbb{H}}$ is always a deformed permutahedron, as it is a Minkowski sum of faces of the standard simplex.

Example 2.1. For the hypergraph $\mathbb{H} = \{123, 134\}$, we have



which is a 3-dimensional polytope sitting in \mathbb{R}^4 . We simplify notation, writing 123 for $\{1, 2, 3\}$.

Remark 2.2. Note that the singleton hyperedges are irrelevant for our purposes. Namely, adding to \mathbb{H} the hyperedge $\{i\}$ for some $i \in [n]$ just translates the polytope $\Delta_{\mathbb{H}}$ in the direction \mathbf{e}_i , which does not affect the face structure (nor the normal fan) of the polytope. For some statements, it is convenient to assume that $\{i\} \in \mathbb{H}$ for all $i \in [n]$. However, we ignore the singletons in the figures to simplify the drawings.

Recall that the face of a Minkowski sum $\sum_i \mathbb{P}_i$ minimizing a direction \mathbf{c} is the Minkowski sum of the faces of the summands \mathbb{P}_i minimizing \mathbf{c} . This standard fact immediately yields combinatorial descriptions of the vertices and faces of the hypergraphic polytope $\Delta_{\mathbb{H}}$, which we recall in the next two sections. Our descriptions are similar to (but slightly different from) those of [BBM19, Thm. 2.18].

2.3. Acyclic orientations and vertices of hypergraphic polytopes. We first recall a combinatorial model for the vertices of $\Delta_{\mathbb{H}}$, which will be extended to all faces of $\Delta_{\mathbb{H}}$ later in Section 2.4.

Definition 2.3. An *orientation* of \mathbb{H} is a map $O : \mathbb{H} \rightarrow [n]$ such that $O(H) \in H$ for all $H \in \mathbb{H}$. The orientation O is *acyclic* if there is no H_1, \dots, H_k with $k \geq 2$ such that $O(H_{i+1}) \in H_i \setminus \{O(H_i)\}$ for $i \in [k-1]$ and $O(H_1) \in H_k \setminus \{O(H_k)\}$.

Example 2.4. The hypergraph $\mathbb{H} = \{123, 134\}$ of Example 2.1 has 9 orientations, 7 of which are acyclic as displayed in Example 2.1 (we represent each orientation O by the pair $(O(123), O(134))$). For instance, the orientation $(O(123), O(134)) = (1, 3)$ is cyclic since $O(123) = 1 \in 134$ and $O(134) = 3 \in 123$ yields a cycle with $k = 2$.

Proposition 2.5 ([BBM19, Thm. 2.18]). *The acyclic orientations of \mathbb{H} are in bijection with the vertices of $\Delta_{\mathbb{H}}$. More precisely, an acyclic orientation A of \mathbb{H} corresponds to*

- the vertex $\sum_{H \in \mathbb{H}} e_{A(H)}$ of $\Delta_{\mathbb{H}}$,
- the vertex poset \triangleleft_A of $\Delta_{\mathbb{H}}$ defined as the transitive closure of $\{A(H) \leq h \mid h \in H \in \mathbb{H}\}$,
- the maximal cone $\mathbf{C}_A := \{\mathbf{x} \in \mathbb{R}^n \mid x_{A(H)} \geq x_h \text{ for all } h \in H \in \mathbb{H}\}$ in the normal fan of $\Delta_{\mathbb{H}}$

Definition 2.6. For a permutation σ of $[n]$, we define an orientation \mathcal{O}_σ of \mathbb{H} by

$$\mathcal{O}_\sigma(H) := \sigma(\min\{j \mid \sigma(j) \in H\}).$$

Equivalently, $\mathcal{O}_\sigma(H)$ is the element of H that first appears in the word $\sigma(1)\sigma(2)\dots\sigma(n)$.

Proposition 2.7 ([BBM19, Lem. 2.9]). *The map \mathcal{O} is a surjection from the permutations of $[n]$ to the acyclic orientations of \mathbb{H} . The pre-image $\mathcal{O}^{-1}(A) := \{\sigma \mid \mathcal{O}_\sigma = A\}$ is the set of linear extensions of \triangleleft_A .*

Example 2.8. Continuing with the hypergraph $\mathbb{H} = \{123, 134\}$ of Examples 2.1 and 2.4, let A be the acyclic orientation $(2, 4)$. The order \triangleleft_A is the following

$$\triangleleft_A = \text{Transitive closure} \left(\begin{array}{c} 1 \quad 3 \quad 1 \quad 3 \\ \backslash \quad / \quad \cup \quad \backslash \quad / \\ 2 \quad \quad 4 \end{array} \right) = \begin{array}{c} 1 \quad 3 \\ \times \\ 2 \quad 4 \end{array}.$$

The linear extensions of this order are the permutations 2413, 2431, 4213 and 4231.

2.4. Acyclic preorientations and faces of hypergraphic polytopes. We now recall a combinatorial model for all faces of $\Delta_{\mathbb{H}}$, similar to (but slightly different from) that of [BBM19, Thm. 2.18].

Definition 2.9. A *preorientation* of \mathbb{H} is a map $O : \mathbb{H} \rightarrow 2^{[n]}$ such that $\emptyset \neq O(H) \subseteq H$ for all $H \in \mathbb{H}$. The preorientation O is *acyclic* if there is no H_1, \dots, H_k with $k \geq 2$ such that $O(H_{i+1}) \cap H_i \neq \emptyset$ for $i \in [k-1]$ and $O(H_1) \cap (H_k \setminus \{O(H_k)\}) \neq \emptyset$.

Proposition 2.10 ([BBM19, Thm. 2.18]). *The acyclic preorientations of \mathbb{H} are in bijection with the faces of $\Delta_{\mathbb{H}}$. More precisely, an acyclic preorientation A of \mathbb{H} corresponds to*

- the face $\sum_{H \in \mathbb{H}} \Delta_{A(H)}$ of $\Delta_{\mathbb{H}}$,
- the face preposet \blacktriangleleft_A of $\Delta_{\mathbb{H}}$ defined as the transitive closure of $\{a \leq h \mid h \in H \in \mathbb{H}, a \in A(H)\}$,
- the cone $\mathbf{C}_A := \{\mathbf{x} \in \mathbb{R}^n \mid x_a \geq x_h \text{ for all } h \in H \in \mathbb{H}, a \in A(H)\}$ in the normal fan of $\Delta_{\mathbb{H}}$.

Definition 2.11. For an ordered partition (aka. set composition) $X = (X_1, \dots, X_k)$ of $[n]$, we define a preorientation \mathcal{O}_X of \mathbb{H} by

$$\mathcal{O}_X(H) := H \cap X_{\min\{i \in [k] \mid H \cap X_i \neq \emptyset\}}.$$

Proposition 2.12 ([BBM19, Lem. 2.9]). *The map \mathcal{O} is a surjection from the ordered partitions of $[n]$ to the acyclic preorientations of \mathbb{H} .*

Remark 2.13. Note that an (acyclic) orientation of \mathbb{H} is essentially a (acyclic) preorientation of \mathbb{H} whose images are all singletons. In this case, the orientation just records the element while the preorientation records the singleton. It thus slightly simplifies the notation to work with orientations when focusing on vertices of $\Delta_{\mathbb{H}}$.

2.5. Three families of hypergraphic polytopes. We briefly recall three specific families of hypergraphic polytopes, which are illustrated in Figure 2.

2.5.1. *Graphical zonotopes.* We start with graphical zonotopes, which are extensively studied in the literature, see *e.g.* [Sta73, Gre77, GZ83, PRW08, Pos09, Pil24, PPP25, Pou25, PP26].

Definition 2.14. A *graphical zonotope* is the hypergraphic polytope $\Delta_{\mathbb{G}}$ of a graph \mathbb{G} , *i.e.* a hypergraph such that $|H| = 2$ for all $H \in \mathbb{G}$.

Example 2.15.

- The graphical zonotope of a tree on n nodes is a cube of dimension $n - 1$.
- The graphical zonotope of the complete graph on n nodes is the permutahedron $\text{Perm}(n)$, see Figure 2.

Note that the normal fan of the graphical zonotope $\Delta_{\mathbb{G}}$ is the fan defined by the graphical arrangement of \mathbb{G} , that is, the collection of hyperplanes $\{\mathbf{x} \in \mathbb{R}^n \mid x_i = x_j\}$ for all arcs $\{i, j\}$ of \mathbb{G} . The following description of the vertex posets of $\Delta_{\mathbb{G}}$ is classical, and traces back to the work of C. Greene [Gre77] (see also [GZ83, Lem. 7.1]).

Proposition 2.16 ([Gre77], [GZ83, Lem. 7.1]). *The vertex posets of a graphical zonotope $\Delta_{\mathbb{G}}$ are the transitive closures of the acyclic orientations of \mathbb{G} . Moreover, any poset is the vertex poset of some graphical zonotope.*

Finally, simple graphical zonotopes were characterized in [Kim08, Rem. 6.2] (see also [PRW08, Prop. 5.2] and [Pil24, Prop. 53]). We say that a graph \mathbb{G} is *chordful* (*aka.* a *block graph*, *aka.* *clique tree*) when the following equivalent conditions are satisfied:

- any cycle in \mathbb{G} induces a clique of \mathbb{G} ,
- the 2-connected components of \mathbb{G} are cliques,
- \mathbb{G} is the line graph of some forest \mathbb{F} (the line graph of \mathbb{F} is the graph whose vertices are the arcs of \mathbb{F} , and where two arcs of \mathbb{F} are connected if they are incident to a common node).

Proposition 2.17 ([Kim08, Rem. 6.2]). *The graphical zonotope $\Delta_{\mathbb{G}}$ is simple if and only if \mathbb{G} is chordful.*

2.5.2. *Nestohedra.* Nestohedra of building sets were defined in the work of A. Postnikov [Pos09] and E.-M. Feichtner and B. Sturmfels [FS05] in connection to the wonderful compactifications of subspace arrangements of C. De Concini and C. Procesi [DCP95].

Definition 2.18. A hypergraph \mathbb{B} is a *building set* if $A \cap B \neq \emptyset$ implies $A \cup B \in \mathbb{B}$ for all $A, B \in \mathbb{B}$. The hypergraphic polytope $\Delta_{\mathbb{B}}$ is the *nestohedron* of \mathbb{B} .

Example 2.19.

- The collection $2^{[n]}$ of all subsets of $[n]$ is a building set. The corresponding nestohedron is (normally equivalent to) the permutahedron $\text{Perm}(n)$, see Figure 2.
- The collection of all intervals of $[n]$ is a building set. The corresponding nestohedron is the usual (Loday) associahedron $\text{Asso}(n)$, see Figure 2.
- The collection of *tubes* of a graph \mathbb{G} (*i.e.* subsets of vertices inducing a connected subgraph) is a building set, called the *graphical building set* of \mathbb{G} . The corresponding nestohedron is called a *graphical associahedron* [CD06].
- More generally, the collection of tubes of a hypergraph \mathbb{H} (*i.e.* subsets of vertices inducing a connected subhypergraph) is a building set, whose nestohedron is the *hypergraph associahedron* of \mathbb{H} [DP11].
- A collection \mathbb{B} of nested sets (*i.e.* if $A, B \in \mathbb{B}$ satisfy $A \cap B \neq \emptyset$, then either $A \subseteq B$ or $B \subseteq A$) is a building set. The corresponding nestohedron is called a *fertilityope* [Def23].

In a rooted tree T with associated order relation \triangleleft , the *descendant set* of a node $a \in T$ is $a^{\triangleleft} := \{b \in T \mid a \triangleleft b\}$, and two vertices $a, b \in T$ are *incomparable* if neither $a \in b^{\triangleleft}$ nor $b \in a^{\triangleleft}$. For a building set \mathbb{B} , a directed tree is a *\mathbb{B} -tree* if for all $a \in T$, we have $a^{\triangleleft} \in \mathbb{B}$, and for all incomparable vertices $a_1, \dots, a_r \in T$, we have $\bigcup_{i=1}^r a_i^{\triangleleft} \notin \mathbb{B}$. A rooted forest F is a *\mathbb{B} -forest* if the connected components of F are connected components of \mathbb{B} (*i.e.* inclusion maximal elements of \mathbb{B}), each inducing a *\mathbb{B} -tree*. Especially, if \mathbb{B} is connected (*i.e.* $[n] \in \mathbb{B}$), then all \mathbb{B} -forests are \mathbb{B} -trees.

Proposition 2.20 ([Pos09, Prop. 7.8]). *The vertex digraphs of the nestohedron $\Delta_{\mathbb{B}}$ are precisely the \mathbb{B} -forests. In particular, all nestohedra are simple polytopes. Moreover, any rooted forest is the vertex digraph of a nestohedron.*

Proof. The first part of the statement is [Pos09, Prop. 7.8]. For the last sentence of the statement, fix a rooted forest F , and let $\mathbb{B} = \{a^{\triangleleft} \mid a \in F\}$. Then \mathbb{B} is a collection of nested sets, because $a^{\triangleleft} \cap b^{\triangleleft} \neq \emptyset$ implies $a \in b^{\triangleleft}$ (hence $a^{\triangleleft} \subseteq b^{\triangleleft}$) or $b \in a^{\triangleleft}$ (hence $b^{\triangleleft} \subseteq a^{\triangleleft}$). Hence, \mathbb{B} is a building set and F is a \mathbb{B} -forest. Thus, by the first part of the statement, F is a vertex digraph of the nestohedron $\Delta_{\mathbb{B}}$. \square

In [PRW08], the authors conjectured that nestohedra are recognizable (among the deformed permutahedra) by their vertex digraphs.

Conjecture 2.21 ([PRW08, Question 8.3]). *A deformed permutahedron has the normal fan of a nestohedron if and only if all its vertex digraphs are rooted forest.*

We will prove this conjecture in an upcoming paper. In Proposition 5.17, we prove a weaker version of this conjecture, which can be phrased in two different but equivalent ways. Namely, we prove that Conjecture 2.21 holds when we replace

- either “deformed permutahedron” by “deformed associahedron” (or equivalently “interval hypergraphic polytope”, see Section 2.5.3),
- or “rooted trees” by “rooted weeping willows” (see Section 5).

We conclude with a relevant family of examples of nestohedra.

Example 2.22. A *fertilitepe* [Def23] is a nestohedron $\Delta_{\mathbb{B}}$ where all elements of \mathbb{B} are either nested or disjoint. To describe its vertices, it is convenient to assume that \mathbb{B} contains all singletons. For $B \in \mathbb{B}$, let ∂B be the set of inclusion maximal elements of $\{A \in \mathbb{B} \mid A \subsetneq B\}$ if $|B| > 1$, and $\partial B = \{B\}$ if $|B| = 1$. The vertices of the fertilitepe $\Delta_{\mathbb{B}}$ are in bijection with the sequences $(x_B)_{B \in \mathbb{B}} \in [n]^{\mathbb{B}}$ such that $x_B \in \{x_A \mid A \in \partial B\}$ and $x_{\{b\}} = b$ for $b \in [n]$. Hence, the fertilitepe $\Delta_{\mathbb{B}}$ has $\prod_{B \in \mathbb{B}} |\partial B|$ vertices and is actually combinatorially equivalent to the product of simplices $\prod_{B \in \mathbb{B}} \Delta_{|\partial B|}$. The \mathbb{B} -tree associated to $(x_B)_{B \in \mathbb{B}}$ is formed by the arcs from x_B to x_A for all $A \in \partial B$ with $x_A \neq x_B$. The i -th coordinate of the vertex associated to $(x_B)_{B \in \mathbb{B}}$ is the number of $B \in \mathbb{B}$ satisfying $x_B = i$.

2.5.3. *Interval hypergraphic polytopes.* Following [BP26], we focus in this paper on the following family of hypergraphs on $[n]$.

Definition 2.23. An *interval hypergraph* \mathbb{I} is a hypergraph on $[n]$ where each $I \in \mathbb{I}$ is an interval of the form $I = [i, j] := [j] \setminus [i-1] = \{i, i+1, i+2, \dots, j-1, j\}$.

Definition 2.24. An *interval building set* is an interval hypergraph which is also a building set.

Example 2.25. Our running example $\mathbb{H} = \{123, 134\}$ of Examples 2.1, 2.4 and 2.8, is not an interval hypergraph, as 134 is not an interval.

Example 2.26. The hypergraph $\mathbb{I} = \{123, 1234, 23, 234\}$ is an interval hypergraph admitting an acyclic orientation $\mathcal{O}_{4132} = (1, 4, 3, 4)$, see Figure 3.

We will prove in Proposition 4.15 some relevant characterizations of interval hypergraphic polytopes. At the moment, we only need the following important observation from [BP26, Prop. 3.6], and its generalization to preorientations. They state that an orientation (resp. preorientation) is acyclic if and only if it contains no cycle of length 2. Proposition 2.27 is proven in [BP26, Prop. 3.6] or follows from Proposition 2.28.

Proposition 2.27 ([BP26, Prop. 3.6]). *An orientation O of an interval hypergraph \mathbb{I} is acyclic if and only if there is no $I, J \in \mathbb{I}$ such that $O(I) \in J \setminus \{O(J)\}$ and $O(J) \in I \setminus \{O(I)\}$.*

Proposition 2.28. *A preorientation O of an interval hypergraph \mathbb{I} is acyclic if and only if there is no $I, J \in \mathbb{I}$ such that $O(I) \cap J \neq \emptyset$ and $O(J) \cap (I \setminus O(I)) \neq \emptyset$.*

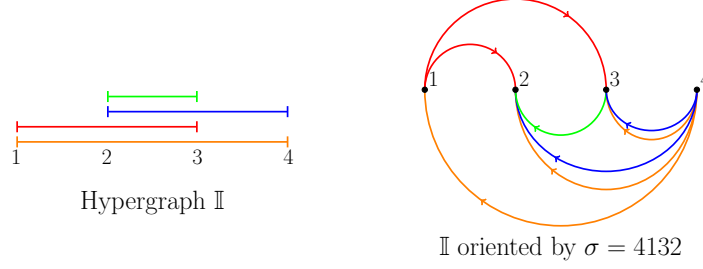


FIGURE 3. (Left) An interval hypergraph \mathbb{I} , (Right) and the graph formed by the directed edges $(\mathcal{O}_{4132}(H), h)$ for each $H \in \mathbb{I}$ and each $h \in H \setminus \{\mathcal{O}_{4132}(H)\}$.

Proof. If there exist $I, J \in \mathbb{I}$ such that $O(I) \cap J \neq \emptyset$ and $O(J) \cap (I \setminus O(I)) \neq \emptyset$, then O is cyclic by Definition 2.9. Conversely, suppose that O is cyclic, and let $I_1, \dots, I_k \in \mathbb{I}$ be such that there are $x_1 \in O(I_1) \cap (I_k \setminus \{O(I_k)\})$ and $x_i \in O(I_i) \cap I_{i-1}$ for $2 \leq i \leq k$, and that $k \geq 3$. We distinguish three cases, proving that there exists a smaller cycle (hence by recursion, a cycle of length 2):

- If $x_1 \leq x_2 \leq x_k$ (resp. $x_k \leq x_2 \leq x_1$), then $x_2 \in I_k$. If $x_2 \in O(I_k)$, then I_1, I_k is a smaller cycle. If $x_2 \notin O(I_k)$, then I_2, \dots, I_k is a smaller cycle.
- If $x_1 \leq x_k \leq x_2$ (resp. $x_2 \leq x_k \leq x_1$), then $x_k \in I_1$, so that I_1, I_k is a smaller cycle.
- If $x_2 \leq x_1 \leq x_k$ (resp. $x_k \leq x_1 \leq x_2$), then there exists $2 \leq i < k$ such that $x_i \leq x_1 \leq x_{i+1}$ (resp. $x_{i+1} \leq x_1 \leq x_i$), hence $x_1 \in I_i$. If $x_1 \in O(I_i)$, then I_i, \dots, I_k is a smaller cycle. If $x_1 \notin O(I_i)$, then I_1, \dots, I_i is a smaller cycle. \square

2.6. Two Genocchi families of interval hypergraphic polytopes. We now consider two families of interval hypergraphs, which are both counted by the famous median Genocchi numbers (see Remark 2.31). The following proposition was advertised in [Pil25], but we reproduce it here in a more formal environment. In this statement, the size of a hypergraph (resp. graph, resp. permutation) is its number of hyperedges (resp. arcs, resp. simple transpositions in any reduced expression).

Proposition 2.29 ([Pil25]). *There are size preserving bijections between:*

- (i) the interval hypergraphs \mathbb{I} on $[n]$ such that $I, J \in \mathbb{I}$ and $I \cap J \neq \emptyset$ implies $I \cap J \in \mathbb{I}$,
- (ii) the interval hypergraphs \mathbb{I} on $[n]$ such that $I, J \in \mathbb{I}$ and $I \cap J \neq \emptyset$ implies $I \cup J \in \mathbb{I}$,
- (iii) the graphs $([n+1], E)$ such that $\{a, c\}, \{b, d\} \in E$ implies $\{b, c\} \in E$ for all $a < b < c < d$,
- (iv) the graphs $([n+1], E)$ such that $\{a, c\}, \{b, d\} \in E$ implies $\{a, d\} \in E$ for all $a < b < c < d$,
- (v) the permutations σ of $[2n]$ such that $\sigma(i) \leq 2i$ and $\sigma(2n-i+1) \geq 2(n-i)+1$ for all $i \in [n]$,
- (vi) the permutations τ of $[2n]$ such that $\tau(2i-1) \geq 2i-1$ and $\tau(2i) \leq 2i$ for all $i \in [n]$.

Proof. Mapping the interval $[i, j]$ to the arc $\{i, j+1\}$ clearly defines size preserving bijections (i) \leftrightarrow (iii) and (ii) \leftrightarrow (iv). Considering the permutation ρ of $[2n]$ with $\rho(2i-1) = n+i$ and $\rho(2i) = i$, the composition $\tau := \sigma\rho$ defines a bijection (v) \leftrightarrow (vi). Finally, the bijections (i) \leftrightarrow (v) \leftrightarrow (ii) are illustrated in Figure 4. Namely, consider the word

$$Q := s_n(s_{n-1}s_{n+1})(s_{n-2}s_n s_{n+2})(s_{n-3}s_{n-1}s_{n+1}s_{n+3}) \cdots (s_1 s_3 \cdots s_{2n-3} s_{2n-1})$$

on the simple transpositions $s_i := (i \ i+1)$ of \mathfrak{S}_{2n} . Then any permutation σ of $[2n]$ with $\sigma(i) \leq 2i$ and $\sigma(2n-i+1) \geq 2(n-i)+1$ for all $i \in [n]$ defines a non-empty subword complex $SC(Q, \sigma)$ (see [KM05, KM04]) which admits unique greedy and anti-greedy facets (see [Pil12, PS13]). The positions of the contacts in the greedy (resp. anti-greedy facet) of $SC(Q, \sigma)$ give an interval hypergraph satisfying (i) (resp. (ii)). \square

Remark 2.30. Note that in Proposition 2.29,

- (i) the interval hypergraphs of (i) are called *intersection closed* and are precisely (up to the singletons) those whose hypergraphic poset (defined as the transitive closure of the graph of the hypergraphic polytope $\Delta_{\mathbb{I}}$ oriented in the linear direction $(1-n, 3-n, \dots, n-3, n-1)$) is a lattice [BP26, Thm. A] (note that not all such hypergraphic polytopes are simple),

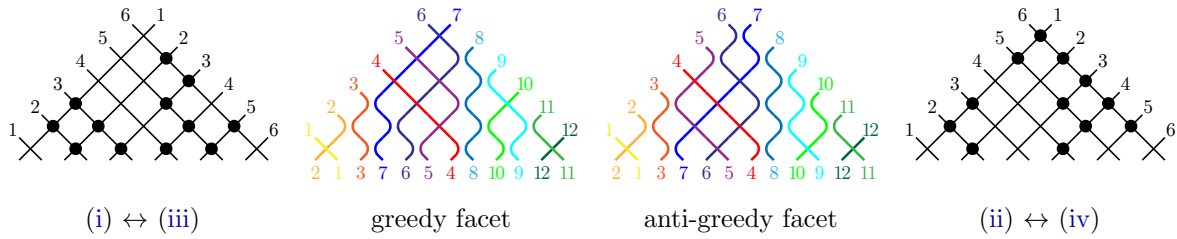


FIGURE 4. Plumbing bijection.

- (ii) the interval hypergraphs of (ii) are called *union closed* and are precisely (up to the singletons) the interval building sets in the sense of [FS05, Pos09], and their hypergraphic polytopes are *interval nestohedra* (in particular, they are simple polytopes),
- (iii) the graphs of (iii) are known as *grounded rectangle graphs* [JT19], *hook graphs* [Hix13], *max point-tolerance graphs* [CCF⁺17], *p-box graphs* [STC15], or *non-jumping graphs* [AFS19],
- (iv) the graphs of (iv) are known as *terrain-like graphs* [FR21, FR24, AFS19],
- (v) the permutations of (v) are called *Yoshi permutations* in [Pil25],
- (vi) the permutations of (vi) are called *Dumont permutations* [DR94].

Note that a similar bijection from (iv) to (vi) was presented in [FR24], but we are not aware that the bijection from (iii) to either (iv) or (vi) was observed earlier, even if the two classes of graphs (iii) and (iv) were compared in [AFS19].

Remark 2.31. The Dumont permutations of Proposition 2.29 (vi) are counted by the famous median Genocchi numbers [OEI10, A005439], whose first values are

$$1, 1, 2, 8, 56, 608, 9440, 198272, 5410688, 186043904, 7867739648, 401293838336, \dots$$

They can be defined, for instance, using every second number $g_{2n-1,1}$ in the leftmost column of the *Seidel triangle*, which is the array of numbers $g_{n,k}$ with $n \geq 1$ and $1 \leq k \leq \frac{n+1}{2}$, defined by $g_{1,1} = 1$ and the induction

$$g_{2n,k} = \sum_{i \geq k} g_{2n-1,i} \quad \text{and} \quad g_{2n+1,k} = \sum_{i \leq k} g_{2n,i}.$$

See Table 1.

$n \setminus k$	1	2	3	4	5	6	...
1	1						
2	1						
3	1	1					
4	2	1					
5	2	3	3				
6	8	6	3				
7	8	14	17	17			
8	56	48	34	17			
9	56	104	138	155	155		
10	608	552	448	310	155		
11	608	1160	1608	1918	2073	2073	
\vdots	\vdots	\vdots	\vdots	\vdots	\vdots	\vdots	\ddots

TABLE 1. Seidel's triangle $g_{n,k}$.

Remark 2.32. The proof actually extends to arbitrary staircase polyomino [Pil25, Sect. 3], but this goes beyond the focus of this paper.

3. SIMPLE INTERVAL HYPERGRAPHIC POLYTOPES

In this section, we prove the characterization of simple interval hypergraphic polytopes stated in Theorem B, and which we recall here. We prove the necessity direction in Section 3.1 and the sufficiency direction in Section 3.2. The set of all interval hypergraphs on 4 nodes whose hypergraphic polytope is simple is illustrated in Figure 5.

Theorem 3.1. *The hypergraphic polytope $\Delta_{\mathbb{I}}$ of an interval hypergraph \mathbb{I} is simple if and only if the following two conditions hold for all $I, J \in \mathbb{I}$:*

- (i) *if $I \cap J \neq \emptyset$ and there exists $K \in \mathbb{I}$ with $I \cup J \subseteq K$, then $I \cup J \in \mathbb{I}$, and*
- (ii) *if $|I \cap J| \geq 2$, then $I \cup J \in \mathbb{I}$ or there exists $K \in \mathbb{I}$ with $I \cap J \subseteq K$ and $I \not\subseteq K$ and $J \not\subseteq K$.*

Example 3.2. We recover from Theorem 3.1 that the hypergraphic polytopes are all simple for:

- interval building sets (that is, interval hypergraphs closed under union of intersecting hyperedges): $I, J \in \mathbb{I}$ and $I \cap J \neq \emptyset$ implies $I \cup J \in \mathbb{I}$, see [FS05, Pos09],
- interval hypergraphs closed under subintervals: $I \in \mathbb{I}$ and $J \subseteq I$ implies $J \in \mathbb{I}$, see [CF26, Prop. 5.5].

In particular the associahedron $\Delta_{\mathbb{I}}$ for $\mathbb{I} = \{[i, j] \mid 1 \leq i < j \leq n\}$ is simple for both reasons.

The following corollary emphasizes that interval nestohedra are special among simple interval hypergraphic polytopes. See Corollary 3.14 for a generalization to all hypergraphs.

Corollary 3.3. *Among the interval hypergraphs containing the ground set $[n]$ as a hyperedge, the only simple hypergraphic polytopes are the interval nestohedra.*

Proof. Suppose $\Delta_{\mathbb{I}}$ is simple and $[n] \in \mathbb{I}$. For $I, J \in \mathbb{I}$ with $I \cap J \neq \emptyset$, applying Theorem 3.1 (i) with $K = [n]$, we obtain that $I \cup J \in \mathbb{I}$. Hence, \mathbb{I} is a building set. \square

Example 3.4. For $S \subseteq [n-1]$, the hypergraphic polytope $\Delta_{\mathbb{I}_S}$ of $\mathbb{I}_S := \{[i, i+1] \mid i \in S\} \cup \{[n]\}$ is simple if and only if $n \leq 3$ or S does not contain two consecutive elements or equivalently no unit intervals intersect, see Example 4.20.

3.1. Necessity. We first prove the forward direction of Theorem 3.1. We start with a standard observation that we will use repeatedly throughout the paper. See also Lemma 3.15 for a discussion on the backward direction of this statement.

Lemma 3.5. *If \triangleleft is the transitive closure of a directed tree, then for any i, j, k, ℓ ,*

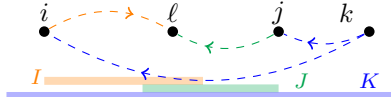
- (i) *if $k \triangleleft i, k \triangleleft j, i \triangleleft \ell$ and $j \triangleleft \ell$, then i and j are comparable in \triangleleft ,*
- (ii) *if $i \triangleleft k, i \triangleleft \ell, j \triangleleft k$, and $j \triangleleft \ell$, then either i and j , or k and ℓ are comparable in \triangleleft .*

We now decompose the proof of the forward direction of Theorem 3.1 into two lemmas, corresponding to the two conditions of Theorem 3.1. In the proof of each lemma, we assume that \mathbb{I} does not fulfill the condition, and we exhibit a non-simple vertex of $\Delta_{\mathbb{I}}$. For this, we define a permutation σ such that the vertex digraph of the acyclic orientation \mathcal{O}_{σ} contains a cycle.

In the following figures, the solid arrows are cover relations \triangleleft and the dashed arrows are comparisons \triangleleft .

Lemma 3.6. *If an interval hypergraph \mathbb{I} contains $I, J, K \in \mathbb{I}$ such that $I \cap J \neq \emptyset, I \cup J \notin \mathbb{I}$ and $I \cup J \subsetneq K$, then the hypergraphic polytope $\Delta_{\mathbb{I}}$ is not simple.*

Proof. Assume by symmetry that $i := \min(I) \in I \setminus J$ and $j := \max(J) \in J \setminus I$, and fix arbitrary $k \in K \setminus (I \cup J)$ and $\ell \in I \cap J$. Note that i, j, k, ℓ exist by assumption, and are all distinct by definition.



Let X (resp. Y) be the word formed by the complement of $I \cup J \cup \{k\}$ in $[n]$ (resp. of $\{i, j, \ell\}$ in $I \cup J$) written in an arbitrary order. Consider the poset \triangleleft of the acyclic orientation \mathcal{O}_{σ} defined

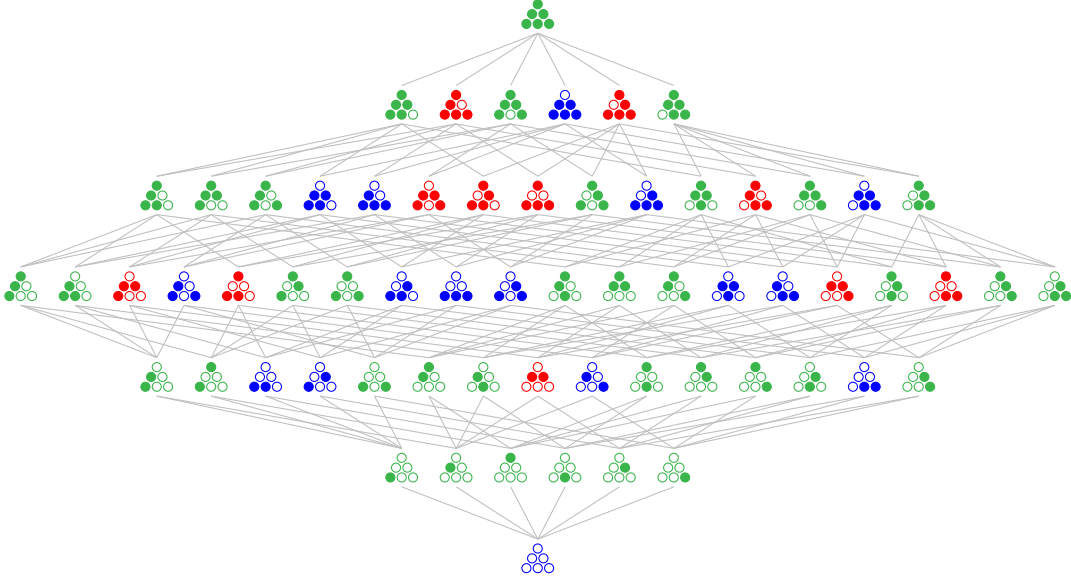

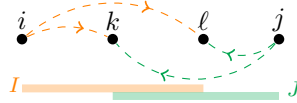


FIGURE 5. The boolean lattice \mathcal{I} of interval hypergraphs (containing all singletons) on 4 nodes, with respect to inclusion. We encode a hypergraph by a subset of the triangle, where the presence of an interval $[i, j]$ appears as a solid dot in diagonal i and antidiagonal $j - 1$. For instance, the interval hypergraph $\{[1, 2], [2, 4], [3, 4]\}$ is encoded by . The green and blue hypergraphs define simple hypergraphic polytopes (green are the interval nestohedra), while the red do not.

by the permutation $\sigma := kXijlY$. As $\{i, j, k\} \subseteq K \in \mathbb{I}$ and $\mathcal{O}_\sigma(K) = k$, we have $k \triangleleft i$ and $k \triangleleft j$. Considering I and J , we obtain similarly that $i \triangleleft \ell$ and $j \triangleleft \ell$. Since \mathbb{I} contains only intervals, if $\{i, j\} \subseteq H \in \mathbb{I}$, then $I \cup J = [i, j] \subseteq H$. Hence, $I \cup J \not\subseteq H$ because $I \cup J \notin \mathbb{I}$, so H contains one of the letters in the word kX , implying that $\mathcal{O}_\sigma(H) \notin \{i, j\}$, hence i and j do not form a cover relation of \triangleleft . As i and j are consecutive in σ and do not form a cover relation of \triangleleft , we conclude that they are incomparable in \triangleleft . Since $k \triangleleft i, k \triangleleft j, i \triangleleft \ell$ and $j \triangleleft \ell$, and i and j are incomparable in \triangleleft , we obtain by Lemma 3.5 (i) that the Hasse diagram of \triangleleft has a cycle. We conclude that $\Delta_{\mathbb{I}}$ is not simple. \square

Lemma 3.7. *If an interval hypergraph \mathbb{I} contains $I, J \in \mathbb{I}$ such that $|I \cap J| \geq 2$, $I \cup J \notin \mathbb{I}$, and $I \subseteq K$ or $J \subseteq K$ whenever $K \in \mathbb{I}$ satisfies $I \cap J \subseteq K$, then the hypergraphic polytope $\Delta_{\mathbb{I}}$ is not simple.*

Proof. As $I \cup J \notin \mathbb{I}$, by Lemma 3.6, we can assume that there is no $H \in \mathbb{I}$ with $I \cup J \subseteq H$, otherwise $\Delta_{\mathbb{I}}$ is not simple. Assume by symmetry that $i := \min(I) \in I \setminus J$ and $j := \max(J) \in J \setminus I$, and let $k := \min(I \cap J)$ and $\ell := \max(I \cap J)$. Note that i, j, k, ℓ exist and are all distinct by assumption.



Let X be the word formed by the complement of $\{i, j, k, \ell\}$ in $[n]$ written in an arbitrary order. Consider the poset \triangleleft of the acyclic orientation \mathcal{O}_σ defined by the permutation $\sigma := ijklX$. Since $\{i, k, \ell\} \subseteq I \in \mathbb{I}$ and $\mathcal{O}_\sigma(I) = i$, we have $i \triangleleft k$ and $i \triangleleft \ell$. Considering J , we obtain similarly that $j \triangleleft k$ and $j \triangleleft \ell$. As we assume that there is no $H \in \mathbb{I}$ satisfying $[i, j] = I \cup J \subseteq H$, and since \mathbb{I} contains only intervals, there is no $H \in \mathbb{I}$ such that $\{i, j\} \subseteq H$. As i and j are consecutive in σ , we conclude that they are incomparable in \triangleleft . Moreover, for any $\{k, \ell\} \subseteq H \in \mathbb{I}$,

we have $I \cap J = [k, \ell] \subseteq H$, hence $I \subseteq H$ or $J \subseteq H$, implying that $\mathcal{O}_\sigma(H) \notin \{k, \ell\}$. As k and ℓ are consecutive in σ , we conclude that they are incomparable in \triangleleft . Since $i \triangleleft k$, $i \triangleleft \ell$, $j \triangleleft k$, and $j \triangleleft \ell$, and both $\{i, j\}$ and $\{k, \ell\}$ are incomparable pairs in \triangleleft , we obtain by Lemma 3.5 (ii) that the Hasse diagram of \triangleleft has a cycle. We conclude that $\triangleleft_{\mathbb{I}}$ is not simple. \square

Proof of forward direction of Theorem 3.1. Follows from Lemmas 3.6 and 3.7. \square

3.2. Sufficiency. We now prove the backward direction of Theorem 3.1. We start with some observations on the vertex posets of interval hypergraphic polytopes.

Lemma 3.8. *Consider an acyclic orientation of an interval hypergraph on $[n]$, and denote by \triangleleft the associated poset on $[n]$ from Proposition 2.5 and by \triangleleft its cover relations. For any $1 \leq a < b < c \leq n$,*

- (i) $a \triangleleft b \triangleright c$ (or $a \triangleright b \triangleleft c$) implies that a and c are incomparable (i.e. $a \not\triangleleft c$ and $c \not\triangleleft a$),
- (ii) $a \triangleleft c$ implies $a \triangleleft b$ (and symmetrically $a \triangleright c$ implies $b \triangleright c$),
- (iii) $a \triangleleft c$ or $a \triangleright c$ implies that $b \not\triangleleft c$ (and symmetrically $a \not\triangleright b$).

Proof. Point (i) obviously holds for any poset. Indeed, if for instance $a \triangleleft c$, then $a \triangleleft b$ is not a cover relation as it is implied by $a \triangleleft c$ and $c \triangleleft b$.

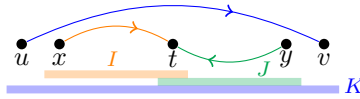
Point (ii) already appeared as [BP26, Prop. 3.10], we repeat the short proof for convenience. Assume that $a \triangleleft c$. By Proposition 2.5, there are $I_1, \dots, I_k \in \mathbb{I}$ such that $a = A(I_1)$, $A(I_{i+1}) \in I_i$ for all $i \in [k-1]$, and $c \in I_k$. As $\bigcup_{i \in [k]} I_i$ is an interval containing a and c and $a < b < c$, it also contains b . Hence, there is $j \in [k]$ such that $b \in I_j$, and the sequence I_1, \dots, I_j proves that $a \triangleleft b$.

Finally, for Point (iii), assume that a and c are comparable and that $b \triangleleft c$. We distinguish:

- if $a \triangleleft c$, then $a \triangleleft b$ by (ii), so that $a \triangleleft b \triangleleft c$ implies that $a \triangleleft c$ is not a cover relation,
- if $a \triangleright c$, then $b \triangleright c$ by (ii), so that $b \triangleleft c$ and $b \triangleright c$ contradict the acyclicity of the orientation. \square

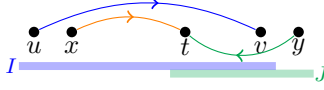
Proof of backward direction of Theorem 3.1. Assume that $\triangleleft_{\mathbb{I}}$ is not simple. Consider a non-simple vertex, and denote by A the corresponding acyclic orientation of \mathbb{I} , by \triangleleft the associated poset on $[n]$, and by \triangleleft its cover relations. As the vertex is not simple, \triangleleft contains an unoriented cycle Γ , which contains a sink $t \in [n]$. Let $x, y \in [n]$ be such that $x \triangleleft t \triangleright y$ in the cycle Γ . By Lemma 3.8 (iii), x and y cannot both lie on the same side of t , so we can assume by symmetry that $1 \leq x < t < y \leq n$. Moreover, as Γ is a cycle, it contains an arc $\{u, v\}$ with $1 \leq u < t < v \leq n$. Assume by symmetry that this arc is oriented $u \triangleleft v$. Note that $u \triangleleft v$ implies $u \triangleleft t$ by Lemma 3.8 (ii). If $x < u < t$, then $x \triangleleft t$ and $u \triangleleft t$ contradict Lemma 3.8 (iii). Hence, $u \leq x < t$ and we distinguish two situations depending on the relative positions of v and y .

Assume first that $y \leq v$, so that we have $1 \leq u \leq x < t < y \leq v \leq n$. As $x \triangleleft t$, $t \triangleright y$, and $u \triangleleft v$, there are intervals $I, J, K \in \mathbb{I}$ such that $[x, t] \subseteq I$ and $A(I) = x$, $[t, y] \subseteq J$ and $A(J) = y$, and $[u, v] \subseteq K$ and $A(K) = u$. If $u \in I$, then we have $u \triangleright x$, which contradicts Lemma 3.8 (iii) since $u \triangleleft v$. Similarly, we have $v \notin I$, $u \notin J$, and $v \notin J$. We thus obtain that $I \cup J \subset K$.



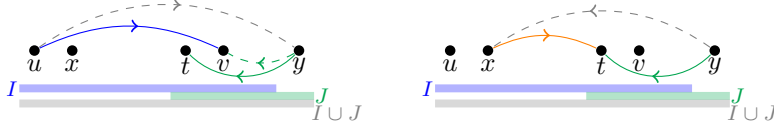
Assume now that $I \cup J \in \mathbb{I}$. If $A(I \cup J) \in I$, then $A(I \cup J) = x$ (as otherwise I and $I \cup J$ would contradict the acyclicity of A). Similarly, if $A(I \cup J) \in J$, then $A(I \cup J) = y$. In both cases, we obtain that x and y are comparable for \triangleleft , which contradicts Lemma 3.8 (i) since $x \triangleleft t \triangleright y$. We conclude that $I \cup J \notin \mathbb{I}$, so that our interval hypergraph \mathbb{I} does not satisfy Condition (i) in Theorem 3.1.

Assume now that $v < y$, so that we have $1 \leq u \leq x < t < v < y \leq n$. As $u \triangleleft v$ and $t \triangleright y$, there are $I, J \in \mathbb{I}$ such that $[u, v] \subseteq I$ and $A(I) = u$, and $[t, y] \subseteq J$ and $A(J) = y$. We moreover pick these intervals $I, J \in \mathbb{I}$ such that $\min(I)$ is maximal while $\max(J)$ is minimal among all possible intervals satisfying these properties. Note that $I \cap J$ contains at least t and v .



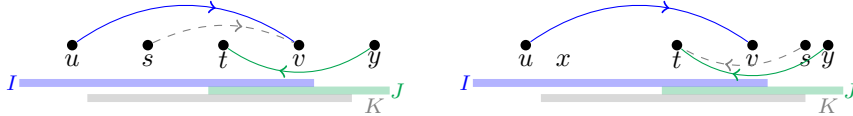
We now separate two cases:

- Assume first that $I \cup J \in \mathbb{I}$. We again distinguish two cases:
 - If $A(I \cup J) \in I$, then $A(I \cup J) = u$ by acyclicity of A . We thus obtain that $u \triangleleft y$. As $A(J) = y$ and $v \in [t, y] \subseteq J$, we also have $v \triangleright y$. We conclude that $u \triangleleft y \triangleleft v$, contradicting that $u \triangleleft v$ is a cover relation.
 - If $A(I \cup J) \in J$, then $A(I \cup J) = y$ by acyclicity of A . As $x \in [u, y] \subseteq I \cup J$, this implies that $x \triangleright y$, which contradicts Lemma 3.8 (i) since $x \triangleleft t \triangleright y$.



As $A(I \cup J) \in I \cup J$, we obtain a contradiction, and conclude that $I \cup J \notin \mathbb{I}$.

- Assume now that there is $K \in \mathbb{I}$ with $I \cap J \subseteq K$ but $I \not\subseteq K$ and $J \not\subseteq K$. Set $s = A(K)$. If $s < u$, then $A(I) = u \in K$ and $A(K) = s \in I$ (otherwise $I \subseteq K$), which contradicts the acyclicity of A . If $s = u$, then $[u, v] \subseteq K$ with $A(K) = u$, which contradicts the maximality of $\min(I)$. Hence, we have $u < s$. By a symmetric argument, we get that $u < s < y$. We again discuss two cases:
 - If $s < v$, we have $s = A(K)$ and $v \in I \cap J \subseteq K$, so that $s \triangleleft v$, which contradicts Lemma 3.8 (iii) since $u \triangleleft v$ and $u < s < v$.
 - If $t < s$, we have $s = A(K)$ and $t \in I \cap J \subseteq K$, so that $s \triangleleft t$, which contradicts Lemma 3.8 (iii) since $t \triangleright y$ and $t < s < y$.



As $t < v$, we conclude that there is no $K \in \mathbb{I}$ with $I \cap J \subseteq K$ but $I \not\subseteq K$ and $J \not\subseteq K$.

We thus obtained that $|I \cap J| \geq 2$ but $I \cup J \notin \mathbb{I}$ and there is no $K \in \mathbb{I}$ with $I \cap J \subseteq K$ but $I \not\subseteq K$ and $J \not\subseteq K$, so that our interval hypergraph \mathbb{I} does not satisfy Condition (ii) in Theorem 3.1. \square

3.3. Counting simple interval hypergraphic polytopes. In this section, we discuss the problem of counting simple interval hypergraphic polytopes. Remember that singleton hyperedges are irrelevant for hypergraphic polytopes (see Remark 2.2). We thus ignore singletons in all our counting (taking them into account would only amount to multiply by a factor 2^n).

Denote by I_n (resp. S_n , resp. N_n , resp. C_n) the number of interval hypergraphs (resp. interval hypergraphs \mathbb{I} whose hypergraphic polytope $\Delta_{\mathbb{I}}$ is simple, resp. interval building sets, resp. interval hypergraphs closed under subintervals) containing all singletons. See Table 2 for the first few values of the sequences $(I_n)_{n \geq 1}$, $(S_n)_{n \geq 1}$, $(N_n)_{n \geq 1}$ and $(C_n)_{n \geq 1}$.

As any nestohedron is simple, we clearly have

$$\frac{1}{16\sqrt{\pi}} \left(\frac{2}{e^2\pi^2} \right)^n n^{2n+3/2} \sim N_n \leq S_n \leq I_n = 2^{\binom{n}{2}} \sim 2^{n^2/2}.$$

The asymptotic expression for N_n is obtained from the standard expression for the median Genocchi numbers [OEI10, A005439], divided by 2^n (since we ignore singletons as discussed earlier).

Finally, we have also reported in Table 3 the number I_n^* (resp. S_n^* , resp. N_n^* , resp. C_n^*) of connected interval hypergraphs (resp. connected interval hypergraphs \mathbb{I} whose hypergraphic polytope $\Delta_{\mathbb{I}}$ is simple, resp. connected interval building sets, resp. connected interval hypergraphs closed under subintervals) containing all singletons. The numbers of Tables 2 and 3 are related by $(\sum_n I_n x^n)(1 - \sum_n I_n^* x^n) = 1$ (and similarly for S_n , N_n , and C_n).

n	1	2	3	4	5	6	7	8	9	...	OEIS
I_n	1	2	8	64	1024	32 768	2 097 152	268 435 456	68 719 476 736	...	A006125
S_n	1	2	8	53	510	6 771	121 036	...			—
N_n	1	2	7	38	295	3 098	42 271	726 734	15 366 679	...	A000366
C_n	1	2	5	14	42	132	429	1 430	4 862	...	A000108

TABLE 2. The numbers $I_n = 2^{\binom{n}{2}}$ of interval hypergraphic polytopes, S_n of simple interval hypergraphic polytopes, N_n of interval nestohedra, and C_n of interval hypergraphs closed under subintervals on $[n]$. Note that $C_n < N_n < S_n < I_n$, for all $n \geq 4$.

n	1	2	3	4	5	6	7	8	9	...	OEIS
I_n^*	1	1	5	49	893	30 649	2 030 213	264 198 625	68 180 168 717	...	A348901
S_n^*	1	1	5	38	401	5 691	106 693	...			—
N_n^*	1	1	4	25	217	2 470	35 647	637 129	13 843 948	...	A218826
C_n^*	1	1	2	5	14	42	132	429	1 430	...	A000108

TABLE 3. The numbers I_n^* of connected interval hypergraphic polytopes, S_n^* of connected simple interval hypergraphic polytopes, N_n^* of connected interval building sets, and C_n^* of connected interval hypergraphs closed under subintervals on $[n]$. Note that $C_n^* < N_n^* < S_n^* < I_n^*$, for all $n \geq 4$.

3.4. Characterizing simple hypergraphic polytopes? In this section, we discuss the extension of Theorem B to all hypergraphic polytopes, beyond those only consisting of intervals. First, it is important to observe that, contrary to the case of interval hypergraphs (where the Minkowski sum $\sum \lambda_{ij} \Delta_{[i,j]}$ uniquely determines the summands), the hypergraph \mathbb{H} is in general not determined by the normal fan of the hypergraphic polytope $\Delta_{\mathbb{H}}$.

Lemma 3.9. *If $J \notin \mathbb{H}$ and for every $e \in \binom{J}{2}$ there exists $H \in \mathbb{H}$ such that $e \subseteq H \subseteq J$, then $\Delta_{\mathbb{H}}$ and $\Delta_{\mathbb{H} \cup \{J\}}$ have the same normal fan.*

Proof. Remember that

- two fans coincide if and only if they have the same walls (*i.e.* codimension 1 cones),
- the union of the walls of the normal fan of a Minkowski sum is the union of the walls of the normal fans of the summands,
- the normal fan of a simplex Δ_J with $J \subseteq [n]$ has a wall for each $\{u, v\} \in \binom{J}{2}$, given by $\{\mathbf{x} \in \mathbb{R}^n \mid x_u = x_v < x_j \text{ for all } j \in J \setminus \{u, v\}\}$.

Consequently, the hypergraphic polytopes $\Delta_{\mathbb{H}}$ and $\Delta_{\mathbb{H} \cup \{J\}}$ have the same normal fan if and only if the walls of the normal fan of the simplex Δ_J are all contained in the union of the walls of $\Delta_{\mathbb{H}}$, that is, if and only if, for each $e \in \binom{J}{2}$, there is $H \in \mathbb{H}$ such that $e \subseteq H \subseteq J$. \square

Example 3.10. The hypergraphic polytopes of the hypergraphs $\{12, 23, 13\}$ and $\{12, 23, 13, 123\}$ have the same normal fan. More generally, the braid fan is the normal fan of the hypergraphic polytope of any hypergraph containing the complete graph $\binom{[n]}{2}$, for example of the complete hypergraph $\sum_{X \subseteq [n]} \Delta_X$.

We say that a hypergraph \mathbb{H} is *saturated* if there is no J as in Lemma 3.9, that is, if \mathbb{H} is inclusion maximal among all hypergraphs whose hypergraphic polytope have a given normal fan. (Note that this differs from the notion of saturated hypergraph of [DP11, Sect. 4], which just means building set.) For instance, all interval hypergraphs are saturated.

To extend Theorem B, it is convenient to restrict our attention to saturated hypergraphs, as this entails no loss of generality. First, Lemmas 3.6 and 3.7 extend straightforward to all saturated hypergraphs (we give similar proofs), which yields the following necessary conditions on \mathbb{H} for $\Delta_{\mathbb{H}}$ to be simple.

Lemma 3.11. *If a saturated hypergraph \mathbb{H} contains $I, J, K \in \mathbb{H}$ such that $I \cap J \neq \emptyset$, $I \cup J \notin \mathbb{H}$, and $I \cup J \subsetneq K$, then the hypergraphic polytope $\Delta_{\mathbb{H}}$ is not simple.*

Proof. As \mathbb{H} is saturated and $I \cup J \notin \mathbb{H}$, there exist $i, j \in I \cup J$ such that there is no $H \in \mathbb{H}$ with $\{i, j\} \subseteq H \subseteq I \cup J$. Fix moreover $k \in K \setminus (I \cup J)$ and $\ell \in I \cap J$. Note that $i, j \in (I \cup J) \setminus (I \cap J)$, so that i, j, k, ℓ are all distinct. Consider the poset \triangleleft of the acyclic orientation \mathcal{O}_{σ} defined by a permutation $\sigma := kXij\ell Y$ where X (resp. Y) is the word formed by the complement of $I \cup J \cup \{k\}$ in $[n]$ (resp. of $\{i, j, \ell\}$ in $I \cup J$) written in an arbitrary order. The choice of i, j, k, ℓ ensures that $k \triangleleft i \triangleleft \ell$ and $k \triangleleft j \triangleleft \ell$. Moreover, as i and j are consecutive in σ and there is no $H \in \mathbb{H}$ with $\{i, j\} \subseteq H \subseteq I \cup J = \{i, j, \ell\} \cup Y$, we obtain that i and j are incomparable in \triangleleft . We conclude by Lemma 3.5 (i) that the Hasse diagram of \triangleleft has a cycle, hence that $\Delta_{\mathbb{H}}$ is not simple. \square

Lemma 3.12. *If a saturated hypergraph \mathbb{H} contains $I, J \in \mathbb{H}$ such that $|I \cap J| \geq 2$, $I \cup J \notin \mathbb{H}$, and there exists $k, \ell \in I \cap J$ such that there is no $H \in \mathbb{H} \setminus \{I, J\}$ satisfying $\{k, \ell\} \subseteq H \subseteq I \cup J$, then the hypergraphic polytope $\Delta_{\mathbb{H}}$ is not simple.*

Proof. As \mathbb{H} is saturated and $I \cup J \notin \mathbb{H}$, there exist $i, j \in I \cup J$ such that there is no $H \in \mathbb{H}$ with $\{i, j\} \subseteq H \subseteq I \cup J$. Note that $i, j \in (I \cup J) \setminus (I \cap J)$, so that i, j, k, ℓ are all distinct. Consider the poset \triangleleft of the acyclic orientation \mathcal{O}_{σ} defined by a permutation $\sigma := XijklY$ where X (resp. Y) is the word formed by the complement of $I \cup J$ in $[n]$ (resp. of $\{i, j, k, \ell\}$ in $I \cup J$) written in an arbitrary order. The choice of i, j, k, ℓ ensures that $i \triangleleft k$, $i \triangleleft \ell$, $j \triangleleft k$ and $j \triangleleft \ell$. Moreover, as i and j are consecutive in σ and there is no $H \in \mathbb{H}$ with $\{i, j\} \subseteq H \subseteq I \cup J = \{i, j, k, \ell\} \cup Y$, we obtain that i and j are incomparable in \triangleleft . Similarly, as k and ℓ are consecutive in σ and there is no $H \in \mathbb{H}$ with $\{k, \ell\} \subseteq H \subseteq (I \cup J) \setminus \{i, j\} = \{k, \ell\} \cup Y$, we obtain that k and ℓ are incomparable in \triangleleft . We conclude by Lemma 3.5 (ii) that the Hasse diagram of \triangleleft has a cycle, hence that $\Delta_{\mathbb{H}}$ is not simple. \square

Example 3.13. The hypergraphic polytope of the saturated hypergraph $\{123, 234, 145, 12345\}$ is not simple by Lemma 3.11 with $I = 123$, $J = 234$, $K = 12345$. The same hypergraphic polytope is not simple by Lemma 3.12 with $I = 123$ and $J = 234$.

The following consequence of Lemma 3.11 generalizes Corollary 3.3. Roughly speaking, among the hypergraphic polytopes containing the full simplex $\Delta_{[n]}$ as a summand, the simple hypergraphic polytopes are precisely the nestohedra.

Corollary 3.14. *Consider a saturated hypergraph \mathbb{H} containing the ground set $[n]$ as a hyperedge. Then the hypergraphic polytope $\Delta_{\mathbb{H}}$ is simple if and only if \mathbb{H} is a building set.*

Proof. Suppose $\Delta_{\mathbb{H}}$ is simple and $[n] \in \mathbb{H}$. For $A, B \in \mathbb{H}$ with $A \cap B \neq \emptyset$, applying Lemma 3.11 with $K = [n]$, we obtain that $A \cup B \in \mathbb{H}$. Hence, \mathbb{H} is a building set. \square

To prove Lemmas 3.11 and 3.12, we heavily relied on Lemma 3.5 which describes two kinds of patterns that prevent a Hasse diagram from being a directed forest. However, more general obstructions can arise, demanding for more convoluted criteria on \mathbb{H} characterizing when is $\Delta_{\mathbb{H}}$ a simple polytope. The following classical strengthening of Lemma 3.5 characterizes the posets whose Hasse diagrams are forests.

Lemma 3.15. *The Hasse diagram D of the order relation \triangleleft is a directed forest if and only if:*

- (i) *there exist no i, j, k, ℓ with i and j incomparable by \triangleleft such that $k \triangleleft i$, $k \triangleleft j$, $i \triangleleft \ell$ and $j \triangleleft \ell$,*
- (ii) *there exist no $k_1, \dots, k_r, \ell_1, \dots, \ell_r$ for $r \geq 2$ with k_p and k_q (resp. ℓ_p and ℓ_q) incomparable by \triangleleft for $p \neq q$ such that $k_p \triangleleft \ell_p$, $k_p \triangleleft \ell_{p+1}$ and $k_r \triangleleft \ell_1$.*

See Figure 6 for illustrations of these posets.

Proof. The proof is classical from the literature, we give here a very short idea. Fix a cycle in D and consider k_1, \dots, k_r to be its sources and ℓ_1, \dots, ℓ_r its sinks, enumerated in cyclic order. If $r \geq 2$, then one is in the case of (ii). If $r = 1$, then there are two directed paths from k_1 to ℓ_1 : taking some i on the first path and some j on the second yields case (i). \square

Example 3.16. Let C_n be a cycle on $n \geq 4$ vertices. The graphical zonotope Δ_{C_n} is not simple, even if it does not violate the necessary conditions of Lemmas 3.11 and 3.12.

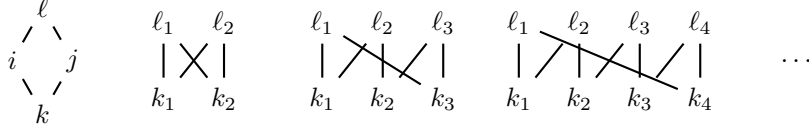


FIGURE 6. Diamond and crown posets.

However, searching in general for patterns in \mathbb{H} which yield vertex digraphs of $\Delta_{\mathbb{H}}$ containing the cycles of Lemma 3.15 seems combinatorially intricate and computationally inefficient. We thus leave the following problem open.

Problem 3.17. *What is the complexity of the decision problem “Given a hypergraph $\mathbb{H} \subseteq \binom{[n]}{m}$, is the hypergraphic polytope $\Delta_{\mathbb{H}}$ simple?”*

Remark 3.18. Note that the problem “Does $\Delta_{\mathbb{H}}$ have a non-simple vertex?” is **NP** as one can provide as certificate a vertex poset of $\Delta_{\mathbb{H}}$ (given as an acyclic orientation of \mathbb{H}), and one of the patterns of Lemma 3.15.

Remark 3.19. We have seen three classes of hypergraphs \mathbb{H} for which determining whether $\Delta_{\mathbb{H}}$ is simple can be done in polynomial time:

- for a building set \mathbb{B} , the nestohedron $\Delta_{\mathbb{B}}$ is always simple,
- for a graph \mathbb{G} , the graphical zonotope $\Delta_{\mathbb{G}}$ is simple if and only if any cycle of \mathbb{G} induces a clique (this can be checked in $O(n+m)$ time),
- for interval hypergraphs \mathbb{I} , the conditions of Theorem B can be checked in $O(m^4)$ time.

Besides, note that verifying that \mathbb{H} is a building set (resp. a graph, resp. an interval hypergraph) can be done in $O(m^3)$ (resp. $O(m)$, resp. $O(nm)$) time. These families however do not cover all simple hypergraphic polytopes.

4. TAMARI INTERVAL POSETS AND VERTICES OF INTERVAL HYPERGRAPHIC POLYTOPES

In this section, we consider the vertex posets of the interval hypergraphic polytopes. These posets are precisely the Tamari interval posets defined by G. Chatel and V. Pons [CP15].

4.1. Tamari interval posets. Recall that the *weak order* is the lattice on permutations of \mathfrak{S}_n whose cover relations are pairs of permutations related by the swap of two values at adjacent positions. Equivalently $\sigma \leq \tau$ if and only if $\text{inv}(\sigma) \subseteq \text{inv}(\tau)$ where $\text{inv}(\sigma)$ is the *inversion set* of the permutation σ , defined by $\text{inv}(\sigma) := \{(\sigma(i), \sigma(j)) \mid 1 \leq i < j \leq n \text{ and } \sigma(i) > \sigma(j)\}$. The Hasse diagram of the weak order is the graph of the permutahedron oriented in the direction $\omega := (n, \dots, 1) - (1, \dots, n) = (n-1, n-3, \dots, 3-n, 1-n)$. The *Tamari lattice* [Tam51] is the lattice on binary trees on n nodes whose cover relations are pairs of binary trees related by a right rotation. The Hasse diagram of the Tamari lattice is the graph of the associahedron oriented in the direction ω . The following are classical characterizations of the intervals in the weak order and in the Tamari lattice.

Definition 4.1 ([BW91, Thm. 6.8], [CPP19, Prop. 2.5]). A *weak order interval poset* is a poset \triangleleft on $[n]$ with the following equivalent properties:

- the set of linear extensions of \triangleleft forms an interval $[\sigma, \tau]$ of the weak order,
- for $1 \leq a < b < c \leq n$, one has $(a \triangleleft c \implies a \triangleleft b \text{ or } b \triangleleft c)$ and $(a \triangleright c \implies a \triangleright b \text{ or } b \triangleright c)$.

Definition 4.2 ([CP15, Def. 2.7 & Thm. 2.8], [CPP19, Coro. 2.24]). A *Tamari interval poset* is a poset \triangleleft on $[n]$ with the following equivalent properties:

- the set of linear extensions of \triangleleft is the union of the sets of linear extensions of the binary trees in an interval of the Tamari lattice,
- the set of linear extensions of \triangleleft is an interval $[\sigma, \tau]$ of the weak order such that σ avoids the pattern 231 and τ avoids the pattern 213,
- for $1 \leq a < b < c \leq n$, one has $(a \triangleleft c \implies a \triangleleft b)$ and $(a \triangleright c \implies b \triangleright c)$,
- for any $a \in [n]$, the principal upper set $a^{\triangleleft} := \{b \in [n] \mid a \triangleleft b\}$ of a is an interval of $[n]$.

Remark 4.3. Following [CPP19], we represent a Tamari interval poset \triangleleft on $[n]$ by its Hasse diagram, with node a at coordinates $(a, 0)$ and with increasing (resp. decreasing) cover relations $a \triangleleft b$ (resp. $a \triangleright b$) with $a < b$ drawn above (resp. below) the horizontal axis. Note that it yields a non-crossing graph (as for any $a < b < c < d$, if $a \triangleleft c$ and $b \triangleleft d$, then $a \triangleleft b$ and $b \triangleleft c$ so that $a \triangleleft c$ is not a cover relation). A typical example of Tamari interval poset is illustrated in Figure 7.

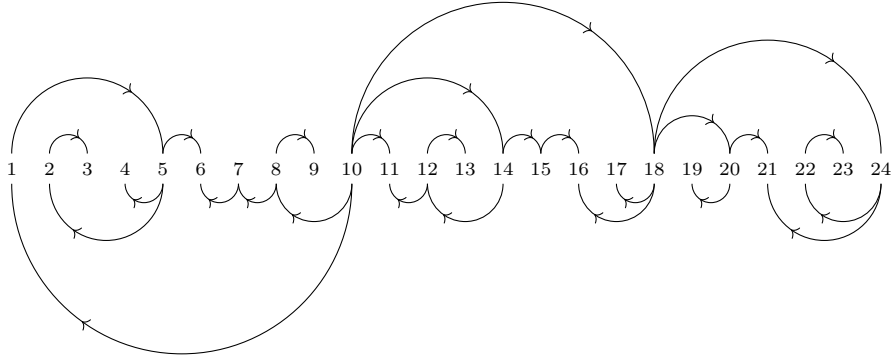


FIGURE 7. The Hasse diagram of a typical Tamari interval poset.

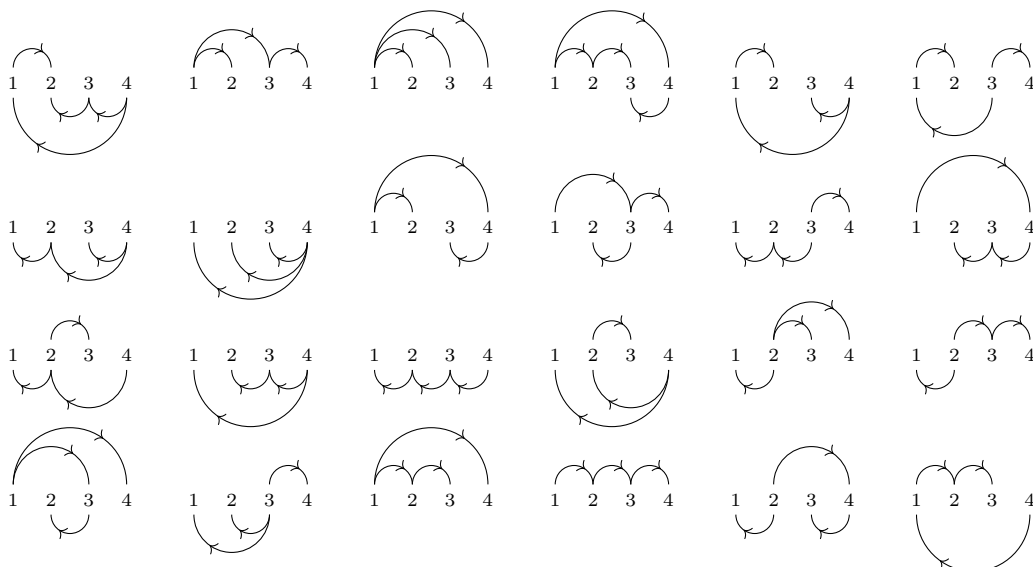
4.2. Two families of Tamari interval posets. We describe two interesting families of Tamari interval posets, which will later appear as the vertex posets of certain families of hypergraphic polytopes (see also Section 5.2 for other families where all Hasse diagrams are trees).

4.2.1. Capped unit interval posets. We begin by considering the following posets, whose full significance will become clear in Example 4.20 (see also Section 6.3.1 and Example 6.16).

Definition 4.4. A *capped unit interval poset* is a poset \triangleleft on $[n]$ such that

- \triangleleft admits a unique minimum m ,
- for any cover relation $a \triangleleft b$, either $a = m$ or $|a - b| = 1$.

Example 4.5. For instance, the capped unit interval posets for $n = 4$ are the following



Proposition 4.6. *Capped unit interval posets are Tamari interval posets.*

Proof. Assume that $a \triangleleft c$ for some $1 \leq a < b < c \leq n$. Consider any saturated chain from a to c in \triangleleft . If b belongs to this chain, then $a \triangleleft b$. Otherwise, let a' be the last element $< b$ and c' be the first element $> b$ along this chain. Hence, we have $a \triangleleft a' \triangleleft c' \triangleleft c$ and $1 \leq a' < b < c' \leq n$. As $a' \triangleleft c'$ and $|a' - c'| > 1$, we get that $a' = m$, hence that $a = m$. We conclude that $a \triangleleft b$. The proof is symmetric if $a \triangleright c$. \square

Remark 4.7. The number of capped unit interval posets is

$$3^{n-2} + \left(\sum_{m=2}^{n-1} 3^{m-2} 3^{n-m-1} \right) + 3^{n-2} = (n+5)3^{n-2} \quad [\text{OEI10, A038765}],$$

because they are determined by their minimum m together with their restrictions to each consecutive pair of integers of $[n] \setminus \{m\}$ (and for each pair $\{i, i+1\}$, there are three possibilities: either i and $i+1$ are incomparable, or $i \triangleleft i+1$, or $i+1 \triangleleft i$). The number of capped unit interval posets whose Hasse diagram is a tree is

$$G_{n-2} + \left(\sum_{m=2}^{n-1} G_{m-2} G_{n-m-1} \right) + G_{n-2} \quad [\text{OEI10, A290917}],$$

where $G_n = 3G_{n-1} - G_{n-2}$ is the bisection of the Fibonacci sequence [OEI10, A001906] (now for each pair $\{i, i+1\}$, say with $m > i$, there are three possibilities: either i and $i+1$ are incomparable, or i is smaller than $i+1$, or $i+1$ is smaller than i which forbids $i-1$ to be smaller than i). Note that this implies that asymptotically, most capped unit interval posets on n nodes are not trees.

We now consider subfamilies of capped unit interval posets indexed by subsets S of $[n-1]$. Again, the significance will become clear in Example 4.20 (see also Section 6.3.1 and Example 6.16).

Definition 4.8. For $S \subseteq [n-1]$, a *capped S -unit interval poset* is a capped unit interval poset \triangleleft with minimum m such that

- i and $i+1$ are comparable in \triangleleft for any $i \in S$,
- if i and $i+1$ form a cover relation in \triangleleft , then $i \in S$ or $m \in \{i, i+1\}$.

Remark 4.9. By the same argument as above, capped S -unit interval posets are counted by

$$\sum_{m=1}^n 2^{|S \setminus \{m-1, m\}|},$$

and those whose Hasse diagram is a tree are counted by

$$\sum_{m=1}^n \ell_S(1, m) \cdot r_S(m, n)$$

where $\ell_S(j, m)$ (resp. $r_S(m, j)$) are defined inductively for $1 \leq j \leq m$ (resp. $m \leq j \leq n$) by $\ell_S(j, m) = 1$ if $j \geq m-1$ (resp. $r_S(m, j) = 1$ if $j \leq m+1$) and

$$\begin{aligned} \ell_S(j, m) &= (1 + \delta_{j \in S}) \cdot \ell_S(j+1, m) - \delta_{\{j, j+1\} \subseteq S \setminus \{m-1\}} \cdot \ell_S(j+2, m) \\ (\text{resp. } r_S(m, j) &= (1 + \delta_{j-1 \in S}) \cdot r_S(m, j-1) - \delta_{\{j-1, j-2\} \subseteq S \setminus \{m\}} \cdot r_S(m, j-2) \quad) \end{aligned}$$

otherwise. (Here, δ_X denotes the Kronecker symbol, meaning that $\delta_X = 1$ if X holds true, and $\delta_X = 0$ otherwise).

Example 4.10. In particular:

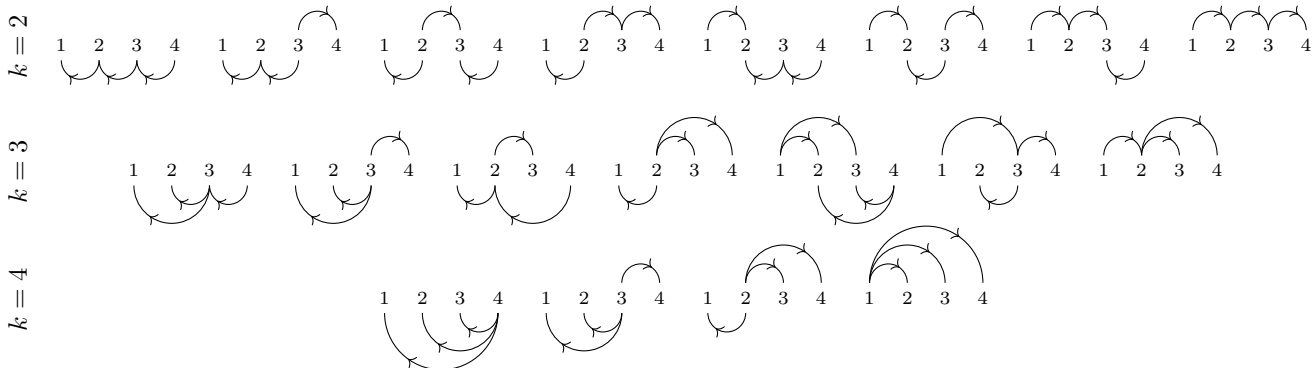
- The capped \emptyset -unit interval posets are the star posets with a minimum m covered by all elements of $[n] \setminus \{m\}$. They are counted by n , and their Hasse diagrams are all trees.
- The capped $[n-1]$ -unit interval posets are the capped unit interval posets in which any consecutive integers are comparable. They are counted by $(n+2)2^{n-3}$ [OEI10, A045623], and those whose Hasse diagram is a tree are counted by $(n-1)(n^2 - 2n + 12)/6$ [OEI10, A177787].

4.2.2. *Uniform interval posets.* We now consider the following posets, whose significance will become clear in Example 4.21 (see also Section 6.3.2 and Example 6.17).

Definition 4.11. For $k \geq 1$, a *k-uniform interval poset* is a poset \triangleleft on $[n]$ such that

- every length k subinterval of $[n]$ admits a unique minimum in \triangleleft , and
- every cover relation connects the minimum in \triangleleft of a length k subinterval to another element of that subinterval.

Example 4.12. The antichain is the only 1-uniform interval poset. The k -uniform interval posets on $[4]$ for $k = 2, 3, 4$ are the following



Proposition 4.13. All k -uniform interval posets are Tamari interval posets.

Proof. Assume that $a \triangleleft c$ for some $1 \leq a < b < c \leq n$. Consider any saturated chain from a to c in \triangleleft . If b belongs to this chain, then $a \triangleleft b$. Otherwise, let a' be the last element $< b$ and c' be the first element $> b$ along this chain. Hence, we have $a \triangleleft a' \triangleleft c' \triangleleft c$ and $1 \leq a' < b < c' \leq n$. Thus, a' is the minimal element of a length k interval I and $c' \in I$. We thus obtain that $b \in I$, so that $a' \triangleleft b$. We conclude that $a \triangleleft b$. The proof is symmetric if $a \triangleright c$. \square

Remark 4.14. The first few numbers of such posets are gathered in Table 4. We leave as an open problem to compute explicit formulas.

$k \setminus n$	1	2	3	4	5	6	7	8	9	10	11	12	...
2	1	2	4	8	16	32	64	128	256	512	1024	2048	...
3	1	1	3	7	16	36	81	182	409	919	2065	4640	...
4	1	1	1	4	10	24	56	128	292	664	1508	3424	...
5	1	1	1	1	5	13	32	76	176	400	905	2038	...
6	1	1	1	1	1	6	16	40	96	224	512	1152	...
7	1	1	1	1	1	1	7	19	48	116	272	624	...

TABLE 4. The numbers of k -uniform interval posets on $[n]$.

4.3. **Counting Tamari interval posets.** A celebrated result of F. Chapoton [Cha07] states that the Tamari intervals are enumerated by

$$\frac{2}{(3n+1)(3n+2)} \binom{4n+1}{n+1}.$$

The first few values can be found in Table 5 or [OEI10, A000260]. These numbers also count the rooted 3-connected planar triangulations with $2n+2$ faces. An explicit bijection between Tamari intervals and 3-connected triangulations was given in [BB09]. A more recent and powerful approach can be found in [FFN25]. We also refer to [BCP26] for intriguing refined counting for Tamari interval posets, providing explicit product formulas for the f -vectors of the canonical complex of the Tamari lattice and of the cellular diagonal of the associahedron.

The number of connected Tamari interval posets (*i.e.* whose Hasse diagram is connected) is also reported in Table 5 or [OEI10, A294084]. The generating functions f of the Tamari interval posets and g of the connected Tamari interval posets are clearly related by $f = 1 + g + g^2 + \dots = 1/(1-g)$.

n	1	2	3	4	5	6	7	8	9	10	...	OEIS
TIP_n	1	3	13	68	399	2530	16965	118668	857956	6369883	...	A000260
$CTIP_n$	1	2	8	41	240	1528	10312	72647	528992	3954488	...	A294084
WW_n	1	2	8	38	196	1062	5948	34120	199316	1181126	...	A047098
RWW_n	1	2	7	30	143	728	3876	21318	120175	690690	...	A006013
$TIPX_n$	1	2	5	17	67	287	...					—
WWX_n	1	2	5	16	67	316	1599	8480	46512	261668	...	—

TABLE 5. The numbers TIP_n of Tamari interval posets, $CTIP_n$ of connected Tamari interval posets, WW_n of weeping willows, RWW_n of rooted weeping willows, $TIPX_n$ of Tamari interval posets satisfying Proposition 4.22 (ii), and WWX_n of weeping willows satisfying Proposition 5.23 (ii).

4.4. Tamari interval posets and interval hypergraphic polytopes. In this section, we prove Proposition A connecting Tamari interval posets to interval hypergraphic polytopes. In the following proposition, we allow for positive scaling of the Minkowski summands (which preserves the normal fan) in the definition of hypergraphic polytopes. That is, we still call hypergraphic polytope the Minkowski sum $\sum_{I \subseteq [n]} \lambda_I \Delta_I$ for any $\lambda_I \geq 0$ for $I \subseteq [n]$ with $|I| > 1$.

Proposition 4.15. *The following are equivalent for a polytope \mathbb{P} :*

- (i) \mathbb{P} is an interval hypergraphic polytope,
- (ii) \mathbb{P} is a deformed permutahedron whose vertex posets are Tamari interval posets,
- (iii) \mathbb{P} is a deformed associahedron, *i.e.* a deformation of $\text{Asso}(n)$.

Proof. (i) \Rightarrow (ii). We already mentioned that all hypergraphic polytopes are deformed permutahedra, so we just need to show that all vertex posets of an interval hypergraphic polytope are Tamari interval posets. This was already observed in [BP26, Prop. 3.10], and we already repeated the argument in Lemma 3.8 (ii).

(ii) \Rightarrow (iii). Consider a Tamari interval poset \triangleleft , corresponding to an interval $[T, T']$ between two binary trees T and T' in the Tamari lattice. The cone defined by \triangleleft is then the union of the cones of the sylvester fan corresponding to the binary trees in $[T, T']$. Hence, if all vertex posets of \mathbb{P} are Tamari interval posets, then the normal fan of \mathbb{P} coarsens the sylvester fan, so that \mathbb{P} is a deformed associahedron.

(iii) \Rightarrow (i). It follows from [BMCLD⁺23, PPPP23, PPP23] that the deformation cone of the associahedron $\text{Asso}(n)$ is simplicial, and its rays are the faces $\Delta_{[i,j]}$ of the standard simplex corresponding to intervals $[i, j]$ of $[n]$. Hence, any deformed associahedron is a non-negative Minkowski sum of $\Delta_{[i,j]}$, in other words, an interval hypergraphic polytope. \square

Proposition 4.16. *Any Tamari interval poset is a vertex poset of an interval hypergraphic polytope.*

Proof. For a Tamari interval poset \triangleleft , recall that we denote $a^{\triangleleft} := \{b \in [n] \mid a \triangleleft b\}$ for $a \in [n]$. By Definition 4.2 (iv), the set a^{\triangleleft} is an interval for all $a \in [n]$. Consider the orientation A_{\triangleleft} of the interval hypergraph $\mathbb{I}_{\triangleleft} := \{a^{\triangleleft} \mid a \in [n]\}$ defined by $A_{\triangleleft}(a^{\triangleleft}) = a$ for all $a \in [n]$. It is clear that A_{\triangleleft} is acyclic and that $\triangleleft_{A_{\triangleleft}} = \triangleleft$. \square

We now give explicitly the coordinates of the vertex of $\Delta_{\mathbb{I}}$ associated to a given Tamari interval poset, see Figure 8 for an example.

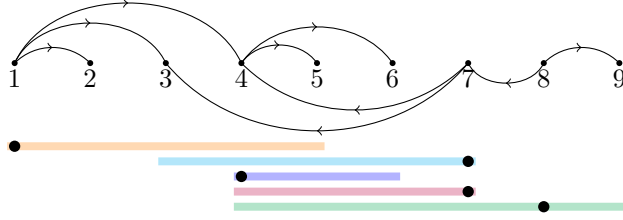


FIGURE 8. An interval hypergraph \mathbb{I} with a Tamari interval poset associated to the vertex \mathbf{v} of $\Delta_{\mathbb{I}}$. By Proposition 4.17, counting the number of intervals of \mathbb{I} with minimum element i for each $i \in [9]$ yields $\mathbf{v} = (1, 0, 0, 1, 0, 0, 2, 1, 0)$

Proposition 4.17. *The vertex of an interval hypergraphic polytope $\Delta_{\mathbb{I}}$ corresponding to a Tamari interval poset \triangleleft has i -th coordinate $\#\{I \in \mathbb{I} \mid i \in I \subseteq i^{\triangleleft}\}$, that is the number of intervals of \mathbb{I} having i as its minimum.*

Proof. Consider any vector \mathbf{c} such that $a \triangleleft b$ implies $c_a < c_b$. Recall that the vertex of a Minkowski sum $\sum_i \mathbb{P}_i$ minimizing a generic direction \mathbf{c} is the Minkowski sum of the vertices of the summands \mathbb{P}_i minimizing \mathbf{c} . Moreover, the vertex minimizing \mathbf{c} on a simplex Δ_I is \mathbf{e}_j , where $j \in I$ is such that $c_j = \min\{c_k \mid k \in I\}$. Hence, the vertex of $\Delta_{\mathbb{I}}$ minimizing \mathbf{c} has i -th coordinate $\#\{I \in \mathbb{I} \mid i \in I \subseteq i^{\triangleleft}\}$. \square

4.5. A finer description. We now refine Proposition 4.16 to describe which Tamari interval poset appears as a vertex poset in which interval hypergraphic polytope.

Theorem 4.18. *A poset \triangleleft is a vertex poset of an interval hypergraphic polytope $\Delta_{\mathbb{I}}$ if and only if*

- (i) *for any $I \in \mathbb{I}$, there is $a \in [n]$ such that $a \in I \subseteq a^{\triangleleft}$,*
- (ii) *for any cover relation $a \triangleleft b$, there is $I \in \mathbb{I}$ such that $\{a, b\} \subseteq I \subseteq a^{\triangleleft}$.*

Proof. Assume first that $\triangleleft = \triangleleft_A$ is the vertex poset of the hypergraphic polytope $\Delta_{\mathbb{I}}$ corresponding to the acyclic orientation A of \mathbb{I} . Then, by Proposition 2.5:

- (i) For any $I \in \mathbb{I}$, we have $A(I) \in I \subseteq A(I)^{\triangleleft}$.
- (ii) For any cover relation $a \triangleleft b$, there is $I \in \mathbb{I}$ such that $a = A(I)$ and $b \in I$. In particular, $\{a, b\} \subseteq I \subseteq A(I)^{\triangleleft} = a^{\triangleleft}$.

Hence, \triangleleft and \mathbb{I} satisfy (i) and (ii).

Conversely, consider a poset \triangleleft and an interval hypergraph \mathbb{I} that satisfy (i) and (ii). We now construct an acyclic orientation A of \mathbb{I} such that $\triangleleft = \triangleleft_A$. For all $I \in \mathbb{I}$, we define $A(I)$ to be the unique $a \in [n]$ such that $a \in I \subseteq a^{\triangleleft}$. Note that it exists by (i), and it is unique by antisymmetry of \triangleleft . We claim that

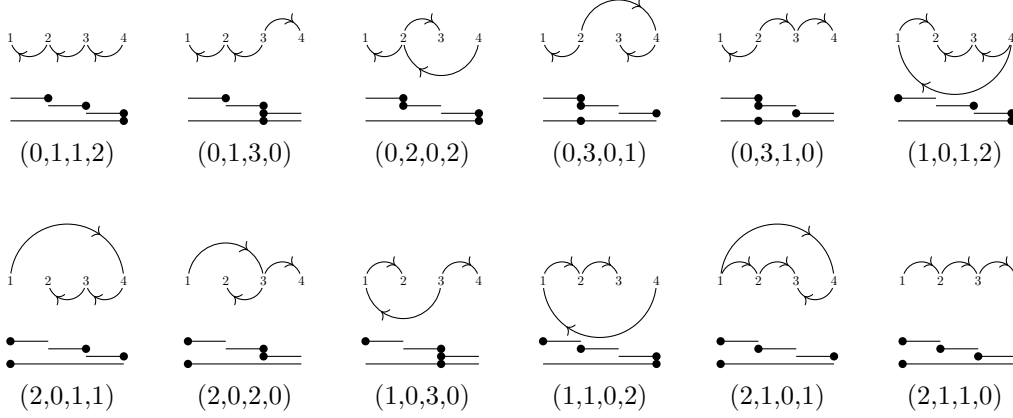
- A is acyclic. Otherwise, there are $I, J \in \mathbb{I}$ with $A(I) \in J$ and $A(J) \in I$ by Proposition 2.27. By definition of A , we then get $A(I) \in J \subseteq A(J)^{\triangleleft}$ and $A(J) \in I \subseteq A(I)^{\triangleleft}$. This implies that $A(I) = A(J)$ by antisymmetry of \triangleleft .
- $\triangleleft = \triangleleft_A$. Indeed, any cover relation of \triangleleft_A is clearly a relation in \triangleleft . Conversely, for any cover relation $a \triangleleft b$, there exists $I \in \mathbb{I}$ such that $\{a, b\} \subseteq I \subseteq a^{\triangleleft}$ by (ii). Hence, $a = A(I)$ and $b \in I$ so that we get $a \triangleleft_A b$.

We conclude that $\triangleleft = \triangleleft_A$ is indeed the vertex poset of the hypergraphic polytope $\Delta_{\mathbb{I}}$ corresponding to the acyclic orientation A of \mathbb{I} . \square

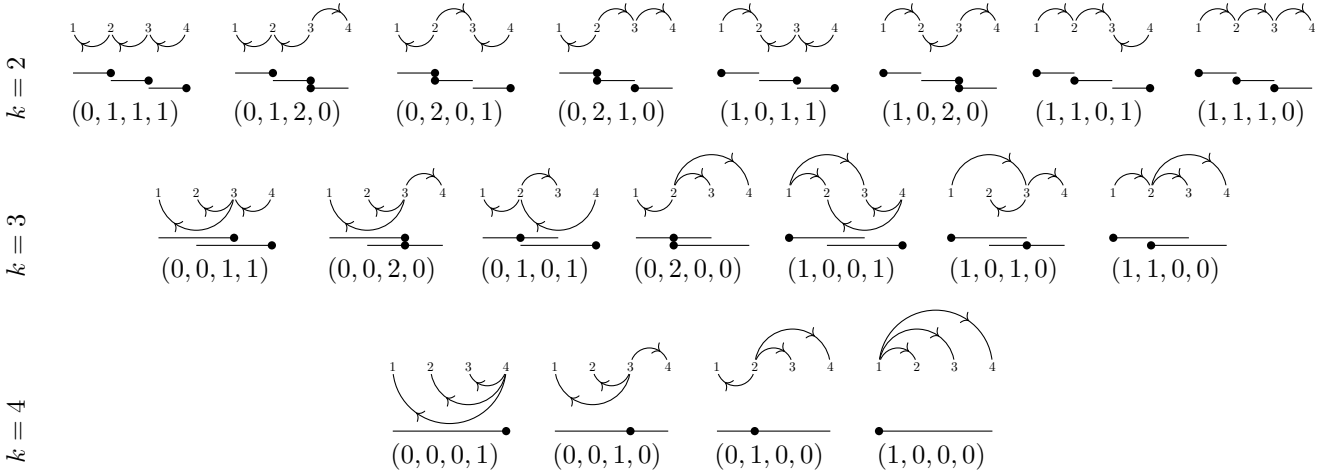
Remark 4.19. Two comments on Theorem 4.18. First, in (i), for any $I \in \mathbb{I}$, there exists a unique $a \in [n]$ such that $a \in I \subseteq a^{\triangleleft}$. Second, (ii) implies that for any $a \in [n]$, there is $I \in \mathbb{I}$ such that $a \in I \subseteq a^{\triangleleft}$. However, the latter is not equivalent to (i) (nor to (ii)).

Example 4.20. For $S \subseteq [n-1]$, the vertex posets of the hypergraphic polytope $\Delta_{\mathbb{I}_S}$ of $\mathbb{I}_S = \{\{i, i+1\} \mid i \in S\} \cup \{[n]\}$ are precisely the capped S -unit interval posets of Definition 4.8.

From Proposition 4.17, we obtain that the i -th coordinate of the vertex \mathbf{v}_\triangleleft of $\Delta_{\mathbb{I}_S}$ corresponding to a capped S -unit interval poset \triangleleft with minimum m is $\delta_{i-1 \triangleright i} + \delta_{i \triangleleft i+1} + \delta_{i=m}$ (here, $n > 2$ so that the intervals $[1, 2]$ and $[n]$ do not coincide). For instance, we illustrate below the correspondence between the capped $[3]$ -unit interval posets on $[4]$ and the acyclic orientations of the interval hypergraph $\{[1, 2], [2, 3], [3, 4], [1, 4]\}$. We mark the minimum of each interval with a bullet \bullet , and the i -th coordinate of the associated vertex is the number of intervals whose bullet \bullet lies at i .



Example 4.21. For the (complete) k -uniform interval hypergraph $\mathbb{I} := \{[i, i + k - 1] \mid i \in [n - k]\}$, the hypergraphic polytope $\Delta_{\mathbb{I}}$ is a non-simple polytope whose vertex posets are precisely the k -uniform interval posets of Definition 4.11. We illustrate below the correspondence for $n = 4$ and $k = 2, 3, 4$.



We now exploit Theorem 4.18 to describe the set of interval hypergraphs for which \triangleleft is a vertex poset. Here, we restrict attention to interval hypergraphs containing all singletons, as dropping this assumption would simply yield a Cartesian product with a boolean lattice (see Remark 2.2). We denote by $U(\triangleleft)$ the maximal cover relations of \triangleleft for the order given by $(a \triangleleft b) \prec (a \triangleleft c)$ for $1 \leq a < b < c \leq n$ or $1 \leq c < b < a \leq n$. In other words, $U(\triangleleft)$ consists of the covers that are maximal among the covers with the same source.

Proposition 4.22. We denote by \mathcal{I} the inclusion poset of interval hypergraphs \mathbb{I} on $[n]$ containing all singletons (which is isomorphic to a boolean lattice on $\binom{n}{2}$ elements). For a given Tamari interval poset \triangleleft , denote by $\mathcal{I}_\triangleleft$ the subposet of \mathcal{I} induced by interval hypergraphs \mathbb{I} on $[n]$ such that \triangleleft is a vertex poset of $\Delta_{\mathbb{I}}$. Then

- (i) $\mathcal{I}_\triangleleft$ is order convex in \mathcal{I} .

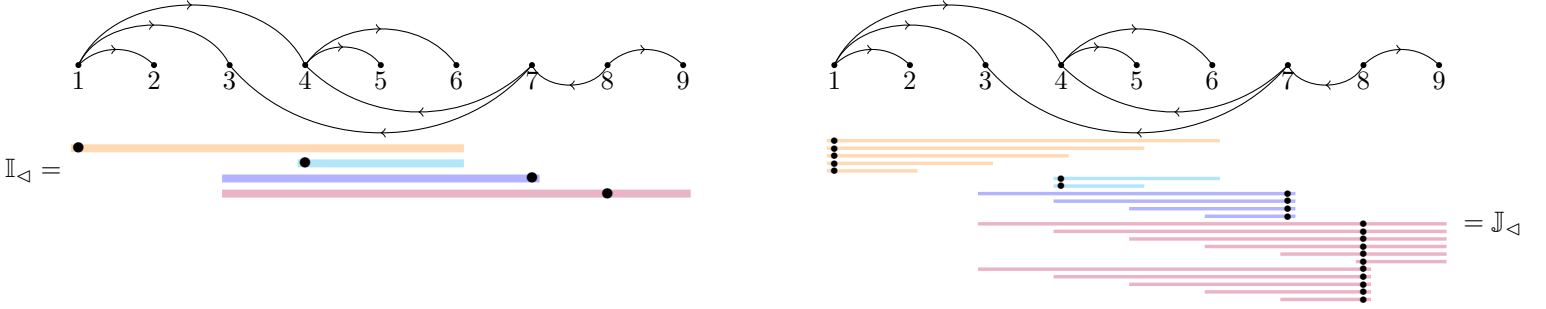


FIGURE 9. The interval hypergraphs $\mathbb{I}_{\triangleleft}$ (left) and $\mathbb{J}_{\triangleleft}$ (right) for the Tamari interval poset \triangleleft drawn on top. We did not draw the singletons they contain. The vertex corresponding to \triangleleft is $\mathbf{v}_{\triangleleft} = (2, 1, 1, 2, 1, 1, 2, 2, 1)$ in the polytope $\Delta_{\mathbb{I}_{\triangleleft}}$ and $\mathbf{v}_{\triangleleft} = (6, 1, 1, 3, 1, 1, 5, 12, 1)$ in the polytope $\Delta_{\mathbb{J}_{\triangleleft}}$. (Count the number of \bullet above each coordinate and add 1 to account for the singleton which is not drawn.) Note that $U(\triangleleft) = \{1 \triangleleft 4, 4 \triangleleft 6, 7 \triangleleft 3, 8 \triangleleft 7, 8 \triangleleft 9\}$.

- (ii) The interval hypergraph $\mathbb{I}_{\triangleleft} := \{a^{\triangleleft} \mid a \in [n]\}$ is a minimal element of $\mathcal{I}_{\triangleleft}$. Moreover, it is the unique minimal element of $\mathcal{I}_{\triangleleft}$ if and only if there are no $1 \leq a < b < c \leq n$ such that $a \triangleleft b \triangleleft c$, or $a \triangleright b \triangleright c$, or $a \triangleright b \triangleleft c$ in $U(\triangleleft)$.
- (iii) The interval hypergraph $\mathbb{J}_{\triangleleft} := \bigcup_{a \in [n]} \{I \mid a \in I \subseteq a^{\triangleleft}\}$ is the unique maximal element of $\mathcal{I}_{\triangleleft}$.

Example 4.23. The interval hypergraphs $\mathbb{I}_{\triangleleft}$ and $\mathbb{J}_{\triangleleft}$ are illustrated in Figure 9 for the Tamari interval poset drawn in Figure 8. Note that $\mathbb{I}_{\triangleleft}$ is not the unique minimal element of $\mathcal{I}_{\triangleleft}$ since we have $1 \triangleleft 4 \triangleleft 6$ in $U(\triangleleft)$. Another minimal element of $\mathcal{I}_{\triangleleft}$ is obtained by replacing $[1, 6]$ by $[1, 4]$.

Example 4.24. Proposition 4.22 is illustrated in Figure 10 with the Tamari interval poset \triangleleft given by the transitive closure of the tree WW . The set $\mathcal{I}_{\triangleleft}$ contains a unique maximal element $\mathbb{J}_{\triangleleft} = \bullet\bullet\bullet$ but three minimal elements $\mathbb{I}_{\triangleleft} = \bullet\bullet\bullet$, and also $\bullet\bullet\bullet$, and $\bullet\bullet\bullet$.

Proof of Proposition 4.22. Recall that $\mathbb{I} \in \mathcal{I}_{\triangleleft}$ if and only if $\mathbb{C}_{\triangleleft} := \{\mathbf{x} \in \mathbb{R} \mid x_i \geq x_j \text{ if } i \triangleleft j\}$ is a maximal cone in the normal fan $\Delta_{\mathbb{I}}$. Observe that for any polytopes $\mathbb{P}, \mathbb{Q}, \mathbb{R}$, if \mathbb{C} is a cone in the normal fan of \mathbb{P} and a cone in the normal fan of $\mathbb{P} + \mathbb{Q} + \mathbb{R}$, then \mathbb{C} is a cone in the normal fan of $\mathbb{P} + \mathbb{Q}$. Hence for interval hypergraphs $\mathbb{I} \subseteq \mathbb{J} \subseteq \mathbb{K}$, if $\mathbb{I}, \mathbb{K} \in \mathcal{I}_{\triangleleft}$, then $\mathbb{C}_{\triangleleft}$ is a cone in the normal fan of $\Delta_{\mathbb{I}}$ and of $\Delta_{\mathbb{K}} = \Delta_{\mathbb{I}} + \sum_{J \in \mathbb{J} \setminus \mathbb{I}} \Delta_J + \sum_{K \in \mathbb{K} \setminus \mathbb{J}} \Delta_K$, thus also in the normal fan of $\Delta_{\mathbb{J}} = \Delta_{\mathbb{I}} + \sum_{J \in \mathbb{J} \setminus \mathbb{I}} \Delta_J$, implying that $\mathbb{J} \in \mathcal{I}_{\triangleleft}$. This shows that $\mathcal{I}_{\triangleleft}$ is order convex inside \mathcal{I} .

Note that both $\mathbb{I}_{\triangleleft}$ and $\mathbb{J}_{\triangleleft}$ belong to $\mathcal{I}_{\triangleleft}$ as they clearly satisfy the conditions (i) and (ii) of Theorem 4.18. Moreover, $\mathbb{I}_{\triangleleft}$ is an inclusion minimal interval hypergraph satisfying (ii) (because for any $a \in [n]$, the interval a^{\triangleleft} is the only interval of $\mathbb{I}_{\triangleleft}$ containing a and contained in a^{\triangleleft}), while $\mathbb{J}_{\triangleleft}$ is the unique inclusion maximal interval hypergraph satisfying (i) (since $\mathbb{J}_{\triangleleft}$ contains all intervals I for which there exists $a \in [n]$ with $a \in I \subseteq a^{\triangleleft}$). Hence, we just have to discuss when $\mathbb{I}_{\triangleleft}$ is the unique inclusion minimal element of $\mathcal{I}_{\triangleleft}$.

Assume first that there are no $1 \leq a < b < c \leq n$ such that $a \triangleleft b \triangleleft c$, or $a \triangleright b \triangleright c$, or $a \triangleright b \triangleleft c$ in $U(\triangleleft)$. As \triangleleft is a Tamari interval poset, any path of cover relations from a to $\min(a^{\triangleleft})$ (resp. $\max(a^{\triangleleft})$) is actually a path in $U(\triangleleft)$. The forbidden patterns thus force a^{\triangleleft} to be either trivial or to be an interval defined by a unique arc in $U(\triangleleft)$. That is, for any $a \in [n]$, either $a^{\triangleleft} = \{a\}$, or $a^{\triangleleft} = [a, b]$ with $a \triangleleft b$, or $a^{\triangleleft} = [b, a]$ with $a \triangleleft b$. We thus obtain that any interval hypergraph satisfying (ii) must contain the interval a^{\triangleleft} . We conclude that $\mathbb{I}_{\triangleleft}$ is the unique inclusion minimal element of $\mathcal{I}_{\triangleleft}$.

Conversely, assume that there are $1 \leq a < b < c \leq n$ such that $a \triangleleft b \triangleleft c$ in $U(\triangleleft)$. Consider $\mathbb{I} := \mathbb{I}_{\triangleleft} \setminus \{a^{\triangleleft}\} \cup \{\{\min(a^{\triangleleft}), b\}\}$. It is immediate that \mathbb{I} still satisfies the conditions (i) and (ii) of Theorem 4.18. As $\mathbb{I}_{\triangleleft} \not\subseteq \mathbb{I}$, we get that $\mathcal{I}_{\triangleleft}$ does not admit a unique inclusion minimal element. The proof is identical if $a \triangleright b \triangleright c$ (resp. $a \triangleright b \triangleleft c$) are both in $U(\triangleleft)$, considering the interval hypergraph $\mathbb{I}_{\triangleleft} \setminus \{c^{\triangleleft}\} \cup \{\{b, \max(c^{\triangleleft})\}\}$ (resp. $\mathbb{I}_{\triangleleft} \setminus \{b^{\triangleleft}\} \cup \{\{\min(b^{\triangleleft}), b\}, [b, \max(b^{\triangleleft})]\}$). \square

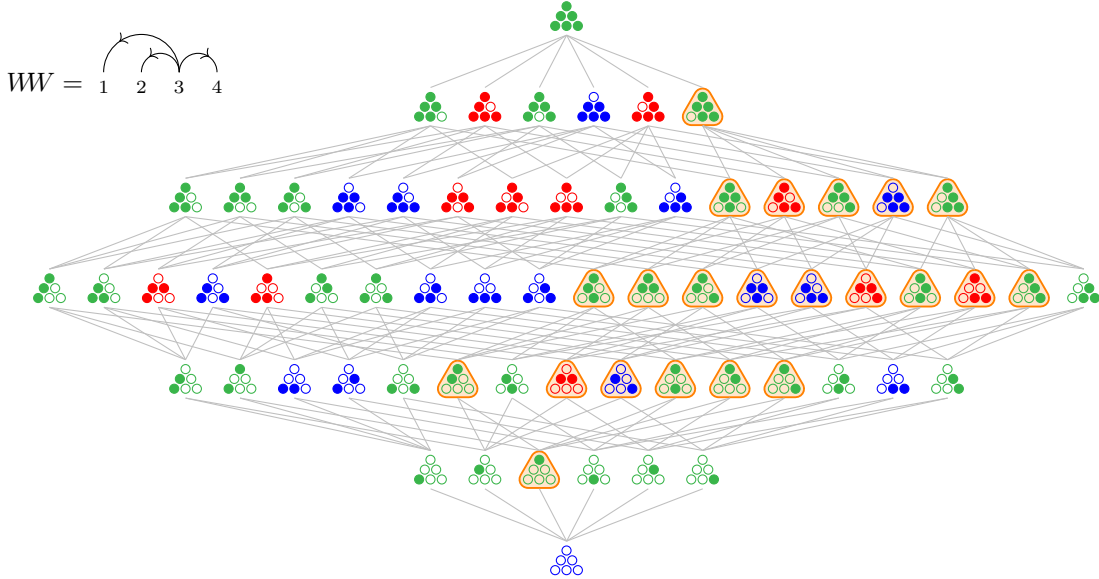


FIGURE 10. The boolean lattice \mathcal{I} of interval hypergraphs on 4 nodes (see Figure 5 for the encoding and color conventions: **red** yield non-simple interval hypergraphic polytopes; **blue** and **green** yield simple ones; **green** yield nestohedra), we have encircled (in **orange**) the interval hypergraphs containing a given tree WW as a vertex poset.

Remark 4.25. It immediately follows from Proposition 4.17 that

- the vertex of $\Delta_{\mathbb{I}_{\triangleleft}}$ corresponding to \triangleleft is the characteristic vector of the nodes of \triangleleft with at least one outgoing neighbor (*i.e.* of the non-maximal elements of \triangleleft), translated by $(1, \dots, 1)$ to account for singletons, and
- the coordinates of the vertex of $\Delta_{\mathbb{J}_{\triangleleft}}$ corresponding to \triangleleft are given by Loday's product formula

$$\left((a - \min(a^{\triangleleft}) + 1)(\max(a^{\triangleleft}) - a + 1) \right)_{a \in [n]}.$$

See Figure 9. Note that these formulas hold since $\mathbb{I}_{\triangleleft}$ and $\mathbb{J}_{\triangleleft}$ contain all singletons (in contrast to the vertex coordinates presented in Figure 8 and Examples 4.20 and 4.21).

Remark 4.26. The number of Tamari interval posets \triangleleft on $[n]$ for which there are no $1 \leq a < b < c \leq n$ such that $a \triangleleft b \triangleleft c$, or $a \triangleright b \triangleright c$, or $a \triangleright b \triangleleft c$ in $U(\triangleleft)$ as described in Proposition 4.22 (ii) are reported in Table 5.

5. WEEPING WILLOWS AND VERTICES OF SIMPLE INTERVAL HYPERGRAPHIC POLYTOPES

In this section, we consider the vertex trees of the simple interval hypergraphic polytopes. These trees are certain relevant non-crossing trees, closely connected to Tamari interval posets.

5.1. Weeping willows. We now focus on the following trees, whose name will be explained by Remark 5.4. A typical example is illustrated in Figure 11, and four interesting families will be presented in Section 5.2.

Definition 5.1. A *weeping willow* is a directed tree WW on $[n]$ such that for all $1 \leq a < b < c \leq n$, if WW contains the arc (a, c) (resp. (c, a)), then it contains a directed path from a to b (resp. from c to b). Moreover, WW is *rooted* if it has a unique source $a \in [n]$ (*i.e.* if there is a directed path from a to any node in $[n]$).

Definition 5.2. We call *crown arcs* of a weeping willow WW the arcs of WW which are maximal for the order given by $(i, j) \preceq (k, \ell)$ for $\min(k, \ell) \leq \min(i, j)$ and $\max(i, j) \leq \max(k, \ell)$.

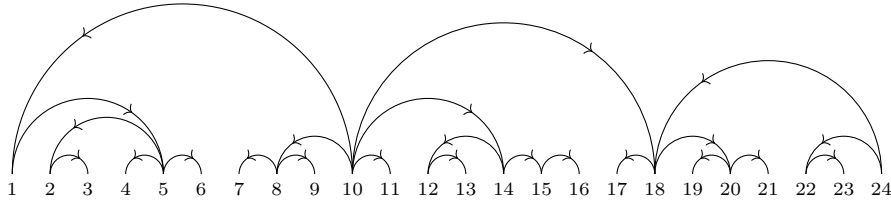


FIGURE 11. A typical weeping willow. The crown arcs are $(10, 1)$, $(10, 18)$ and $(24, 18)$. In contrast, $U(\triangleleft)$ contains all cover relations except $5 \triangleleft 4$, $10 \triangleleft 8$, $10 \triangleleft 11$, $10 \triangleleft 14$ and $24 \triangleleft 22$.

In our figures, the crown arcs are the topmost arcs. In particular, every crown arc is a cover relation in $U(\triangleleft)$ (where \triangleleft is the transitive closure of the weeping willow), but the reverse is false, see Figure 11. We now explore a few basic properties of weeping willows.

Lemma 5.3. *For any arc (i, j) of a weeping willow WW , the subtree of WW induced by $[\min(i, j), \max(i, j)]$ is rooted at i .*

Proof. Assume for instance that $i < j$ and let $k \in [i + 1, j]$. As (i, j) is an arc of the weeping willow WW , we obtain that there is a directed path from i to k . This implies that k is not a source, so that i is the only source of WW . \square

Remark 5.4. Lemma 5.3 justifies our choice of name for “weeping willows”. Namely, except their crown arcs which can be directed in both directions, all their other arcs are weeping away from the crown arcs and towards the leaves.

Proposition 5.5. *The weeping willows are precisely the Hasse diagrams of the Tamari interval posets which are trees.*

Proof. Consider a weeping willow WW , and let \triangleleft be its transitive closure. As WW is a tree, it is the Hasse diagram of \triangleleft , so we just need to show that \triangleleft is a Tamari interval poset. Consider any $1 \leq a < b < c \leq n$ such that $a \triangleleft c$. As \triangleleft is the transitive closure of WW , there are $a = x_0, \dots, x_k = c$ such that $(x_{i-1}, x_i) \in WW$ for each $i \in [k]$. Since $x_0 = a < b < c = x_k$, there exists $i \in [k]$ such that $x_{i-1} \leq b \leq x_i$. As WW is a weeping willow, it contains a directed path from x_{i-1} to b , hence also in a directed path from a to b , implying that $a \triangleleft b$. Similarly, if $1 \leq a < b < c \leq n$ such that $a \triangleright c$, then $b \triangleright c$. Thus, \triangleleft is a Tamari interval poset, whose Hasse diagram is WW .

Conversely, consider a Tamari interval poset \triangleleft whose Hasse diagram is a directed tree WW . Consider $1 \leq a < b < c < d \leq n$. For any $1 \leq a < b < c \leq n$, if $(a, c) \in WW$ then $a \triangleleft c$ implies $a \triangleleft b$, hence there is a path from a to b . Similarly, if $(c, a) \in WW$, there is a path from c to b . Hence, WW is weeping. \square

Proposition 5.6. *Any weeping willow WW is non-crossing, i.e. for all $1 \leq a < b < c < d \leq n$, the pairs $\{a, c\}$ and $\{b, d\}$ cannot both be undirected arcs of WW .*

Proof. Assume that there are $1 \leq a < b < c < d \leq n$ such that both $\{a, c\}$ and $\{b, d\}$ are undirected arcs of WW . As WW is a tree, it is the Hasse diagram of its transitive closure \triangleleft . We distinguish three cases, depending on the orientation of $\{a, c\}$ and $\{b, d\}$:

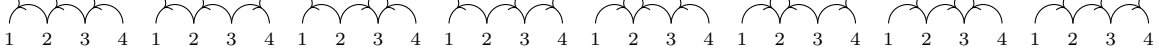
- (i) If $(a, c), (b, d) \in WW$, then $a \triangleleft b \triangleleft c$ since WW is weeping, contradicting that $(a, c) \in WW$. The situation where $(c, a), (d, b) \in WW$ is symmetric.
- (ii) If $(c, a), (b, d) \in WW$, then $c \triangleleft b$ and $b \triangleleft c$, contradicting the antisymmetry of \triangleleft .
- (iii) If $(a, c), (d, b) \in WW$, then $a \triangleleft b$ and $d \triangleleft c$. If $b \triangleleft c$ (resp. $a \triangleleft d$), then $a \triangleleft b \triangleleft c$ (resp. $a \triangleleft d \triangleleft c$) contradicts that $(a, c) \in WW$. By symmetry, we obtain that both pairs $\{a, d\}$ and $\{b, c\}$ are incomparable in \triangleleft . As $a \triangleleft b$, $a \triangleleft c$, $d \triangleleft b$ and $d \triangleleft c$, and $\{a, d\}$ and $\{b, c\}$ are incomparable in \triangleleft , we conclude that WW is not a tree by Lemma 3.5(ii). \square

Remark 5.7. Proposition 5.5 implies that we can represent weeping willows as non-crossing trees using our drawing convention of Remark 4.3 for Tamari interval posets. Proposition 5.6 implies

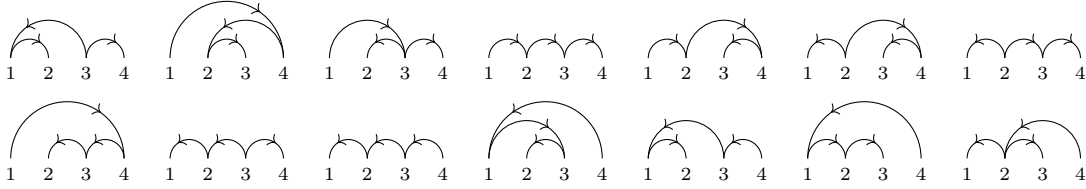
that we can actually also represent weeping willows as non-crossing trees with all increasing and decreasing arcs drawn above the horizontal line. For the sake of compactness, we will prefer the later drawing convention of weeping willows.

5.2. Four families of weeping willows. We now describe four interesting families of weeping willows, which we illustrate when $n = 4$.

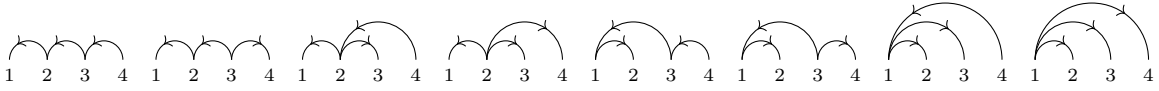
Example 5.8. Any orientation of the path graph $\{\{i, i + 1\} \mid i \in [n - 1]\}$ is a weeping willow. Only n of them are rooted. See also Example 5.19.



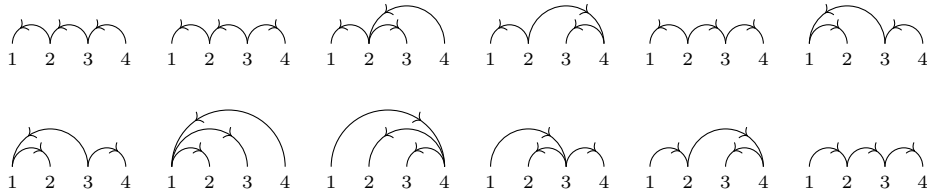
Example 5.9. Any rooted binary tree, with arcs oriented away from its root, and with nodes labeled in inorder (meaning that for each node, we first label its left subtree, then the node, then its right subtree) is a rooted weeping willow. See also Example 5.20.



Example 5.10. We inductively define the *Pitman–Stanley trees* of size n as all trees obtained by adding an arbitrarily oriented arc between n and the root of a Pitman–Stanley tree of size $n - 1$. By construction, Pitman–Stanley trees are rooted weeping willows. Moreover, there are 2^{n-1} Pitman–Stanley trees of size n , and there is a natural bijection sending a Pitman–Stanley tree to the subset of integers $i \in [n - 1]$ such that $i + 1$ has an incoming neighbor in $[i]$. See also Example 5.21.



Example 5.11. Let us denote PS_n^- the Pitman–Stanley trees of size n for which the arc incident to n is oriented away from n . Clearly $|\text{PS}_n^-| = 2^{n-2}$. The *frehedron trees* are all trees we get by taking the concatenation of W_i, \overline{W}_j where $W_i \in \text{PS}_i^-, W_j \in \text{PS}_j^-, i + j = n + 1$ and \overline{W}_j is W_j reflected. Their total number is $2^{n-2} + \sum_{i=2}^{n-1} 2^{i-2} 2^{n-i-1} + 2^{n-2} = (n + 2)2^{n-3}$ [OEI10, A045623]. They are rooted weeping willows. See also Example 5.22.



5.3. Counting weeping willows. We now exploit Proposition 5.6 to count (rooted) weeping willows. See also Table 5.

Proposition 5.12. *Let*

$$f = 1 + x + 3x^2 + 12x^3 + 55x^4 + 273x^5 + 1428x^6 + 7752x^7 + 43263x^8 + 246675x^9 + \dots$$

$$g = 1 + 2x + 8x^2 + 38x^3 + 196x^4 + 1062x^5 + 5948x^6 + 34120x^7 + 199316x^8 + 1181126x^9 + \dots$$

$$h = 1 + 2x + 7x^2 + 30x^3 + 143x^4 + 728x^5 + 3876x^6 + 21318x^7 + 120175x^8 + 690690x^9 + \dots$$

denote the ordinary generating functions of unoriented non-crossing trees [OEI10, A001764], of weeping willows [OEI10, A047098], and of rooted weeping willows [OEI10, A006013] respectively, where x counts the number of arcs. Then

$$f = 1 + xf^3, \quad g = 1 + 2xgf^2, \quad \text{and} \quad h = 1 + xf^2(h + f).$$

Hence, f , g , and h are solutions of

$$xf^3 - f + 1 = 0, \quad (8x - 1)g^3 - g^2 + g + 1 = 0, \quad \text{and} \quad x^2h^3 - 2xh^2 + h - 1 = 0,$$

and, on n nodes, there are $\frac{1}{2n+1}\binom{3n}{n}$ non-crossing trees, $2\binom{3n}{n} - \sum_{k=0}^n \binom{3n}{k}$ weeping willows, and $\frac{1}{n+1}\binom{3n+1}{n}$ rooted weeping willows.

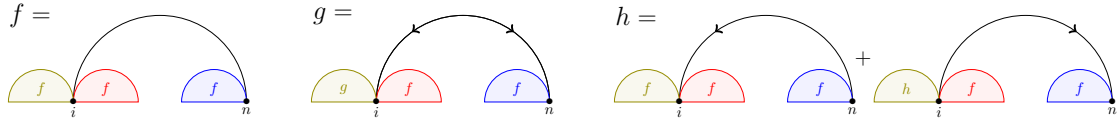


FIGURE 12. Illustration for the proof of Proposition 5.12.

Proof. We refer the reader to Figure 12 for an illustration of the following decompositions. The longest arc $\{i, n\}$ incident to node n in a non-crossing tree decomposes it into three non-crossing trees (one on the left of i , one on the right of i , and one on the left of n), which yields the formula $f = 1 + xf^3$. The longest arc $\{i, n\}$ incident to node n in a weeping willow is oriented arbitrarily and decomposes it into a weeping willow (left of i) and two non-crossing trees by Lemma 5.3 (one on the right of i , and one on the left of n), which yields $g = 1 + 2xgf^2$. The longest arc $\{i, n\}$ incident to node n in a rooted weeping willow with root n (resp. distinct from n) decomposes it into three non-crossing trees by Lemma 5.3 (resp. into a rooted weeping willow and two non-crossing trees), which yields $h = 1 + xf^2(h + f)$. Observing that $xf^2 = 1 - 1/f$, we obtain that $g = 1/(1 - 2xf^2) = f/(2 - f)$ and $h = f/(1 - xf^2) = f^2$. The functional equations can be verified by straightforward computations, and the explicit numbers can be recovered by Lagrange inversion (or extracted from their respective OEIS pages). \square

Remark 5.13. It follows from Section 4.3 and Proposition 5.12 that asymptotically, most Tamari interval posets are not weeping willows.

It is also interesting to refine the enumeration of weeping willows with respect to increasing and decreasing arcs. The proof is similar and left to the reader.

Proposition 5.14. *Let*

$$f = 1 + x + 2x^2 + xy + 5x^3 + 5x^2y + 2xy^2 + 14x^4 + 21x^3y + 15x^2y^2 + 5xy^3 + \dots$$

$$g = 1 + x + y + 2x^2 + 4xy + 2y^2 + 5x^3 + 14x^2y + 14xy^2 + 5y^3 + 14x^4 + 49x^3y + 70x^2y^2 + 49xy^3 + 14y^4 + \dots$$

$$h = 1 + x + y + 2x^2 + 4xy + y^2 + 5x^3 + 14x^2y + 9xy^2 + 2y^3 + 14x^4 + 49x^3y + 50x^2y^2 + 25xy^3 + 5y^4 + \dots$$

denote the ordinary generating functions of non-crossing trees oriented towards n , of weeping willows, and of rooted weeping willows respectively, where x and y count the number of increasing and decreasing arcs respectively. Then

$$f = 1 + xf^2\bar{f}, \quad g = 1 + (x + y)gf\bar{f}, \quad \text{and} \quad h = 1 + f\bar{f}(xh + yf),$$

where $\bar{f}(x, y) = f(y, x)$.

Proof. Similar to the proof of Proposition 5.12. \square

5.4. Weeping willows and simple interval hypergraphic polytopes. We now specialize Section 4.4 to prove Proposition C.

Proposition 5.15. *The following are equivalent for a polytope \mathbb{P} :*

- (i) \mathbb{P} is a simple interval hypergraphic polytope,
- (ii) \mathbb{P} is a deformed permutahedron whose vertex digraphs are forests of weeping willows.
- (iii) \mathbb{P} is a simple deformed associahedron.

Proof. Immediate from Propositions 4.15 and 5.5. \square

Proposition 5.16. *Any weeping willow is a vertex tree of some simple interval hypergraphic polytope.*

Proof. It immediately follows from Propositions 4.16 and 5.5 that any weeping willow is the vertex tree of a simple vertex in some interval hypergraphic polytope. However, we have to work slightly more to prove that any weeping willow appears as a vertex tree in some *simple* interval hypergraphic polytope.

Consider a weeping willow WW , its transitive closure \triangleleft , and the interval hypergraph $\mathbb{I}_{\triangleleft} := \{a^{\triangleleft} \mid a \in [n]\}$ defined in Proposition 4.22 (ii). We just need to prove that $\Delta_{\mathbb{I}_{\triangleleft}}$ is simple, or equivalently, that $\mathbb{I}_{\triangleleft}$ satisfies the conditions of Theorem B:

- (i) If there are $i, j, k, \ell \in [n]$ such that $\ell \in i^{\triangleleft} \cap j^{\triangleleft}$ and $i^{\triangleleft} \cup j^{\triangleleft} \subseteq k^{\triangleleft}$, then we have $k \triangleleft i, j \triangleleft \ell$. As WW is a tree, we obtain by Lemma 3.5 (i) that i and j are comparable in \triangleleft . Hence, we get that i^{\triangleleft} and j^{\triangleleft} are nested, so that $i^{\triangleleft} \cup j^{\triangleleft} \in \{i^{\triangleleft}, j^{\triangleleft}\} \subseteq \mathcal{I}_{\triangleleft}$.
- (ii) If there are $i, j, k, \ell \in [n]$ such that $k, \ell \in i^{\triangleleft} \cap j^{\triangleleft}$, then we have $i, j \triangleleft k, \ell$. As WW is a tree, we obtain by Lemma 3.5 (ii) that either i and j , or k and ℓ are comparable in \triangleleft . If i and j are comparable, then i^{\triangleleft} and j^{\triangleleft} are nested, so that $i^{\triangleleft} \cup j^{\triangleleft} \in \{i^{\triangleleft}, j^{\triangleleft}\} \subseteq \mathcal{I}_{\triangleleft}$. Otherwise, we obtain that $i^{\triangleleft} \cap j^{\triangleleft}$ is a chain in \triangleleft , and we can assume that k is its minimal element. Note that $i \notin k^{\triangleleft}$ and $j \notin k^{\triangleleft}$ by antisymmetry of \triangleleft . Hence, we obtained that $i^{\triangleleft} \cap j^{\triangleleft} \subseteq k^{\triangleleft}$ and $i^{\triangleleft} \not\subseteq k^{\triangleleft}$ and $j^{\triangleleft} \not\subseteq k^{\triangleleft}$. \square

We can now prove a weaker version of Conjecture 2.21, in the case of *interval* hypergraphic polytopes.

Proposition 5.17. *A deformed permutahedron has the normal fan of an interval nestohedron if and only if all its vertex digraphs are forests of rooted weeping willows.*

Proof. By Proposition 2.20, vertex digraphs of nestohedra are \mathbb{B} -forests, notably rooted forests. Thus, the vertex digraphs of interval nestohedra are forests of rooted weeping willows.

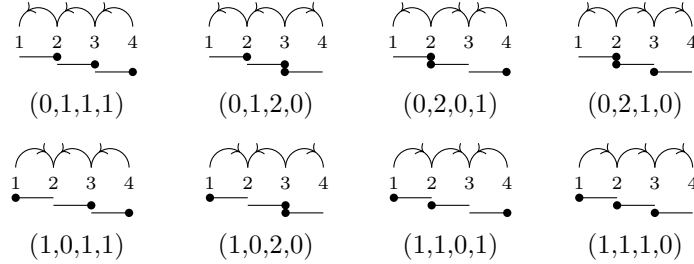
We now prove the converse. Fix a deformed permutahedron \mathbb{P} whose vertex digraphs are forests of rooted weeping willows. Thus, by Propositions 4.15 and 5.5, there exists an interval hypergraph \mathbb{I} such that \mathbb{P} is normally equivalent to $\Delta_{\mathbb{I}}$. Moreover, since weeping willows are trees, the polytope $\Delta_{\mathbb{I}}$ is simple, so \mathbb{I} satisfies the conditions of Theorem B. Consider $I, J \in \mathbb{I}$ with $I \cap J \neq \emptyset$. Without loss of generality, we assume that $i := \min I < \max J =: j$. Construct the permutation $\sigma := ijX$ where X is the word formed by $[n] \setminus \{i, j\}$ written in an arbitrary order, and let WW be the associated forest of weeping willows (*i.e.* the vertex digraph of the vertex of $\Delta_{\mathbb{I}}$ whose normal cone contains \mathbb{C}_{σ}). Then, i is a source of WW (because i is the first letter of σ). Since WW is a vertex digraph of $\Delta_{\mathbb{I}}$, it is rooted, and node i is necessarily its root. Moreover, as $I \cap J \neq \emptyset$, the node j is in the same rooted tree of the forest WW as i is. Hence, j is not a source of WW , and j precedes every $[n] \setminus \{i, j\}$ in σ . Thus, the couple (i, j) must be an arc of WW . It follows that there exists $K \in \mathbb{I}$ with $\{i, j\} \subseteq K$, implying $[i, j] = (I \cup J) \subseteq K$. By Theorem B (i), we get $I \cup J \in \mathbb{I}$. Therefore, \mathbb{I} is a building set, and \mathbb{P} is normally equivalent to the interval nestohedron $\Delta_{\mathbb{I}}$. \square

Proposition 5.18. *Any rooted weeping willow is a vertex tree of some interval nestohedron.*

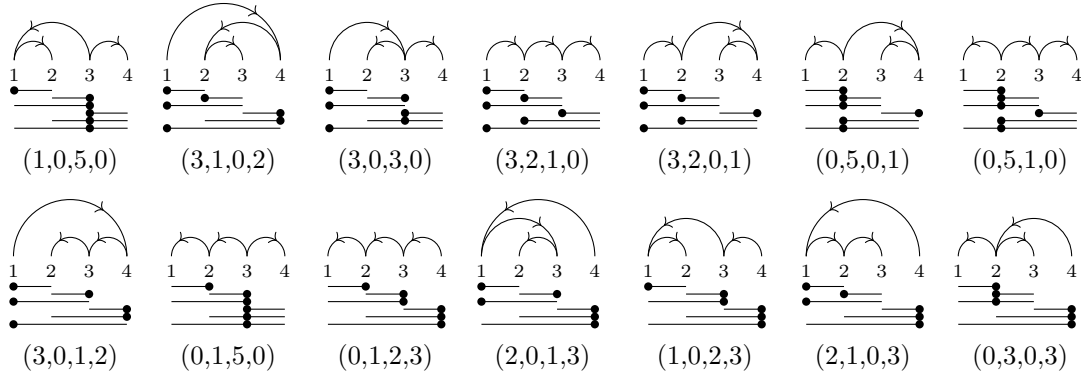
Proof. Consider a rooted weeping willow WW , its transitive closure \triangleleft , and the interval hypergraph $\mathbb{I}_{\triangleleft} := \{a^{\triangleleft} \mid a \in [n]\}$ defined in the proof of Proposition 4.22 (ii). As WW is rooted, for any $a, b \in [n]$, the sets a^{\triangleleft} and b^{\triangleleft} are nested (resp. disjoint) if the unique path between a and b in WW is directed (resp. not directed). Hence, $\mathbb{I}_{\triangleleft}$ is an interval building set and WW is indeed a vertex tree of the interval nestohedron $\Delta_{\mathbb{I}_{\triangleleft}}$. \square

5.5. A finer description. Specializing Theorem 4.18, we know which weeping willow appear in which simple interval hypergraphic polytope. This yields the following examples (in each example, by convention, our interval hypergraphs contain no singleton).

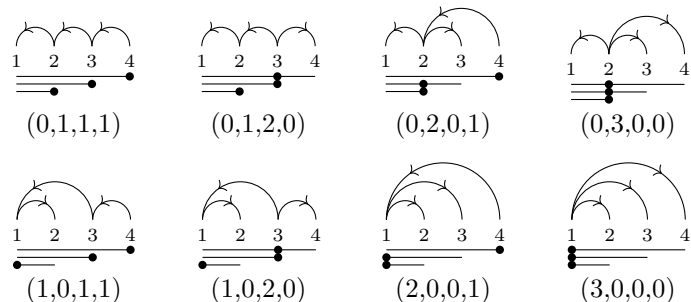
Example 5.19. For $\mathbb{I} = \{[i, i + 1] \mid 1 \leq i < n\}$, the hypergraphic polytope $\Delta_{\mathbb{I}}$ is the cube (graphical zonotope of the path-graph), and its weeping willows (*i.e.* vertex trees) are all orientations of the path graph considered in Example 5.8. The coordinate of the vertex associated to a given weeping willow is its out-degree vector.



Example 5.20. For $\mathbb{I} = \{[i, j] \mid 1 \leq i < j \leq n\}$, the hypergraphic polytope $\Delta_{\mathbb{I}}$ is the associahedron [SS93, Lod04], and its vertex trees are the rooted binary trees oriented and labeled as in Example 5.9. The coordinates of the vertex associated to each rooted binary tree is the product of the number of left leaves times the number of right leaves, see [Lod04, Section 1] or Remark 4.25.

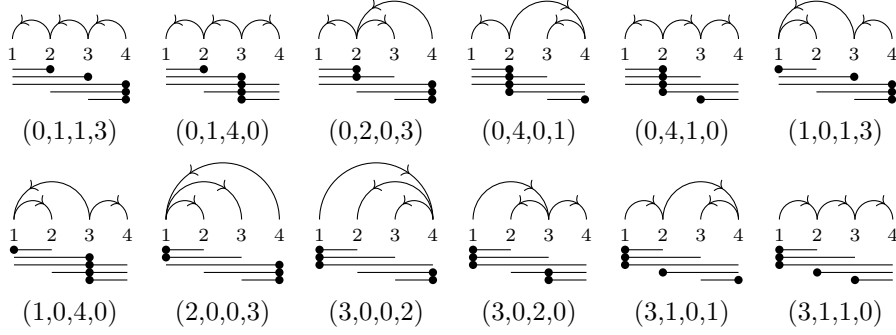


Example 5.21. For $\mathbb{I} = \{[1, i] \mid 1 < i \leq n\}$, the hypergraphic polytope $\Delta_{\mathbb{I}}$ is the Pitman–Stanley polytope [SP02], and its vertex trees are the Pitman–Stanley trees of Example 5.10. The vertex \mathbf{v}_{WW} of $\Delta_{\mathbb{I}}$ corresponding to a Pitman–Stanley tree WW is the out-degree sequence of WW . Through the bijection discussed in Example 5.10, the vertex $\mathbf{v}_{\mathbf{a}} = (v_1, \dots, v_n)$ of $\Delta_{\mathbb{I}}$ corresponding to a binary sequence $\mathbf{a} := (a_1, a_2, \dots, a_{n-1}) \in \{0, 1\}^n$ is given by $v_i = k + \ell$ where k (resp. ℓ) is maximal such that $a_{i-k} = \dots = a_{i-1} = 0$ (resp. $a_i = \dots = a_{i+\ell-1} = 1$).



Example 5.22. For $\mathbb{I} = \{[1, i], [n] \setminus [i] \mid 1 \leq i \leq n\}$, the hypergraphic polytope $\Delta_{\mathbb{I}}$ is the freehedron [San09], and its vertex trees are the freehedron trees of Example 5.11. The vertex of $\Delta_{\mathbb{I}}$, namely $\mathbf{v}_{WW} = (v_1, \dots, v_n)$, corresponding to a freehedron tree WW is given by

$$v_i = \begin{cases} \text{out-degree}(i) & \text{if } i \text{ is not the root,} \\ n+1 & \text{if } i \text{ is the root and } 1 < i < n, \\ n & \text{if } i \text{ is the root and } i \in \{1, n\}. \end{cases}$$



Moreover, we exploit Theorem 4.18 to give an analogue of Proposition 4.22 for simple interval hypergraphic polytopes. See Figure 10. Recall from Theorem 4.18 that, for a Tamari interval poset \triangleleft , we defined the interval hypergraphs $\mathbb{I}_{\triangleleft} := \{a^{\triangleleft} \mid a \in [n]\}$ and $\mathbb{J}_{\triangleleft} := \bigcup_{a \in [n]} \{I \mid a \in I \subseteq a^{\triangleleft}\}$. See Figure 9 for illustrations of $\mathbb{I}_{\triangleleft}$ and $\mathbb{J}_{\triangleleft}$. Recall that we call *crown arcs* of WW the arcs of WW which are maximal for the order given by $(a, b) \preceq (c, d)$ for $\min(c, d) \leq \min(a, b)$ and $\max(a, b) \leq \max(c, d)$.

Proposition 5.23. *We denote by \mathcal{S} the inclusion poset of interval hypergraphs \mathbb{I} on $[n]$ such that $\Delta_{\mathbb{I}}$ is simple. For a given weeping willow WW with transitive closure \triangleleft , denote by $\mathcal{S}_{\triangleleft} := \mathcal{I}_{\triangleleft} \cap \mathcal{S}$ the subposet of \mathcal{S} induced by interval hypergraphs \mathbb{I} on $[n]$ such that WW is a vertex tree of $\Delta_{\mathbb{I}}$. Then*

- (i) $\mathcal{S}_{\triangleleft}$ is order convex in \mathcal{S} .
- (ii) The interval hypergraph $\mathbb{I}_{\triangleleft}$ is a minimal element of $\mathcal{S}_{\triangleleft}$. Moreover, it is the unique minimal element of $\mathcal{S}_{\triangleleft}$ if and only if there are no $1 \leq a < b < c \leq n$ such that $a \triangleleft b \triangleleft c$, or $a \triangleright b \triangleright c$, or $a \triangleright b \triangleleft c$, where at least one of the two cover relations is a crown arc of WW .
- (iii) The interval hypergraph $\mathbb{J}_{\triangleleft}$ is the unique maximal element of $\mathcal{S}_{\triangleleft}$.

Example 5.24. Proposition 5.23 is illustrated in Figure 10. Recall that the set \mathcal{S} appears in blue and green and is not order convex inside the boolean lattice \mathcal{I} . The set $\mathcal{S}_{\triangleleft}$ contains a unique maximal element $\mathbb{J}_{\triangleleft} = \text{green}$ but three minimal elements $\mathbb{I}_{\triangleleft} = \text{green}$, and also blue and blue . The latter is not a minimal element of $\mathcal{I}_{\triangleleft}$.

Proof of Proposition 5.23. The order convexity of $\mathcal{S}_{\triangleleft}$ is argued as in the proof of Proposition 4.22.

We know that $\mathbb{I}_{\triangleleft} \in \mathcal{S}_{\triangleleft}$ from the proof of Proposition 5.16. With a very similar approach, we now prove that $\mathbb{J}_{\triangleleft}$ satisfies the conditions of Theorem B. Consider $I, J \in \mathbb{J}_{\triangleleft}$ such that $I \cap J \neq \emptyset$, and let $i, j \in [n]$ be such that $i \in I \subseteq i^{\triangleleft}$ and $j \in J \subseteq j^{\triangleleft}$. Then

- (i) Assume that $I \cap J \neq \emptyset$ and there is $K \in \mathbb{J}_{\triangleleft}$ with $I \cup J \subseteq K$. Let $\ell \in I \cap J$ and $k \in [n]$ be such that $k \in K \subseteq k^{\triangleleft}$. Then we have $k \triangleleft i, j \triangleleft \ell$. As WW is a tree, we obtain by Lemma 3.5(i) that i and j are comparable in \triangleleft , say for instance that $i \triangleleft j$. Then $j^{\triangleleft} \subseteq i^{\triangleleft}$, so that $i \in I \cup J \subseteq i^{\triangleleft}$, which implies that $I \cup J \in \mathbb{J}_{\triangleleft}$ by construction of $\mathbb{J}_{\triangleleft}$.
- (ii) Assume that $|I \cap J| \geq 2$. If i and j are comparable, then i^{\triangleleft} and j^{\triangleleft} are nested, and we conclude as above that $I \cup J \in \mathbb{J}_{\triangleleft}$. Otherwise, consider $k, \ell \in I \cap J$. As $I \cap J \subseteq i^{\triangleleft} \cap j^{\triangleleft}$, there are paths from both i and j to both k and ℓ . If k and ℓ are incomparable, then these four paths contradict that WW is non-crossing. Hence, $I \cap J$ is a chain in \triangleleft , with minimal element k_{\circ} . Note that $i \notin k_{\circ}^{\triangleleft}$ and $j \notin k_{\circ}^{\triangleleft}$ by antisymmetry of \triangleleft . Hence, we obtained that $K = k_{\circ}^{\triangleleft} \in \mathbb{J}_{\triangleleft}$ satisfies $I \cap J \subseteq K$ and $I \not\subseteq K$ and $J \not\subseteq K$.

As $\mathcal{S}_{\triangleleft} = \mathcal{I}_{\triangleleft} \cap \mathcal{S}$, note that $\mathbb{I}_{\triangleleft}$ (resp. $\mathbb{J}_{\triangleleft}$) is still an inclusion minimal (resp. the *unique* inclusion maximal) element of $\mathcal{S}_{\triangleleft}$ as it was already an inclusion minimal (resp. the unique inclusion maximal) element of $\mathcal{I}_{\triangleleft}$. We thus just need to discuss when is $\mathbb{I}_{\triangleleft}$ inclusion-minimally unique.

Assume first that there are no $1 \leq a < b < c \leq n$ such that $a \triangleleft b \triangleleft c$, or $a \triangleright b \triangleright c$, or $a \triangleright b \triangleleft c$, where at least one of the two cover relations is a crown arc of WW , see Figure 13. For any $a \in [n]$, consider a path π_{\min} (resp. π_{\max}) in WW from a to $\min(a^{\triangleleft})$ (resp. to $\max(a^{\triangleleft})$). If $\pi_{\min} \cup \pi_{\max}$ contains at most one arc, then any interval hypergraph containing all singletons and satisfying Theorem 4.18 (ii) must contain a^{\triangleleft} . Otherwise, either π_{\min} contains at least two consecutive arcs, or π_{\max} does, or there are two arcs of WW incoming at a . In all three cases, our assumption ensures that no arc of $\pi_{\min} \cup \pi_{\max}$ is a crown arc of WW . Hence, there is a crown arc (k, k') passing above $\pi_{\min} \cup \pi_{\max}$. In particular, there is an interval $K \in \mathbb{I}$ such that $K \supseteq [k, k'] \supseteq a^{\triangleleft}$. Besides, any interval hypergraph \mathbb{I} such that $\Delta_{\mathbb{I}}$ is simple and admits WW as a vertex tree must contain an interval containing the endpoints of each arc of $\pi_{\min} \cup \pi_{\max}$ by Theorem 4.18 (ii). Thus, by Theorem B (i), the existence of K implies that the union X of these intervals, belongs to \mathbb{I} . On the one hand, $X \supseteq [\min(a^{\triangleleft}), \max(a^{\triangleleft})] = a^{\triangleleft}$, by construction. On the other hand, all elements of X belong to intervals whose minimum according to \triangleleft is in the path $\pi_{\min} \cup \pi_{\max}$, hence all elements in X are bigger than a , *i.e.* $X \subseteq a^{\triangleleft}$. Thus, $X = a^{\triangleleft}$, yielding $a^{\triangleleft} \in \mathbb{I}$. We conclude that any such interval hypergraph \mathbb{I} must contain $\mathbb{I}_{\triangleleft}$: it is the *unique* inclusion minimal element of $\mathcal{S}_{\triangleleft}$.

Conversely, assume that there are $1 \leq a < b < c \leq n$ such that $a \triangleleft b \triangleleft c$ where $a \triangleleft b$ is a crown arc of WW . Without loss of generality, we can consider that a is a root of WW . Consider the interval hypergraph $\mathbb{I} := \mathbb{I}_{\triangleleft} \setminus \{a^{\triangleleft}\} \cup \{[\min(a^{\triangleleft}), b]\}$. We have seen at the end of the proof of Proposition 4.22 that WW is a vertex tree of $\Delta_{\mathbb{I}}$, it remains to prove that \mathbb{I} satisfies the conditions of Theorem B. First, note that a^{\triangleleft} is inclusion maximal in $\mathbb{I}_{\triangleleft}$, and $[\min(a^{\triangleleft}), b]$ is inclusion maximal in \mathbb{I} . As $[\min(a^{\triangleleft}), b] \subseteq a^{\triangleleft}$, this ensures that Theorem B (i) is satisfied for \mathbb{I} . Besides, we have that for all $H \in \mathbb{I}$ and $j \in [n]$, there exists $k \in [n]$ such that $H \cap j^{\triangleleft} = k^{\triangleleft}$. Hence, \mathbb{I} still satisfies Theorem B (ii). The proof is similar if $a \triangleleft b \triangleleft c$ and $b \triangleleft c$ is a crown arc (resp. if $a \triangleright b \triangleright c$ and $b \triangleright c$ is a crown arc, resp. if $a \triangleright b \triangleright c$ and $a \triangleright b$ is a crown arc, resp. $a \triangleright b \triangleleft c$ and one of them is a crown arc), considering the interval hypergraph $\mathbb{I} := \mathbb{I}_{\triangleleft} \setminus \{a^{\triangleleft}\} \cup \{[b, \max(a^{\triangleleft})]\}$ (resp. $\mathbb{I}_{\triangleleft} \setminus \{c^{\triangleleft}\} \cup \{[b, \max(c^{\triangleleft})]\}$, resp. $\mathbb{I}_{\triangleleft} \setminus \{c^{\triangleleft}\} \cup \{[\min(c^{\triangleleft}), b]\}$, resp. $\mathbb{I}_{\triangleleft} \setminus \{b^{\triangleleft}\} \cup \{[\min(b^{\triangleleft}), b], [b, \max(b^{\triangleleft})]\}$). \square

Remark 5.25. Let

$$f = 1 + x + 3x^2 + 12x^3 + 55x^4 + 273x^5 + 1428x^6 + 7752x^7 + 43263x^8 + 246675x^9 + \dots$$

$$k = 1 + 2x + 5x^2 + 16x^3 + 67x^4 + 316x^5 + 1599x^6 + 8480x^7 + 46512x^8 + 261668x^9 + \dots$$

denote the ordinary generating functions of unoriented non-crossing trees and of the weeping willows described in Proposition 5.23 (ii). Then

$$k = 1 + (2x + x^2)f^2,$$

and there are $\frac{2}{2n-1} \binom{3n-2}{n} + \frac{1}{2n-3} \binom{3n-5}{n-1}$ such weeping willows on $n \geq 1$ nodes. See Table 5 for the first values. The proof is left to the reader, after contemplation of Figure 13.

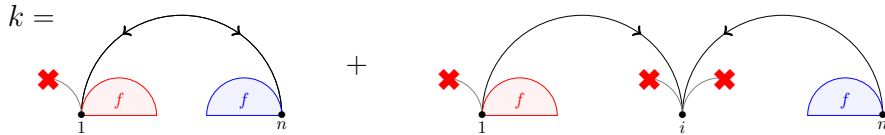


FIGURE 13. The two possible decomposition of the weeping willows described in Proposition 5.23 (ii). Red crosses \times indicate forbidden arcs.

Remark 5.26. For the transitive closure \triangleleft of a weeping willow, the condition of Proposition 5.23 (ii) clearly implies the condition of Proposition 4.22 (ii). The converse however is false. For instance, for the total order \triangleleft given by $4 \triangleleft 1 \triangleleft 2 \triangleleft 3$, the interval hypergraph $\mathbb{I}_{\triangleleft}$ is not the unique minimal element of $\mathcal{I}_{\triangleleft}$, while it is the unique minimal element of $\mathcal{S}_{\triangleleft}$.

Proposition 5.27. We denote by \mathcal{N} the inclusion poset of interval building sets on $[n]$ (i.e. interval hypergraphs \mathbb{I} containing all singletons, and such that $I, J \in \mathbb{I}$ and $I \cap J \neq \emptyset$ implies $I \cup J \in \mathbb{I}$). For a given rooted weeping willow WW with transitive closure \triangleleft , denote by $\mathcal{N}_{\triangleleft} := \mathcal{I}_{\triangleleft} \cap \mathcal{N}$ the subposet of \mathcal{N} induced by interval building sets \mathbb{I} on $[n]$ such that WW is a vertex tree of $\Delta_{\mathbb{I}}$. Then $\mathcal{N}_{\triangleleft}$ is the interval between $\mathbb{I}_{\triangleleft}$ and $\mathbb{J}_{\triangleleft}$.

Example 5.28. Proposition 5.27 is illustrated in Figure 10. Recall that the set \mathcal{N} appears in green and is not order convex inside the boolean lattice \mathcal{I} . The set $\mathcal{N}_{\triangleleft}$ is the interval of \mathcal{N} between $\mathbb{I}_{\triangleleft} = \circ \circ \circ$ and $\mathbb{J}_{\triangleleft} = \bullet \bullet \bullet$.

Proof of Proposition 5.27. The order convexity of $\mathcal{N}_{\triangleleft}$ is argued as in the proof of Proposition 4.22.

We know that $\mathbb{I}_{\triangleleft}$ is an interval building set from the proof of Proposition 5.18. Moreover, if \mathbb{I} is an interval building set satisfying Theorem 4.18 (ii), then it contains an interval containing $[\min(a, b), \max(a, b)]$ for any arc (a, b) of WW by Theorem 4.18 (ii), hence an interval containing $[\min(a, b), \max(a, b)]$ for any directed path from a to b by the building set property. It immediately follows that it contains $\mathbb{I}_{\triangleleft}$.

We now prove that $\mathbb{J}_{\triangleleft}$ is also an interval building set. Consider $I, J \in \mathbb{J}_{\triangleleft}$ such that $I \cap J \neq \emptyset$, let $i, j \in [n]$ be such that $i \in I \subseteq i^{\triangleleft}$ and $j \in J \subseteq j^{\triangleleft}$. As i^{\triangleleft} and j^{\triangleleft} intersect, they are nested (since WW is rooted), say $i^{\triangleleft} \subseteq j^{\triangleleft}$. We conclude that $j \in I \cup J \subseteq i^{\triangleleft} \cup j^{\triangleleft} = j^{\triangleleft}$, so that $I \cup J \in \mathbb{J}_{\triangleleft}$. (An alternative proof is given by Corollary 3.3.) As $\mathcal{N}_{\triangleleft} \subseteq \mathcal{I}_{\triangleleft}$ and $\mathbb{J}_{\triangleleft}$ is the unique maximal element of $\mathcal{I}_{\triangleleft}$, we conclude that $\mathbb{J}_{\triangleleft}$ is also the unique inclusion maximal element of $\mathcal{N}_{\triangleleft}$. \square

6. TAMARI INTERVAL PREPOSETS AND FACES OF INTERVAL HYPERGRAPHIC POLYTOPES

In this section, we consider the face preposets of the interval hypergraphic polytopes. They naturally generalize the Tamari interval posets of Section 4.

6.1. Tamari interval preposets. We first generalize the Tamari interval posets to preposets.

Definition 6.1. A *Tamari interval preposet* is a preposet \triangleleft on $[n]$ with the following equivalent properties:

- (i) for $1 \leq a < b < c \leq n$, one has $a \triangleleft c \implies a \triangleleft b$ and $a \triangleright c \implies b \triangleright c$,
- (ii) for any $a \in [n]$, the principal upper set $a^{\triangleleft} := \{b \in [n] \mid a \triangleleft b\}$ of a is an interval of $[n]$.

Remark 6.2. The Tamari interval posets of Definition 4.2 are precisely the Tamari interval preposets Definition 6.1 which are antisymmetric.

Remark 6.3. Note that the Tamari interval preposets could also be defined by properties similar to (i) and (ii) of Definition 4.2, but using the facial Tamari lattice and the facial weak order [DHP18]. We skip these definitions here as they are slightly technical and not needed for our purposes.

We next introduce a way to draw a Tamari interval preposet as a non-crossing diagram.

Definition 6.4. For $A = \{a_1 < \dots < a_k\} \subseteq [n]$, define $\text{tour}(A) := \{(a_1, a_2), \dots, (a_{k-1}, a_k), (a_k, a_1)\}$. For two non-crossing subsets $A, B \subseteq [n]$, define the *canonical relation* $A \frown B$ by

- $A \frown B := (\max A, \min B)$ if A lies entirely to the left of B , i.e. if $\max A < \min B$,
- $A \frown B := (a, \min B)$ if B lies inside a gap of A , i.e. if there are $a < a'$ in A such that $B \subseteq]a, a'[\subseteq [n] \setminus A$,
- otherwise, $A \frown B := (a, b)$ where $(b, a) := B \frown A$.

The *canonical arc* of (A, B) is the oriented arc $a \rightarrow b$ where $(a, b) := A \frown B$.

Remark 6.5. We then represent a Tamari interval preposet \triangleleft by the union of the tours of its nodes and the canonical arcs of its cover relations, drawn above or below the horizontal axis depending on whether they are increasing or decreasing relations (as in Remark 4.3). To alleviate the figures, we draw the arcs of the tour above the horizontal axis, but the reader can imagine them drawn both above and below: drawing both still yields a non-crossing diagram. A typical example of Tamari interval poset is illustrated in Figure 14.

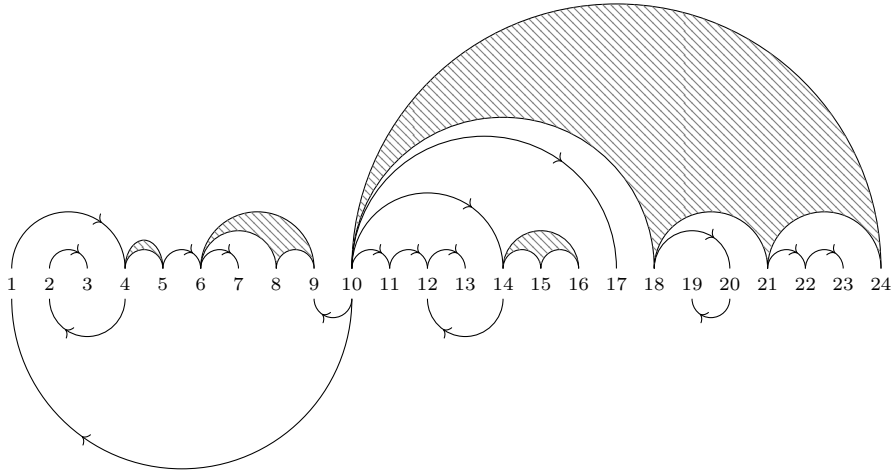


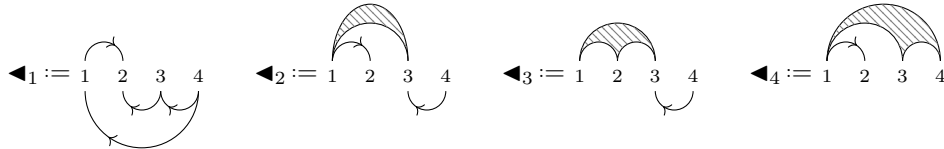
FIGURE 14. A typical Tamari interval preposet.

6.2. Inclusion versus refinement. Denote by $\mathbf{C}_{\blacktriangleleft} := \{\mathbf{x} \in \mathbb{R}^n \mid x_i \geq x_j \text{ if } i \blacktriangleleft j\}$ the cone of a preposet \blacktriangleleft on $[n]$. One can compare two preposets \blacktriangleleft and \blacktriangleleft' on $[n]$ in two natural ways:

- either by *inclusion*: $\mathbf{C}_{\blacktriangleleft} \subseteq \mathbf{C}_{\blacktriangleleft'}$, that is, $i \blacktriangleleft' j$ implies $i \blacktriangleleft j$,
- or by *refinement*: $\mathbf{C}_{\blacktriangleleft}$ is a face of $\mathbf{C}_{\blacktriangleleft'}$.

Note that refinement implies inclusion. We are mostly interested in the refinement order on Tamari interval preposets, but it is unfortunately not a lattice, as illustrated in our next example.

Example 6.6. Consider the four Tamari interval preposets



Then \blacktriangleleft_1 and \blacktriangleleft_2 do not refine each other, and \blacktriangleleft_3 and \blacktriangleleft_4 do not refine each other. Moreover, \blacktriangleleft_1 and \blacktriangleleft_2 refine \blacktriangleleft_3 and \blacktriangleleft_4 , and the relation between \blacktriangleleft_2 and \blacktriangleleft_3 is a cover relation. Hence, \blacktriangleleft_1 and \blacktriangleleft_2 have no join, while \blacktriangleleft_3 and \blacktriangleleft_4 have no meet.

In contrast, although it is less meaningful geometrically, the inclusion poset is a lattice

Proposition 6.7. *The inclusion poset of Tamari interval preposets is a lattice.*

Proof. The intersection of two Tamari interval preposets is a Tamari interval preposet. The inclusion poset of Tamari interval preposets thus admits a meet, thus is a lattice as it is bounded by the empty preposet and the full preposet. \square

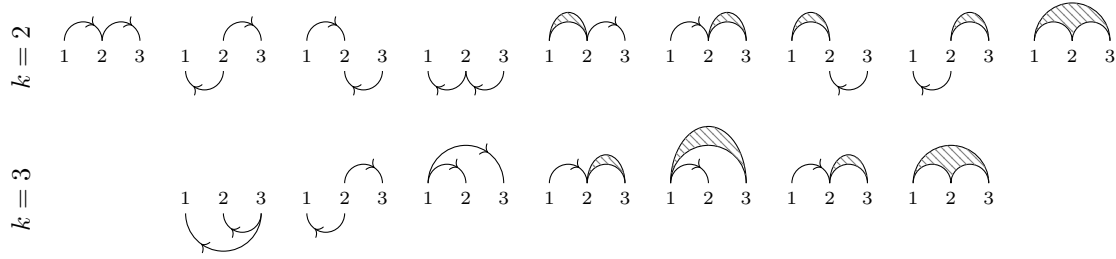
6.3. Two families of Tamari interval preposets. Similarly as in Section 4.2, we now describe two interesting families of Tamari interval preposets, which will later appear as the face preposets of certain families of hypergraphic polytopes (see also Section 7.3 for other families where all Hasse diagrams are trees).

6.3.1. Capped unit interval preposets. Continuing Section 4.2.1, we first consider the following preposets, which will take their significance in Example 6.16. Recall that for a preposet \blacktriangleleft , we denote by \triangleleft the poset on the equivalence classes of \blacktriangleleft , and by \triangleleft its cover relations.

Definition 6.8. We call *capped unit interval preposets* the preposets \blacktriangleleft on $[n]$ such that

- \triangleleft admits a unique minimum M ,
- for any cover relation $A \triangleleft B$, either $A = M$ or there is $a \in A$ and $b \in B$ with $|a - b| = 1$,

Example 6.13. The k -uniform interval preposets on $[3]$ for $k = 2, 3$ are the following



6.4. Counting Tamari interval preposets. The numbers of Tamari interval preposets and connected Tamari interval preposets on $[n]$ with k nodes are gathered in Table 7. The former were enumerated in and already appeared as [OEI10, A234268]. In contrast to Section 4.3, no simple formulas appear to exist for these numbers.

$n \setminus k$	1	2	3	4	5	6	Σ	$n \setminus k$	1	2	3	4	5	6	Σ
1	1						1	1	1						1
2	1	3					4	2	1	2					3
3	1	7	13				21	3	1	5	8				14
4	1	12	48	68			129	4	1	9	31	41			82
5	1	18	116	342	399		876	5	1	14	78	213	240		546
6	1	25	230	1060	2530	2530	6376	6	1	20	160	680	1556	1528	3945

TABLE 7. The number of Tamari interval preposets (left) and connected Tamari interval preposets (right) on $[n]$ with k nodes.

6.5. Tamari interval preposets and interval hypergraphic polytopes. Extending Section 4.4, we connect Tamari interval preposets to interval hypergraphic polytopes.

Proposition 6.14. *The face preposets of an interval hypergraphic polytope are Tamari interval preposets. Conversely, any Tamari interval preposet is a face poset of an interval hypergraphic polytope.*

Proof. The following proof mimics the proof of Lemma 3.8 (ii) and Proposition 4.16.

By Proposition 2.10, the faces of an interval hypergraphic polytope $\Delta_{\mathbb{I}}$ are in bijection with acyclic preorientations A of \mathbb{I} . Let \blacktriangleleft_A be the preposet of an acyclic preorientation of \mathbb{I} , fix integers $1 \leq a < b < c \leq n$, and assume that $a \blacktriangleleft_A c$. By Proposition 2.10, there are $I_1, \dots, I_k \in \mathbb{I}$ such that $a \in A(I_1)$, $A(I_{i+1}) \cap I_i \neq \emptyset$ for all $i \in [k-1]$, and $c \in I_k$. As $\bigcup_{i \in [k]} I_i$ is an interval containing a and c and $a < b < c$, it also contains b . Hence, there is $i \in [k]$ such that $b \in I_i$, and the sequence I_1, \dots, I_i proves that $a \blacktriangleleft_A b$. Similarly, $a \blacktriangleright_A c$ implies $b \blacktriangleright_A c$. We conclude that \blacktriangleleft_A is indeed a Tamari interval preposet by Definition 6.1.

Consider a Tamari interval preposet \blacktriangleleft . By Definition 6.1 (ii), the set a^{\blacktriangleleft} is an interval for all $a \in [n]$. Consider the orientation A_{\blacktriangleleft} of the interval hypergraph $\mathbb{I}_{\blacktriangleleft} := \{a^{\blacktriangleleft} \mid a \in [n]\}$ defined by $A_{\blacktriangleleft}(a^{\blacktriangleleft}) = \{b \mid a \blacktriangleleft b \text{ and } b \blacktriangleleft a\}$ for all $a \in [n]$. It is clear that A_{\blacktriangleleft} is acyclic, and that $\blacktriangleleft_{A_{\blacktriangleleft}} = \blacktriangleleft$. Hence, \blacktriangleleft is a face preposet of the interval hypergraphic polytope $\Delta_{\mathbb{I}_{\blacktriangleleft}}$. \square

6.6. A finer description. Extending Section 4.5, we now refine Proposition 6.14 to describe which Tamari interval preposet appears as a face preposet in which interval hypergraphic polytope.

Theorem 6.15. *A preposet \blacktriangleleft is a face preposet of an interval hypergraphic polytope $\Delta_{\mathbb{I}}$ if and only if*

- (i) for any $I \in \mathbb{I}$, there is $a \in [n]$ such that $a \in I \subseteq a^{\blacktriangleleft}$,
- (ii) for any equivalence class of \blacktriangleleft given as $\{a_1 < \dots < a_q\}$, and any $1 \leq p < q$, there is $I \in \mathbb{I}$ such that $\{a_p, a_{p+1}\} \subseteq I \subseteq a_p^{\blacktriangleleft} = a_{p+1}^{\blacktriangleleft}$,
- (iii) for any cover relation $X \blacktriangleleft Y$, there is $a \in X$, $b \in Y$, and $I \in \mathbb{I}$ such that $\{a, b\} \subseteq I \subseteq a^{\blacktriangleleft}$.

Proof. Assume first that $\blacktriangleleft = \blacktriangleleft_A$ is the face preposet of the hypergraphic polytope $\Delta_{\mathbb{I}}$ corresponding to the acyclic preorientation A of \mathbb{I} . Then, by Proposition 2.10:

- (i) For $I \in \mathbb{I}$, and any $a \in A(I) \subseteq I$, we have $a \in I \subseteq a^{\blacktriangleleft}$.
- (ii) For any $p \in [q-1]$, as $a_p \blacktriangleleft a_{p+1}$ is a cover relation, there exists $I \in \mathbb{I}$ such that $a_p \in A(I)$ and $a_{p+1} \in I$; similarly, as $a_p \blacktriangleright a_{p+1}$ is a cover relation, there exists $J \in \mathbb{I}$ such that $a_p \in J$ and $a_{p+1} \in A(J)$. As A is acyclic, we deduce without loss of generality that $\{a_p, a_{p+1}\} \subseteq A(I)$, and by the previous (i) that $A(I) \subseteq a_p^{\blacktriangleleft} = a_{p+1}^{\blacktriangleleft}$.
- (iii) For any cover relation $X \triangleleft Y$, there is $a \in X$, $b \in Y$ and $I \in \mathbb{I}$ such that $a \in A(I)$ and $b \in I$. In particular, $\{a, b\} \subseteq I \subseteq a^{\blacktriangleleft}$.

Hence, \blacktriangleleft and \mathbb{I} satisfy (i), (ii) and (iii).

Conversely, consider a preposet \blacktriangleleft and an interval hypergraph \mathbb{I} that satisfy (i), (ii) and (iii). We now construct an acyclic preorientation A of \mathbb{I} such that $\blacktriangleleft = \blacktriangleleft_A$. For all $I \in \mathbb{I}$, we define $A(I) = \{a \in [n] \mid a \in I \subseteq a^{\blacktriangleleft}\}$. Note that $A(I)$ is non-empty by (i). We claim that

- A is acyclic. Otherwise, there are $I, J \in \mathbb{I}$ with $a \in A(I) \cap (J \setminus A(J))$ and $b \in A(J) \cap (I \setminus A(I))$ by Proposition 2.28. By definition of A , this would imply that $a \in J \subseteq b^{\blacktriangleleft}$ and $b \in I \subseteq a^{\blacktriangleleft}$, hence $a^{\blacktriangleleft} = b^{\blacktriangleleft}$, so that $a \in A(J)$ and $b \in A(I)$: a contradiction.
- $\blacktriangleleft = \blacktriangleleft_A$. First, for any a, b consecutive in an equivalence class of \blacktriangleleft , there exists $I \in \mathbb{I}$ such that $\{a, b\} \subseteq I \subseteq a^{\blacktriangleleft} = b^{\blacktriangleleft}$ by (ii). Hence, we get that $\{a, b\} \in A(I)$, and thus $a \blacktriangleleft_A b$ and $b \blacktriangleleft_A a$. We conclude by transitivity that the equivalence classes of \blacktriangleleft and \blacktriangleleft_A coincide. Second, for any cover relation $X \triangleleft Y$, there exists a in X , b in Y and $I \in \mathbb{I}$ such that $\{a, b\} \subseteq I \subseteq a^{\blacktriangleleft}$ by (iii). Hence, $a \in A(I)$ and $b \in I$ so that we get $X \triangleleft_A Y$.

We conclude that $\blacktriangleleft = \blacktriangleleft_A$ is indeed the face poset of the hypergraphic polytope $\Delta_{\mathbb{I}}$ corresponding to the acyclic preorientation A of \mathbb{I} . \square

Example 6.16. For $S \subseteq [n-1]$, the face preposets of the hypergraphic polytope $\Delta_{\mathbb{I}_S}$ of $\mathbb{I}_S := \{[i, i+1] \mid i \in S\} \cup \{[n]\}$ are precisely the capped S -unit interval preposets of Definition 6.11.

Example 6.17. For the (complete) k -uniform interval hypergraph $\mathbb{I} = \{[i, i+k-1] \mid i \in [n-k]\}$, the face preposets of the hypergraphic polytope $\Delta_{\mathbb{I}}$ are precisely the k -uniform interval preposets of Definition 6.12.

Finally, Proposition 4.22 extends to face preposets as follows. For a Tamari interval preposet \blacktriangleleft , we denote by $C(\blacktriangleleft)$ the relations of \blacktriangleleft given by:

- all equivalence relations of \blacktriangleleft , i.e. all $a \blacktriangleleft b$ such that $a \blacktriangleright b$,
- the canonical relations $A \frown B$ (see Definition 6.4) for all cover relations $A \triangleleft B$ of the poset \triangleleft of \blacktriangleleft .

We denote by $U(\blacktriangleleft)$ the maximal relations of $C(\blacktriangleleft)$ for the order given by $(a \blacktriangleleft b) \prec (a \blacktriangleleft c)$ for $1 \leq a < b < c \leq n$ or $1 \leq c < b < a \leq n$.

Proposition 6.18. *We still denote by \mathcal{I} the inclusion poset of interval hypergraphs \mathbb{I} on $[n]$ containing all singletons. For a given Tamari interval preposet \blacktriangleleft , denote by $\mathcal{I}_{\blacktriangleleft}$ the subposet of \mathcal{I} induced by interval hypergraphs \mathbb{I} on $[n]$ such that \blacktriangleleft is a face preposet of $\Delta_{\mathbb{I}}$. Then*

- (i) $\mathcal{I}_{\blacktriangleleft}$ is order convex in \mathcal{I} .
- (ii) The interval hypergraph $\mathbb{I}_{\blacktriangleleft} := \{a^{\blacktriangleleft} \mid a \in [n]\}$ is a minimal element of $\mathcal{I}_{\blacktriangleleft}$. Moreover, it is the unique minimal element of $\mathcal{I}_{\blacktriangleleft}$ if and only if there are no $1 \leq a < b < c \leq n$ such that $a \blacktriangleleft b \blacktriangleleft c$, or $a \blacktriangleright b \blacktriangleright c$, or $a \blacktriangleright b \blacktriangleleft c$ in $U(\blacktriangleleft)$.
- (iii) The interval hypergraph $\mathbb{J}_{\blacktriangleleft} := \bigcup_{a \in [n]} \{I \mid a \in I \subseteq a^{\blacktriangleleft}\}$ is the unique maximal element of $\mathcal{I}_{\blacktriangleleft}$.

Proof. The proof is similar to that of Proposition 4.22 and left to the reader. \square

7. SCHRÖDER WEEPING WILLOWS AND FACES OF SIMPLE INTERVAL HYPERGRAPHIC POLYTOPES

In this section, we consider the face trees of the simple interval hypergraphic polytopes.

7.1. Schröder weeping willows. Following Definition 5.1 and Proposition 5.5, we now consider the following trees. A typical example is illustrated in Figure 15, and four interesting families will be presented in Section 7.3.

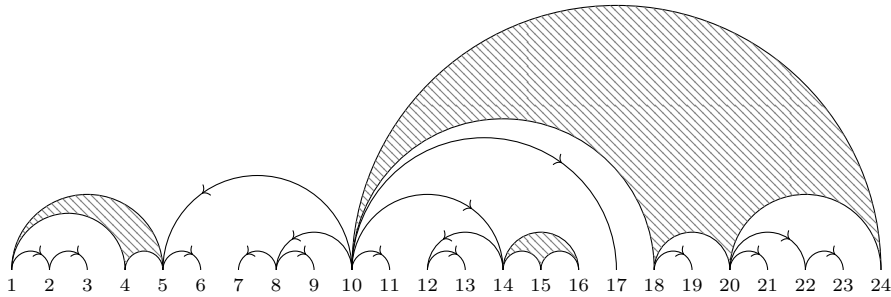


FIGURE 15. A typical Schröder weeping willow.

Definition 7.1. A *Schröder weeping willow* on $[n]$ is a directed tree SWW on a partition of $[n]$ whose associated preposet is a Tamari interval preposet.

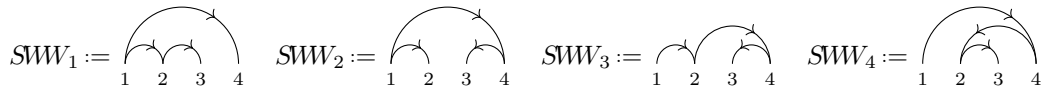
Remark 7.2. The weeping willows of Definition 5.1 are essentially the Schröder weeping willows of Definition 7.1 where each node is a singleton.

Remark 7.3. We represent the Schröder weeping willows as in Remark 6.5, except that we now gather all increasing and decreasing arcs above the horizontal axis. It follows from Proposition 5.6 that the resulting drawing is non-crossing. See Figure 15.

7.2. Inclusion versus refinement. Recall from Section 6.2 that one can order Tamari interval preposets either by inclusion or by refinement. Restricting to weeping willows, the refinement poset is also the *contraction poset*, *i.e.* the transitive closure of the edge contraction on Schröder weeping willows.

Note that in contrast to Proposition 6.7, the inclusion poset on Schröder weeping willow is not a lattice, as illustrated in our next example.

Example 7.4. Consider the four Schröder weeping willows



and their corresponding Tamari interval preposets $\blacktriangleleft_1, \blacktriangleleft_2, \blacktriangleleft_3$ and \blacktriangleleft_4 . Then \blacktriangleleft_1 and \blacktriangleleft_2 are not included in each other, and \blacktriangleleft_3 and \blacktriangleleft_4 are not included in each other. Moreover,

$$\blacktriangleleft_1 \cup \blacktriangleleft_2 = \begin{array}{c} \text{arc } (1,4) \\ \text{arc } (1,2) \\ \text{arc } (2,3) \\ \text{arc } (3,4) \end{array} = \blacktriangleleft_3 \cap \blacktriangleleft_4$$

which is not a Schröder weeping willow. Hence, in the inclusion poset on Schröder weeping willows, SWW_1 and SWW_2 have no join, while SWW_3 and SWW_4 have no meet.

But now, contrarily to Example 6.6, the contraction poset on Schröder weeping willows behaves nicely. See Figure 16.

Proposition 7.5. *The contraction poset on Schröder weeping willows, augmented by an artificial minimal element, is a lattice (that we call *contraction lattice*).*

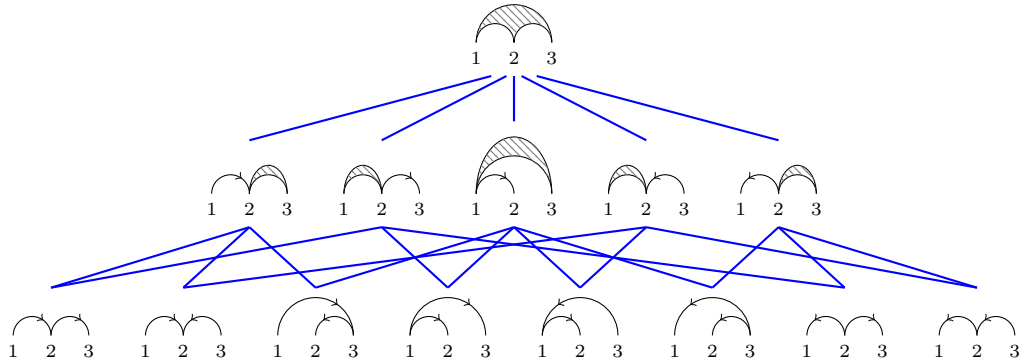


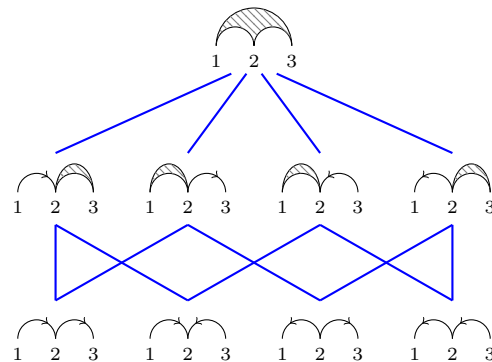
FIGURE 16. The lattice of Schröder weeping willows on 3 nodes (trimmed of its artificial minimum) admits 14 elements.

Proof. As a Schröder weeping willow is a tree, the cone $\mathbb{C}_{\blacktriangleleft}$ associated to some Schröder weeping willow SWW is a simplicial cone. Consider two such simplicial cones \mathbb{C}, \mathbb{C}' , and let $\mathbb{D}_1, \dots, \mathbb{D}_s$ be the faces of both \mathbb{C} and \mathbb{C}' contained in the intersection $\mathbb{C} \cap \mathbb{C}'$. As \mathbb{C} is simplicial, the convex hull $\text{conv}(\mathbb{D}_1, \dots, \mathbb{D}_s)$ is also a face of both \mathbb{C} and \mathbb{C}' , and is the unique inclusion-wise maximal common face. In particular $\text{conv}(\mathbb{D}_1, \dots, \mathbb{D}_s)$ is the cone associated to a certain Schröder weeping willow. Consequently, any two elements of the contraction poset on Schröder weeping willows admit a meet. As this poset has a unique minimum and a unique maximum, it is a lattice. \square

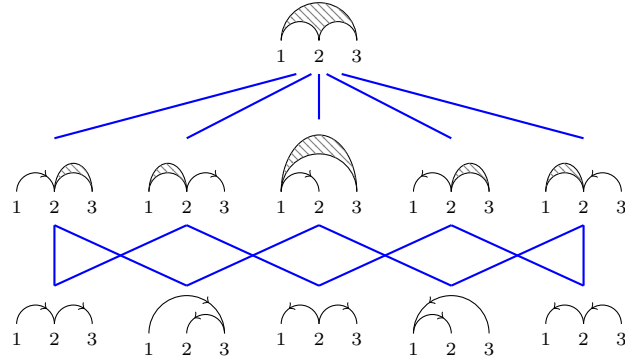
Remark 7.6. In the join semilattice on Schröder weeping willows, the atoms are the weeping willows, and the maximal element is the Schröder weeping willow with a single node $[n]$.

7.3. Four families of Schröder weeping willows. Similarly as in Section 5.2, we now describe four interesting families of Schröder weeping willows, which we illustrate when $n = 3$.

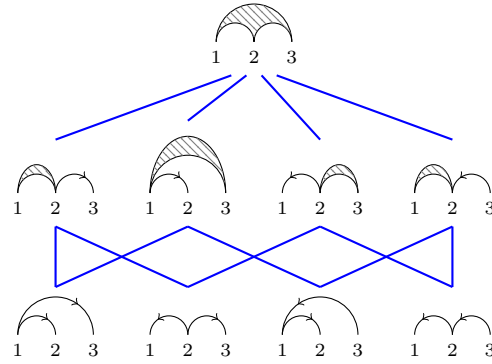
Example 7.7. The weeping willows of Example 5.8 are the minimal elements of the contraction poset on partial orientations of a line. For instance, when $n = 3$, we get the following (which is the face lattice of a square, trimmed of its minimum):



Example 7.8. The weeping willows of Example 5.9 are the minimal elements of the contraction poset on the classical Schröder trees. For instance, when $n = 3$, we get the following (which is the face lattice of a pentagon, trimmed of its minimum):



Example 7.9. The weeping willows of Example 5.10 are the minimal elements of the contraction poset on Schröder Pitman-Stanley trees. For instance, when $n = 3$, we get the following (which is the face lattice of a square, trimmed of its minimum):



Example 7.10. The weeping willows of Example 5.11 are the minimal elements of the contraction poset on Schröder freehedron trees. For instance, when $n = 3$, we get the same contraction poset as in Example 7.8.

7.4. Counting Schröder weeping willows. We now exploit Remark 7.3 to count (rooted) Schröder weeping willows.

Proposition 7.11. *Let*

$$E = 1 + x + 4x^2 + 20x^3 + 113x^4 + 688x^5 + 4404x^6 + 29219x^7 + 199140x^8 + 1385904x^9 + \dots$$

$$F = 1 + 2x + 7x^2 + 33x^3 + 181x^4 + 1083x^5 + 6854x^6 + 45111x^7 + 305629x^8 + 2117283x^9 + \dots$$

$$G = 1 + 3x + 14x^2 + 79x^3 + 489x^4 + 3195x^5 + 21635x^6 + 150296x^7 + 1064427x^8 + 7653367x^9 + \dots$$

$$H = 1 + 3x + 13x^2 + 68x^3 + 395x^4 + 2450x^5 + 15892x^6 + 106489x^7 + 731379x^8 + 5121392x^9 + \dots$$

denote the ordinary generating functions of unoriented non-crossing partition trees where n is in a singleton block [OEI10, A108447], of unoriented non-crossing partition trees [OEI10, A054727], of Schröder weeping willows, and of rooted Schröder weeping willows [OEI10, A200757] respectively, where x counts the size of the ground set minus one. Then,

$$\begin{aligned} E &= 1 + xFE^2, & F &= \frac{E}{1 - xE}, \\ G &= \frac{1 + 2xGE^2}{1 - xE}, & \text{and} & & H &= \frac{1 + x(H + F)E^2}{1 - xE}. \end{aligned}$$

Hence, E , F , G and H are solutions of

$$\begin{aligned} xE^3 + xE^2 - (x + 1)E + 1 &= 0, & xF^3 + (x^2 - x)F^2 + (2x - 1)F + 1 &= 0, \\ (10x - 1)G^3 + (5x^2 - 3x - 1)G^2 + (5x + 1)G + 1 &= 0, & x^2H^3 + x(x - 2)H^2 + (1 - x)H - 1 &= 0. \end{aligned}$$

Proof. The four formulas immediately follow from the decompositions illustrated in Figure 17 (recall that if A is the generating function for a combinatorial family, then $\frac{1}{1-A}$ is the generating function for sequences of objects in this family).

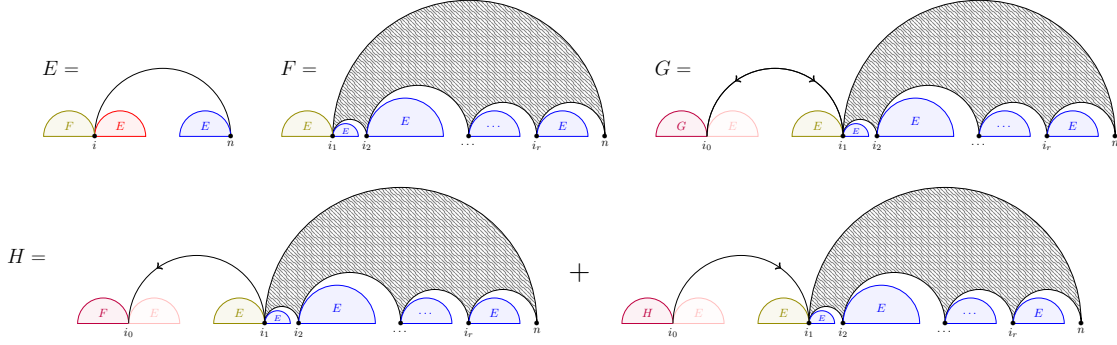


FIGURE 17. Decomposition for E (top left), for F (top middle), for G (top right), and for H (bottom).

Substituting the formula expressing F in the formula for E gives the claimed annihilating polynomial for E . Once this is established, one can express F , G and H as functions of E , then check that their respective annihilating polynomials yields multiples of the one of E (alternatively, each annihilating polynomial can be obtained with the resultant method). \square

Proposition 7.12. *Let*

$$\begin{aligned} E &= 1 + xz + x^2z + x^3z + 3x^2z^2 + x^4z + 7x^3z^2 + x^5z + 12x^4z^2 + 12x^3z^3 + \dots \\ F &= z + xz + x^2z + xz^2 + x^3z + 3x^2z^2 + x^4z + 6x^3z^2 + 3x^2z^3 + x^5z + 10x^4z^2 + 14x^3z^3 + \dots \\ G &= z + xz + x^2z + 2xz^2 + x^3z + 5x^2z^2 + 9x^3z^2 + 8x^2z^3 + x^4z + \dots \\ H &= z + xz + x^2z + 2xz^2 + x^3z + 5x^2z^2 + 9x^3z^2 + 7x^2z^3 + x^4z + \dots \end{aligned}$$

denote the ordinary generating functions of unoriented non-crossing Schröder trees where n is in a singleton block [OEI10, A108447], of unoriented non-crossing Schröder trees [OEI10, A054727], of Schröder weeping willows, and of rooted Schröder weeping willows [OEI10, A200757] respectively, where x counts the size of the ground set minus one, and z counts the number of nodes (i.e. the number of parts in the partition of $[x+1]$). Then,

$$\begin{aligned} E &= 1 + xFE^2, & F &= \frac{zE}{1 - xE}, \\ G &= \frac{z(1 + 2xGE^2)}{1 - xE}, & \text{and} & \\ H &= \frac{z(1 + x(H + F)E^2)}{1 - xE}. \end{aligned}$$

Proof. The proof is similar as the one of Proposition 7.11, using again Figure 17. \square

Remark 7.13. In particular, the f -vector of the contraction poset on Schröder weeping willow, i.e. the number of Schröder weeping willows with ground set $[n]$ counted according to their number of nodes, is formed by the coefficients of the polynomial (in the variable z) which is in factor of x^{n-1} inside G . For instance, for $n = 3$, the f -vector is $(8, 5, 1)$, as can be read off from the size of each row in Figure 16; meanwhile, the polynomial in factor of x^{3-1} inside G is $8z^3 + 5z^2 + z$.

Remark 7.14. One can recover f (resp. g , resp. h) from Proposition 5.12 by looking at the coefficients in front of $x^k z^{k+1}$ in F (resp. G , resp. H) in Proposition 7.12. Indeed, a weeping willow is a Schröder weeping willow with the same number of nodes and parts.

7.5. Schröder weeping willows and simple interval hypergraphic polytopes. Following Section 5.4, we now specialize Section 6.5 to connect Schröder weeping willows with face trees of simple interval hypergraphic polytopes. The next statement extends Propositions 5.15 and 5.16.

Proposition 7.15. *The face preposets of a simple interval hypergraphic polytope are Schröder weeping willows. In fact, the face lattice of a simple interval hypergraphic polytope is a graded sublattice of the contraction lattice on Schröder weeping willows. Conversely, any Schröder weeping willow is a face poset of a simple interval hypergraphic polytope.*

Proof. This immediately follows from three immediate facts:

- the face forests of a simple deformed permutahedron are precisely all contractions of its vertex forests, and its face lattice is isomorphic to the contraction lattice on its face forests,
- the Schröder weeping willows are precisely the contractions of the weeping willows. \square

The same arguments yield the following extension of Propositions 5.17 and 5.18.

Proposition 7.16. *The face preposets of an interval nestohedron are rooted Schröder weeping willows. Conversely, any rooted Schröder weeping willow is a face poset of an interval nestohedron.*

Example 7.17. For instance, the contraction posets of Examples 7.7 to 7.10 are isomorphic to the face lattices of the cube, associahedron, Pitman–Stanley polytope, and freehedron respectively.

7.6. A finer description. Finally, we extend Propositions 5.23 and 5.27 to all Schröder weeping willows. Recall from Proposition 6.18 that, for a Tamari interval preposet \blacktriangleleft , we considered the interval hypergraphs $\mathbb{I}_{\blacktriangleleft} := \{a^{\blacktriangleleft} \mid a \in [n]\}$ and $\mathbb{J}_{\blacktriangleleft} := \bigcup_{a \in [n]} \{I \mid a \in I \subseteq a^{\blacktriangleleft}\}$. For a preposet \blacktriangleleft , recall that we denote by $C(\blacktriangleleft)$ the relations of \blacktriangleleft given by:

- all equivalence relations of \blacktriangleleft , i.e. all $a \blacktriangleleft b$ such that $a \blacktriangleright b$,
- the canonical relations $A \frown B$ (see Definition 6.4) for all cover relations $A \triangleleft B$ of the poset \triangleleft of \blacktriangleleft .

We denote by $K(\blacktriangleleft)$ the maximal relations of $C(\blacktriangleleft)$ for the order given by $(a, b) \prec (c, d)$ if a, b, c, d are not all equivalent for \blacktriangleleft and $\min(c, d) \leq \min(a, b)$ and $\max(a, b) \leq \max(c, d)$,

Proposition 7.18. *We denote by \mathcal{S} the inclusion poset of interval hypergraphs \mathbb{I} on $[n]$ such that $\Delta_{\mathbb{I}}$ is simple. For a given Schröder weeping willow SWW with transitive closure \blacktriangleleft , denote by $\mathcal{S}_{\blacktriangleleft} := \mathcal{I}_{\blacktriangleleft} \cap \mathcal{S}$ the subposet of \mathcal{S} induced by interval hypergraphs \mathbb{I} on $[n]$ such that SWW is a face tree of $\Delta_{\mathbb{I}}$. Then*

- (i) $\mathcal{S}_{\blacktriangleleft}$ is order convex in \mathcal{S} .
- (ii) The interval hypergraph $\mathbb{I}_{\blacktriangleleft}$ is a minimal element of $\mathcal{S}_{\blacktriangleleft}$. Moreover, it is the unique minimal element of $\mathcal{S}_{\blacktriangleleft}$ if and only if there are no $1 \leq a < b < c \leq n$ such that $a \blacktriangleleft b \blacktriangleleft c$, or $a \blacktriangleright b \blacktriangleright c$, or $a \blacktriangleright b \blacktriangleleft c$, where both relations are in $C(\blacktriangleleft)$ and at least one of them is in $K(\blacktriangleleft)$.
- (iii) The interval hypergraph $\mathbb{J}_{\blacktriangleleft}$ is the unique maximal element of $\mathcal{S}_{\blacktriangleleft}$.

Proof. The proof is similar to that of Proposition 5.23 and left to the reader. \square

Proposition 7.19. *We denote by \mathcal{N} the inclusion poset of interval building sets on $[n]$ (i.e. interval hypergraphs \mathbb{I} containing all singletons, and such that $I, J \in \mathbb{I}$ and $I \cap J \neq \emptyset$ implies $I \cup J \in \mathbb{I}$). For a given rooted Schröder weeping willow SWW with transitive closure \blacktriangleleft , denote by $\mathcal{N}_{\blacktriangleleft} := \mathcal{I}_{\blacktriangleleft} \cap \mathcal{N}$ the subposet of \mathcal{N} induced by interval building sets \mathbb{I} on $[n]$ such that SWW is a face tree of $\Delta_{\mathbb{I}}$. Then $\mathcal{N}_{\blacktriangleleft}$ is the interval between $\mathbb{I}_{\blacktriangleleft}$ and $\mathbb{J}_{\blacktriangleleft}$.*

Proof. The proof is similar to that of Proposition 5.27 and left to the reader. \square

ACKNOWLEDGEMENTS

Most of our working group came together during the January 2025 Banff workshop “Lattice Theory”. We are grateful to the organizers (Emily Barnard, Cesar Ceballos, Colin Defant, Osamu Iyama, and Nathan Williams) and to all participants for the friendly and inspiring atmosphere. We also thank Gabe Udell for the suggestion to consider hypergraphs containing $[n]$.

REFERENCES

- [AA23] Marcelo Aguiar and Federico Ardila. Hopf monoids and generalized permutahedra. *Mem. Amer. Math. Soc.*, 289(1437), 2023.
- [ABG⁺25] Antoine Abram, Jose Bastidas, Félix Gélinas, Vincent Pilaud, and Andrew Sack. Ornamentation lattices and intreeval hypergraphic lattices. Preprint, [arXiv:2508.01606](https://arxiv.org/abs/2508.01606), 2025.
- [AD13] Federico Ardila and Jeffrey Doker. Lifted generalized permutahedra and composition polynomials. *Adv. in Appl. Math.*, 50(4):607–633, 2013.
- [AFS19] Stav Ashur, Omrit Filtser, and Rachel Sababn. Terrain-like and non-jumping graphs. In *Proceedings of the 35th European Workshop on Computational Geometry (EuroCG)*, page 51, 2019.
- [Agn17] Geir Agnarsson. On a special class of hyper-permutahedra. *Electron. J. Combin.*, 24(3):Paper No. 3.46, 25, 2017.
- [AM09] Geir Agnarsson and Walter D. Morris. On Minkowski sums of simplices. *Ann. Comb.*, 13(3):271–287, 2009.
- [BB09] Olivier Bernardi and Nicolas Bonichon. Intervals in Catalan lattices and realizers of triangulations. *J. Combin. Theory Ser. A*, 116(1):55–75, 2009.
- [BBM19] Carolina Benedetti, Nantel Bergeron, and John Machacek. Hypergraphic polytopes: combinatorial properties and antipode. *J. Comb.*, 10(3):515–544, 2019.
- [BCP26] Alin Bostan, Frédéric Chyzak, and Vincent Pilaud. Refined Product Formulas for Tamari Intervals. *Electron. J. Combin.*, 33(1):P1.62, 2026.
- [BMCLD⁺23] Véronique Bazier-Matte, Nathan Chapelier-Laguette, Guillaume Douville, Kaveh Mousavand, Hugh Thomas, and Emine Yıldırım. ABHY Associahedra and Newton polytopes of F -polynomials for finite type cluster algebras of simply laced finite type. *J. Lond. Math. Soc. (2)*, 2023.
- [BP22] Nathaniel Bottman and Daria Poliakova. Constraining polytopes. Preprint, [arXiv:2208.14529](https://arxiv.org/abs/2208.14529), 2022.
- [BP26] Nantel Bergeron and Vincent Pilaud. Interval hypergraphic lattices. *European J. Combin.*, 132:Paper No. 104285, 2026.
- [BW91] Anders Björner and Michelle L. Wachs. Permutation statistics and linear extensions of posets. *J. Combin. Theory Ser. A*, 58(1):85–114, 1991.
- [CCF⁺17] Daniele Catanzaro, Steven Chaplick, Stefan Felsner, Bjarni V. Halldórsson, Magnús M. Halldórsson, Thomas Hixon, and Juraj Stacho. Max point-tolerance graphs. *Discrete Appl. Math.*, 216(part 1):84–97, 2017.
- [CD06] Michael P. Carr and Satyan L. Devadoss. Coxeter complexes and graph-associahedra. *Topology Appl.*, 153(12):2155–2168, 2006.
- [CF26] Veronica Calvo Cortes and Hadleigh Frost. Dyck paths, configuration spaces and polytopes for linear nakayama algebras, 2026.
- [Cha07] Frédéric Chapoton. Sur le nombre d’intervalles dans les treillis de Tamari. *Sém. Lothar. Combin.*, 55:Art. B55f, 18, 2005/07.
- [Cha18] Frédéric Chapoton. Une note sur les intervalles de Tamari. *Ann. Math. Blaise Pascal*, 25(2):299–314, 2018.
- [CHM⁺23] Jean Cardinal, Hung P. Hoang, Arturo Merino, Ondřej Mička, and Torsten Mütze. Combinatorial generation via permutation languages. V. Acyclic orientations. *SIAM J. Discrete Math.*, 37(3):1509–1547, 2023.
- [CP15] Grégory Châtel and Viviane Pons. Counting smaller elements in the Tamari and m -Tamari lattices. *J. Combin. Theory Ser. A*, 134:58–97, 2015.
- [CP24] Frédéric Chapoton and Vincent Pilaud. Shuffles of deformed permutahedra, multiplihedra, constrainahedra, and biassociahedra. *Ann. H. Lebesgue*, 7:1535–1601, 2024.
- [CPP19] Grégory Chatel, Vincent Pilaud, and Viviane Pons. The weak order on integer posets. *Algebraic Combinatorics*, 2(1):1–48, 2019.
- [CS25] Jean Cardinal and Raphael Steiner. Shortest paths on polymatroids and hypergraphic polytopes. 2025.
- [DCP95] Conrado De Concini and Claudio Procesi. Wonderful models of subspace arrangements. *Selecta Math. (N.S.)*, 1(3):459–494, 1995.
- [Def23] Colin Defant. Fertilitopes. *Discrete Comput. Geom.*, 70(3):713–752, 2023.
- [DHP18] Aram Dermenjian, Christophe Hohlweg, and Vincent Pilaud. The facial weak order and its lattice quotients. *Trans. Amer. Math. Soc.*, 370(2):1469–1507, 2018.
- [DP11] Kosta Došen and Zoran Petrić. Hypergraph polytopes. *Topology Appl.*, 158(12):1405–1444, 2011.
- [DR94] Dominique Dumont and Arthur Randrianarivony. Dérangements et nombres de Genocchi. *Discrete Math.*, 132(1-3):37–49, 1994.
- [Edm70] Jack Edmonds. Submodular functions, matroids, and certain polyhedra. In *Combinatorial Structures and their Applications (Proc. Calgary Internat. Conf., Calgary, Alta., 1969)*, pages 69–87. Gordon and Breach, New York, 1970.
- [FFN25] Wenjie Fang, Éric Fusy, and Philippe Nadeau. Tamari intervals and blossoming trees. *Comb. Theory*, 5(1):Paper No. 4, 41, 2025.
- [For08] Stefan Forcey. Convex hull realizations of the multiplihedra. *Topology Appl.*, 156(2):326–347, 2008.

- [FR21] Vincent Froese and Malte Renken. A fast shortest path algorithm on terrain-like graphs. *Discrete Comput. Geom.*, 66(2):737–750, 2021.
- [FR24] Vincent Froese and Malte Renken. Terrain-like graphs and the median Genocchi numbers. *European J. Combin.*, 115:Paper No. 103780, 8, 2024.
- [FS05] Eva Maria Feichtner and Bernd Sturmfels. Matroid polytopes, nested sets and Bergman fans. *Port. Math. (N.S.)*, 62(4):437–468, 2005.
- [Gre77] Curtis Greene. Acyclic orientations. In *Proceedings of the NATO Advanced Study Institute held in Berlin (West Germany)*, volume 31 of *Nato Science Series C*., pages 65–68. Springer Netherlands, 1977.
- [GZ83] Curtis Greene and Thomas Zaslavsky. On the interpretation of Whitney numbers through arrangements of hyperplanes, zonotopes, non-Radon partitions, and orientations of graphs. *Trans. Amer. Math. Soc.*, 280(1):97–126, 1983.
- [Hix13] Thomas Stuart Hixon. Hook graphs and more : Some contributions to geometric graph theory. Master’s thesis, Technische Universität Berlin, 2013.
- [JT19] Vít Jelínek and Martin Töpfer. On grounded L-graphs and their relatives. *Electron. J. Combin.*, 26(3):Paper No. 3.17, 13, 2019.
- [Kim08] Sangwook Kim. Shellable complexes and topology of diagonal arrangements. *Discrete Comput. Geom.*, 40(2):190–213, 2008.
- [KM04] Allen Knutson and Ezra Miller. Subword complexes in Coxeter groups. *Adv. Math.*, 184(1):161–176, 2004.
- [KM05] Allen Knutson and Ezra Miller. Gröbner geometry of Schubert polynomials. *Ann. of Math. (2)*, 161(3):1245–1318, 2005.
- [Lod04] Jean-Louis Loday. Realization of the Stasheff polytope. *Arch. Math. (Basel)*, 83(3):267–278, 2004.
- [OEI10] The On-Line Encyclopedia of Integer Sequences. Published electronically at <http://oeis.org>, 2010.
- [Pil12] Vincent Pilaud. The greedy flip tree of a subword complex. Preprint, [arXiv:1203.2323](https://arxiv.org/abs/1203.2323), 2012.
- [Pil24] Vincent Pilaud. Acyclic reorientation lattices and their lattice quotients. *Ann. Comb.*, 2024. Online first.
- [Pil25] Vincent Pilaud. Plumbing bijections. Preprint, [arXiv:2512.05001](https://arxiv.org/abs/2512.05001), 2025.
- [Pos09] Alexander Postnikov. Permutohedra, associahedra, and beyond. *Int. Math. Res. Not. IMRN*, (6):1026–1106, 2009.
- [Pou25] Germain Poullot. Rays of the deformation cones of graphical zonotopes, 2025.
- [PP25] Vincent Pilaud and Germain Poullot. Pivot polytopes of products of simplices and shuffles of associahedra. *Discrete Comput. Geom.*, 2025.
- [PP26] Arnau Padrol and Germain Poullot. Indecomposability and beyond via the graph of edge dependencies, 2026.
- [PPP22] Arnau Padrol, Vincent Pilaud, and Germain Poullot. Deformation cones of hypergraphic polytopes. *Sém. Lothar. Combin.*, 86B:Art. #72, 12 pp., 2022.
- [PPP23] Arnau Padrol, Vincent Pilaud, and Germain Poullot. Deformation cones of graph associahedra and nestohedra. *European J. Combin.*, 107:103594, 2023.
- [PPP25] Arnau Padrol, Vincent Pilaud, and Germain Poullot. Deformed graphical zonotopes. *Discrete Comput. Geom.*, 73(2):447–465, 2025.
- [PPPP23] Arnau Padrol, Yann Palu, Vincent Pilaud, and Pierre-Guy Plamondon. Associahedra for finite type cluster algebras and minimal relations between \mathfrak{g} -vectors. *Proc. London Math. Soc.*, 127(3):513–588, 2023.
- [PPR23] Arnau Padrol, Vincent Pilaud, and Julian Ritter. Shard polytopes. *Int. Math. Res. Not. IMRN*, (9):7686–7796, 2023.
- [PRW08] Alexander Postnikov, Victor Reiner, and Lauren K. Williams. Faces of generalized permutohedra. *Doc. Math.*, 13:207–273, 2008.
- [PS12] Vincent Pilaud and Francisco Santos. The brick polytope of a sorting network. *European J. Combin.*, 33(4):632–662, 2012.
- [PS13] Vincent Pilaud and Christian Stump. EL-labelings and canonical spanning trees for subword complexes. In *Discrete Geometry and Optimization*, Fields Inst. Comm. Series, pages 213–248. Springer, 2013.
- [PS19] Vincent Pilaud and Francisco Santos. Quotientopes. *Bull. Lond. Math. Soc.*, 51(3):406–420, 2019.
- [Rad52] Richard Rado. An inequality. *J. London Math. Soc.*, 27:1–6, 1952.
- [Reh22] Sophie Rehberg. Pruned inside-out polytopes, combinatorial reciprocity theorems and generalized permutahedra. *Electron. J. Combin.*, 29(4):Paper No. 4.36, 31, 2022.
- [San09] Samson Sanedlidze. The bitwisted Cartesian model for the free loop fibration. *Topology Appl.*, 156(5):897–910, 2009.
- [Sch11] Pieter Hendrik Schoute. *Analytical treatment of the polytopes regularly derived from the regular polytopes. Section I: The simplex.*, volume 11. 1911.
- [SP02] Richard P. Stanley and Jim Pitman. A polytope related to empirical distributions, plane trees, parking functions, and the associahedron. *Discrete Comput. Geom.*, 27(4):pp. 603–634, 2002.

- [SS93] Steve Shnider and Shlomo Sternberg. *Quantum groups: From coalgebras to Drinfeld algebras*. Series in Mathematical Physics. International Press, Cambridge, MA, 1993.
- [Sta70] James Stasheff. *H-spaces from a homotopy point of view*. Lecture Notes in Mathematics, Vol. 161. Springer-Verlag, Berlin-New York, 1970.
- [Sta73] Richard P. Stanley. Acyclic orientations of graphs. *Discrete Math.*, 5:171–178, 1973.
- [STC15] Mauricio Soto and Christopher Thraves Caro. p -box: a new graph model. *Discrete Math. Theor. Comput. Sci.*, 17(1):169–186, 2015.
- [SU04] Samson Saneblidze and Ronald Umble. Diagonals on the permutahedra, multiplihedra and associahedra. *Homology Homotopy Appl.*, 6(1):363–411, 2004.
- [Tam51] Dov Tamari. *Monoides préordonnés et chaînes de Malcev*. PhD thesis, Université Paris Sorbonne, 1951.

(J. Bastidas) LACIM, UNIVERSITÉ DU QUÉBEC À MONTRÉAL, CANADA

Email address: `bastidas.math@proton.me`

URL: <https://bastidas-jose.codeberg.page/>

(F. Gélinas) YORK UNIVERSITY, CANADA

Email address: `felixgel@yorku.ca`

URL: <https://felixgelinas.github.io/>

(V. Pilaud) UNIVERSITAT DE BARCELONA & CENTRE DE RECERCA MATEMÀTICA, BARCELONA

Email address: `vincent.pilaud@ub.edu`

URL: <https://www.ub.edu/comb/vincentpilaud/>

(G. Poullot) OSNABRÜCK UNIVERSITÄT, GERMANY

Email address: `germain.poullot@uni-osnabrueck.de`

URL: <https://embrunforestier.github.io/germainpoullot.github.io/>

(A. Sack) UNIVERSITY OF MICHIGAN, UNITED STATES OF AMERICA

Email address: `asack@umich.edu`

URL: <https://andrewsack.com/>

(E. Tzanaki) UNIVERSITY OF CRETE, GREECE

Email address: `etzanaki@uoc.gr`

URL: <https://sites.google.com/view/tzanakel/homepage>